PEETER JOOT

ADVANCED ANTENNA THEORY

ADVANCED ANTENNA THEORY

PEETER JOOT

Notes and problems from UofT ECE1229H 2015

June 2020 – version V0.2.3

COPYRIGHT

DOCUMENT VERSION

Version V0.2.3

Sources for this notes compilation can be found in the github repository

git@github.com:peeterjoot/ece1229-antenna.git

The last commit (Jun/2/2020), associated with this pdf was b9b3a18b12cab31e06c5b2e8e8500208ff95bcd1

Should you wish to actively contribute typo fixes (or even more significant changes) to this book, you can do so by contacting me, or by forking your own copy of the associated git repositories and building the book pdf from source, and submitting a subsequent merge request.

```
#!/bin/bash

git clone git@github.com:peeterjoot/latex-notes-
    compilations.git peeterjoot
cd peeterjoot

submods="figures/ece1229-antenna julia matlab
    mathematica ece1229-antenna latex"
for i in $submods ; do
   git submodule update --init $i
   (cd $i && git checkout master)
done

export PATH=`pwd`/latex/bin:$PATH

cd ece1229-antenna
make
```

I reserve the right to impose dictatorial control over any editing and content decisions, and may not accept merge requests as-is, or at all. That said, I will probably not refuse reasonable suggestions or merge requests.

Dedicated to:
Aurora and Lance, my awesome kids, and
Sofia, who not only tolerates and encourages my studies, but is also awesome enough to think that math is sexy.

PREFACE

This book contains course notes from the Spring 2015 session of the University of Toronto Advanced Antenna Theory course (ECE1229H), taught by Professor G. V. Eleftheriades.

Official course description: "This course deals with the analysis and design of a range of antennas. Topics addressed include: definitions of antenna parameters; vector potentials; solutions to the inhomogeneous wave equation; principles of duality and reciprocity; wire antennas; antenna arrays; phased arrays; synthesis techniques for discrete and continuous line sources; integral equations and solutions using the method of moments; field equivalence principle; aperture antennas; antenna measurement techniques; diffraction; horn antennas; reflector antennas; microstrip antennas; reflectarrays; electrically small antennas; and broadband antennas."

Synopsis

1. Fundamental Antenna Parameters (patterns, directivity, effective aperture, input impedance, Friis transmission equation, radar range equations, RCS)
2. Review of Maxwell's Equations
3. Radiation from arbitrary current distributions
4. Wire and Mobile Communication Antennas: Dipoles, loops, ground effects
5. Reciprocity; Equivalence of transmit and receive radiation patterns
6. Phased Arrays
7. Self Impedance: Integral equations and method of moments (MoM)
8. Mutual Impedance : Induced EMF method

9. Aperture Antennas I : Equivalent current method, rectangular apertures, horn antennas
10. Apertures Antennas II : Plane-wave expansion, slots
11. Printed and IC Antennas : Microstrip patch antennas, miniaturized antennas
12. Metamaterial Antennas
13. Broadband Antennas : Self complementarity, spirals, log periodic, Yagi Uda

References include

- (Main Text) [5] C.A. Balanis, "Antenna Theory," Wiley, 3rd Edition
- (Recommended) [23] W.L. Stutzman and G. A. Thiele, "Antenna Theory and Design" 2nd Edition, Wiley.
- (Recommended) [9] G.V. Eleftheriades and K.G. Balmain (Edt.) "Negative-Refraction Metamaterials", Wiley and IEEE Press.

This document contains:

- Personal notes exploring details that were not clear to me from the lectures, or from the texts associated with the lecture material.
- Assigned problems. Like anything else take these as is. I have attempted to either correct errors or mark them as such.

This set of notes is significantly different from my notes for many other classes. With the class taught on slides (and some of those slides mirroring the text closely), I did not take live notes in class. These notes fill in details that I felt deserved clarification, contain problem sets solutions, as well as a number of loosely related musings on Geometric Algebra equivalents to some of the generalized concepts of electromagnetic theory encountered in this class (i.e. magnetic sources). My thanks go to Professor Eleftheriades for teaching this course.

Peeter Joot peeterjoot@pm.me

CONTENTS

Preface xi

1 FUNDAMENTAL PARAMETERS OF ANTENNAS. 1
- 1.1 Poynting vector. 1
- 1.2 Typical far-field radiation intensity. 1
- 1.3 Field plots. 3
- 1.4 dB vs dBi. 4
- 1.5 Trig integrals. 4
- 1.6 Polarization vectors. 4
- 1.7 Phasor power. 8
- 1.8 Radar cross section examples. 9
- 1.9 Scattering from a sphere vs frequency. 10
- 1.10 EIRP. 11
- 1.11 Free space impedance. 12
- 1.12 Notation. 12
- 1.13 Problems. 12

2 MAXWELL'S EQUATIONS. 27
- 2.1 Review. 27
- 2.2 Constitutive relations. 29
- 2.3 Boundary conditions. 30
- 2.4 Linear time invariant. 30
- 2.5 Green's functions. 30
- 2.6 Tangential and normal field components. 31
- 2.7 Energy momentum conservation. 35
- 2.8 Duality transformation. 40
- 2.9 Reciprocity theorem. 42
- 2.10 Notation. 45
- 2.11 Problems. 46

3 LINEAR WIRE ANTENNAS. 49
- 3.1 Magnetic Vector Potential. 49
- 3.2 Plots of infinitesimal dipole radial dependence. 49
- 3.3 Electric Far field for a spherical potential. 51

3.4 Magnetic Far field for a spherical potential. 53
3.5 Plane wave relations between electric and magnetic fields. 54
3.6 Transverse only nature of the far-field fields. 54
3.7 Duality transformation of the far field fields. 55
3.8 Vertical dipole reflection coefficient. 56
3.9 Horizontal dipole reflection coefficient. 58
3.10 Field resolution w.r.t the reflecting plane. 60
3.11 Image theorem. 64
3.12 Problems. 68

4 ANTENNA ARRAYS. 83
4.1 Chebyscheff polynomials. 83
4.2 Problems. 93

5 APERATURE ANTENNAS. 117
5.1 Problems. 117

6 MICROSTRIP ANTENNAS. 123
6.1 Problems. 123

7 FIELDS AND WAVES. 127
7.1 coupled wave equation in cylindrical coordinates. 127
7.2 Impedance transformation. 128
7.3 Problems. 130

A PROF. ELEFTHERIADES' HANDWRITING DECODER RING. 133

B ELECTRIC SOURCES (GA). 135
B.1 Maxwell's equation in GA phasor form. 135
B.2 Preliminaries. Dual magnetic form of Maxwell's equations. 136
B.3 Constructing a potential representation. 137
B.4 Maxwell's equation in Four vector form. 139
B.5 Helmholtz equation directly from the GA form. 140

C MAGNETIC SOURCES (GA). 143
C.1 Dual-Maxwell's equation in GA phasor form. 143
C.2 Preliminaries. Dual magnetic form of Maxwell's equations. 144

C.3 Constructing a potential representation. 145
C.4 Maxwell's equation in Four vector form. 147
C.5 Helmholtz equation directly from the GA form. 148

D ELECTRIC AND MAGNETIC SOURCES (GA). 151
D.1 Space time split. 151
D.2 Covariant form. 152
D.3 Trial potential solution. 153
D.4 Lorentz gauge application to Helmholtz. 154
D.5 Recovering the fields. 154

E RECIPROCITY THEOREM (GA). 157

F RELATION TO TENSOR FORM (GA). 159

G PARALLEL PROJECTION OF ELECTROMAGNETIC FIELDS (GA). 165

H MATHEMATICA NOTEBOOKS. 169

I JULIA NOTEBOOKS. 173

J MATLAB NOTEBOOKS. 175

INDEX 177

BIBLIOGRAPHY 183

LIST OF FIGURES

Figure 1.1 Plot methods for fields and intensities. 3
Figure 1.2 Cosinusoidal and sinusoidal radiation intensities. 3
Figure 1.3 Square sinusoidal and cosinusoidal radiation intensity. 4
Figure 1.4 Square geometry for RCS example. 10
Figure 1.5 Sphere geometry for RCS example. 10
Figure 1.6 Cylinder geometry for RCS example. 10
Figure 1.7 Trihedral corner reflector geometry for RCS example. 11
Figure 1.8 Scattering from a sphere vs frequency (from Prof. Eleftheriades' class notes). 11
Figure 1.9 Radiation intensity. 21
Figure 1.10 Scattering off of plane surface. 24
Figure 2.1 Pillboxes for tangential and normal field relations 31
Figure 3.1 Radial dependence of Re H_ϕ and Im H_ϕ. 50
Figure 3.2 Radial dependence of Re E_r and Im E_r. 50
Figure 3.3 Radial dependence of Re E_θ and Im E_θ. 50
Figure 3.4 Vertical dipole configuration. 56
Figure 3.5 Electric and magnetic field directions. 57
Figure 3.6 Field components relative to reflecting plane. 60
Figure 3.7 Angle of incidence determination. 62
Figure 3.8 A corner-cube antenna. 64
Figure 3.9 Incorrect Image Theorem source placement for corner cube. 65
Figure 3.10 Correct image source placement for the corner cube. 66
Figure 3.11 Image source placement for horizontal dipole. 66
Figure 3.12 Vertical dipole reflection geometry. 71
Figure 3.13 Electric and magnetic infinitesimal dipole superposition, view from above. 77
Figure 3.14 Electric and magnetic infinitesimal dipole superposition, polar plot in ZY plane. 77

Figure 3.15 Polar plot of radiation intensities for some electric z-axis oriented dipoles. 79
Figure 3.16 Double wavelength radiation intensity. 79
Figure 3.17 Log polar plot of radiation intensities for some electric z-axis oriented dipoles. 80
Figure 4.1 A couple Cheybshev plots. 86
Figure 4.2 $T_3(z_0 x)$ for a few different scale factors z_0. 88
Figure 4.3 T_3 fitting of $N = 4$ array in linear and dB scales. 89
Figure 4.4 Plot with $u_0 = 0, d = \lambda/4$. 92
Figure 4.5 Plot with $u_0 = 3.5, d = 0.4\lambda$. 93
Figure 4.6 Plot of $|\mathrm{AF}|^2$ in XY plane with $\alpha = h/\lambda$. 98
Figure 4.7 Polar plot of AF in XY plane for various values of $\alpha = s/\lambda$. 99
Figure 4.8 Polar plot of $|\mathrm{AF}|^2$ for $\theta = 0$. 99
Figure 4.9 Spherical plot of $|\mathrm{AF}|^2$ for $\alpha = 0.69$. 99
Figure 4.10 Plot $|\mathrm{AF}|$ for $ad = 0, \pi/2, \pi, 3\pi/2$. 106
Figure 4.11 Array factor for specified zeros. 108
Figure 4.12 Five element array on z-axis. 109
Figure 4.13 Polar plot of 5 element binomial power array factor. 110
Figure 4.14 Spherical polar plot of 5 element binomial power array factor. 111
Figure 4.15 Zeros of five element Chebyshev and uniform array elements on z-domain unit circle. 114
Figure 4.16 Chebyshev and uniform power array factor in z-x plane (dB). 114
Figure 4.17 5 element Chebyshev array power pattern in 3D. 115
Figure 4.18 Plots of 5 element Chebyshev and uniform array power patterns for $u = kd \sin\theta \cos 0$. 115
Figure 5.1 Electric field power pattern, 0 dB to -40 dB. 121
Figure 5.2 E-H-plane (power) for $\phi = 0$. 121
Figure 5.3 E,H-plane (power) for $\phi = 0$, dB scale. 122
Figure 6.1 Im Z_{in} variation with m. 126
Figure 7.1 Normal reflection and transmission between two media. 129

Figure A.1 Prof. Eleftheriades' handwriting decoder ring. 133

1 FUNDAMENTAL PARAMETERS OF ANTENNAS.

1.1 POYNTING VECTOR.

The Poynting vector was written in an unfamiliar form

$$\mathcal{W} = \mathcal{E} \times \mathcal{H}. \tag{1.1}$$

I can roll with the use of a different symbol (i.e. not $\mathbf{S}$) for the Poynting vector, but I'm used to seeing a $c/4\pi$ factor ([21] and [16]). I remembered something like that in SI units too, so was slightly confused not to see it here.

Per [11] that something is a μ_0, as in

$$\mathcal{W} = \frac{1}{\mu_0} \mathcal{E} \times \mathcal{B}. \tag{1.2}$$

Note that the use of $\mathcal{H}$ instead of $\mathcal{B}$ is what wipes out the requirement for the $1/\mu_0$ term since $\mathcal{H} = \mathcal{B}/\mu_0$, assuming linear media, and no magnetization.

1.2 TYPICAL FAR-FIELD RADIATION INTENSITY.

It was mentioned that

$$\begin{aligned} U(\theta, \phi) &= \frac{r^2}{2\eta_0} \left|\mathbf{E}(r, \theta, \phi)\right|^2 \\ &= \frac{1}{2\eta_0} \left(\left|E_\theta(\theta, \phi)\right|^2 + \left|E_\phi(\theta, \phi)\right|^2 \right), \end{aligned} \tag{1.3}$$

where the intrinsic impedance of free space is

$$\begin{aligned} \eta_0 &= \sqrt{\frac{\mu_0}{\epsilon_0}} \\ &= 377 \Omega. \end{aligned} \tag{1.4}$$

(this is also eq. 2-19 in the text.) To get an understanding where this comes from, consider the far field radial solutions to the electric and magnetic dipole problems, which have the respective forms (from [11]) of

$$\begin{aligned} \mathcal{E} &= -\frac{\mu_0 p_0 \omega^2}{4\pi} \frac{\sin\theta}{r} \cos\left(wt - kr\right) \hat{\boldsymbol{\theta}} \\ \mathcal{B} &= -\frac{\mu_0 p_0 \omega^2}{4\pi c} \frac{\sin\theta}{r} \cos\left(wt - kr\right) \hat{\boldsymbol{\phi}} \end{aligned} \tag{1.5a}$$

$$\begin{aligned} \mathcal{E} &= \frac{\mu_0 m_0 \omega^2}{4\pi c} \frac{\sin\theta}{r} \cos\left(wt - kr\right) \hat{\boldsymbol{\phi}} \\ \mathcal{B} &= -\frac{\mu_0 m_0 \omega^2}{4\pi c^2} \frac{\sin\theta}{r} \cos\left(wt - kr\right) \hat{\boldsymbol{\theta}}. \end{aligned} \tag{1.5b}$$

In neither case is there a component in the direction of propagation, and in both cases (using $\mu_0 \epsilon_0 = 1/c^2$)

$$\begin{aligned} |\mathcal{H}| &= \frac{|\mathcal{E}|}{\mu_0 c} \\ &= |\mathcal{E}| \sqrt{\frac{\epsilon_0}{\mu_0}} \\ &= \frac{1}{\eta_0} |\mathcal{E}|. \end{aligned} \tag{1.6}$$

Note that the signs of $\mathcal{E}$ vs. $\mathcal{B}$ in eq. (1.5a) and eq. (1.5b) and are determined by the far field relation $\mathbf{E} = c\mathbf{B} \times \hat{\mathbf{r}}$ (see: eq. 9.19,9.39 [16]). The effect of dependency is that the Poynting vector will be radial, which will be seen below. A superposition of the phasors for such dipole fields, in the far field, will have the form

$$\begin{aligned} \mathbf{E} &= \frac{1}{r} \left(E_\theta(\theta, \phi) \hat{\boldsymbol{\theta}} + E_\phi(\theta, \phi) \hat{\boldsymbol{\phi}} \right) \\ \mathbf{B} &= \frac{1}{rc} \left(E_\theta(\theta, \phi) \hat{\boldsymbol{\theta}} - E_\phi(\theta, \phi) \hat{\boldsymbol{\phi}} \right), \end{aligned} \tag{1.7}$$

with a corresponding time averaged Poynting vector

$$\begin{aligned} \mathbf{W}_{\mathrm{av}} &= \frac{1}{2\mu_0} \mathbf{E} \times \mathbf{B}^* \\ &= \frac{1}{2\mu_0 c r^2} \left(E_\theta \hat{\boldsymbol{\theta}} + E_\phi \hat{\boldsymbol{\phi}} \right) \times \left(E_\theta^* \hat{\boldsymbol{\theta}} - E_\phi^* \hat{\boldsymbol{\phi}} \right) \\ &= \frac{\hat{\boldsymbol{\theta}} \times \hat{\boldsymbol{\phi}}}{2\mu_0 c r^2} \left(\left|E_\theta\right|^2 + \left|E_\phi\right|^2 \right) \\ &= \frac{\hat{\mathbf{r}}}{2\eta_0 r^2} \left(\left|E_\theta\right|^2 + \left|E_\phi\right|^2 \right), \end{aligned} \tag{1.8}$$

Figure 1.1: Plot methods for fields and intensities.

```
rcap = {Cos[#], Sin[#]} & ;
scap = {Sin[#1] Cos[#2], Sin[#1] Sin[#2], Cos[#1]} & ;
ParametricPlot[ f[r0, θ, 0] rcap, {θ, 0, Pi}]
ParametricPlot3D[ f[r0, θ, ϕ] scap, {θ, 0, Pi}, {ϕ, 0, 2 Pi}]
```

verifying eq. (1.3) for a superposition of electric and magnetic dipole fields. This can likely be shown for more general fields too.

1.3 FIELD PLOTS.

We can plot the fields, or intensity (or log plots in dB of these). It is pointed out in [11] that when there is r dependence these plots are done by considering the values of at fixed r. The field plots are conceptually the simplest, since that vector parameterizes a surface. Any such radial field with magnitude $f(r, \theta, \phi)$ can be plotted in Mathematica in the $\phi = 0$ plane at $r = r_0$, or in 3D (respectively, but also at $r = r_0$) with code like fig. 1.1 Intensity plots can use the same code, with the only difference being the interpretation. The surface doesn't represent the value of a vector valued radial function, but is the magnitude of a scalar valued function evaluated at $f(r_0, \theta, \phi)$.

The surfaces for $U = \cos\theta, \cos^2\theta$ and for $U = \sin\theta, \sin^2\theta$ in the plane are parametrically plotted in fig. 1.2, and for cosines in **??** to compare with textbook figures. Three dimensional visualizations

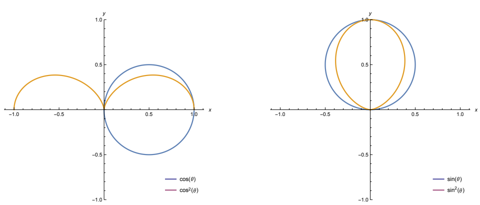

(a) (b)

Figure 1.2: Cosinusoidal and sinusoidal radiation intensities.

Table 1.1: $\int_0^{\pi/2.} \sin^n \theta d\theta = \int_0^{\pi/2} \cos^n \theta d\theta$

n	1	2	3	4	5	6	7
	1	$\pi/4$	$2/3$	$3\pi/16$	$8/15$	$5\pi/32$	$16/35$

Table 1.2: $\int_0^{\pi.} \sin^n \theta d\theta$

n	1	2	3	4	5	6	7
	2	$\pi/2$	$4/3$	$3\pi/8$	$16/15$	$5\pi/16$	$32/35$

of $U = \sin^2 \theta$ and $U = \cos^2 \theta$ can be found in fig. 1.3 Even for such simple functions these look pretty cool.

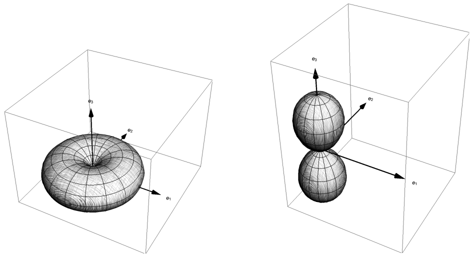

(a) (b)

Figure 1.3: Square sinusoidal and cosinusoidal radiation intensity.

1.4 DB VS DBI.

Note that dBi is used to indicate that the gain is with respect to an "isotropic" radiator. This is detailed more in [7].

1.5 TRIG INTEGRALS.

1.6 POLARIZATION VECTORS.

The text introduces polarization vectors $\hat{\rho}$, but doesn't spell out their form. Consider a plane wave field of the form

$$\mathbf{E} = E_x e^{j\phi_x} e^{j(\omega t - kz)} \hat{\mathbf{x}} + E_y e^{j\phi_y} e^{j(\omega t - kz)} \hat{\mathbf{y}}. \tag{1.9}$$

Table 1.3: $\int_0^{\pi.} \cos^n \theta d\theta$

n	1	2	3	4	5	6	7
	0	$\pi/2$	0	$3\pi/8$	0	$5\pi/16$	0

The x, y plane directionality of this phasor can be written

$$\boldsymbol{\rho} = E_x e^{j\phi_x} \hat{\mathbf{x}} + E_y e^{j\phi_y} \hat{\mathbf{y}}, \tag{1.10}$$

so that

$$\mathbf{E} = \boldsymbol{\rho} e^{j(\omega t - kz)}. \tag{1.11}$$

Separating this direction and magnitude into factors

$$\boldsymbol{\rho} = |\mathbf{E}| \hat{\boldsymbol{\rho}}, \tag{1.12}$$

allows the phasor to be expressed as

$$\mathbf{E} = \hat{\boldsymbol{\rho}} |\mathbf{E}| e^{j(\omega t - kz)}. \tag{1.13}$$

As an example, suppose that $E_x = E_y$, and set $\phi_x = 0$. Then

$$\hat{\boldsymbol{\rho}} = \hat{\mathbf{x}} + \hat{\mathbf{y}} e^{j\phi_y}. \tag{1.14}$$

Demonstrating the geometry. It seems worthwhile to review how a generally polarized field phasor leads to linear, circular, and elliptic geometries.

The most general field polarized in the x, y plane has the form

$$\begin{aligned} \mathbf{E} &= \left(\hat{\mathbf{x}} a e^{j\alpha} + \hat{\mathbf{y}} b e^{j\beta} \right) e^{j(\omega t - kz)} \\ &= \left(\hat{\mathbf{x}} a e^{j(\alpha - \beta)/2} + \hat{\mathbf{y}} b e^{j(\beta - \alpha)/2} \right) e^{j(\omega t - kz + (\alpha + \beta)/2)}. \end{aligned} \tag{1.15}$$

Knowing to factor out the average phase angle above is only because I tried initially without that and things got ugly and messy. I guessed this would help (it does). Let $\mathcal{E} = \operatorname{Re} \mathbf{E} = \hat{\mathbf{x}} x + \hat{\mathbf{y}} y$, $\theta = \omega t + (\alpha + \beta)/2$, and $\phi = (\alpha - \beta)/2$, so that

$$\mathbf{E} = \left(\hat{\mathbf{x}} a e^{j\phi} + \hat{\mathbf{y}} b e^{-j\phi} \right) e^{j\theta}. \tag{1.16}$$

The coordinates can now be read off

$$\frac{x}{a} = \cos\phi\cos\theta - \sin\phi\sin\theta \tag{1.17a}$$

$$\frac{y}{b} = \cos\phi\cos\theta + \sin\phi\sin\theta, \tag{1.17b}$$

or in matrix form

$$\begin{bmatrix} x/a \\ y/b \end{bmatrix} = \begin{bmatrix} \cos\phi & -\sin\phi \\ \cos\phi & \sin\phi \end{bmatrix} \begin{bmatrix} \cos\theta \\ \sin\theta \end{bmatrix}. \tag{1.18}$$

The goal is to eliminate all the θ (i.e. time dependence), converting the parametric relationship into a conic form. Assuming that neither $\cos\theta$, nor $\sin\theta$ are zero for now (those are special cases and lead to linear polarization), inverting the matrix will allow the θ dependence to be eliminated

$$\frac{1}{\sin(2\phi)} \begin{bmatrix} \sin\phi & \sin\phi \\ -\cos\phi & \cos\phi \end{bmatrix} \begin{bmatrix} x/a \\ y/b \end{bmatrix} = \begin{bmatrix} \cos\theta \\ \sin\theta \end{bmatrix}. \tag{1.19}$$

Squaring and summing both rows of these equation gives

$$\begin{aligned} 1 &= \frac{1}{\sin^2(2\phi)} \left(\sin^2\phi \left(\frac{x}{a} + \frac{y}{b} \right)^2 + \cos^2\phi \left(-\frac{x}{a} + \frac{y}{b} \right)^2 \right) \\ &= \frac{1}{\sin^2(2\phi)} \left(\frac{x^2}{a^2} + \frac{y^2}{b^2} + 2\frac{xy}{ab} \left(\sin^2\phi - \cos^2\phi \right) \right) \\ &= \frac{1}{\sin^2(2\phi)} \left(\frac{x^2}{a^2} + \frac{y^2}{b^2} - 2\frac{xy}{ab} \cos(2\phi) \right). \end{aligned} \tag{1.20}$$

Time to summarize and handle the special cases.

1. To have $\cos\phi = 0$, the phase angles must satisfy $\alpha - \beta = (1 + 2k)\pi$, $k \in \mathbb{Z}$. For this case eq. (1.17) reduces to

$$-\frac{x}{a} = \frac{y}{b}, \tag{1.21}$$

which is just a line.

Example 1.1: Linear polarization.

Let $\alpha = 0, \beta = -\pi$, so that the phasor has the value

$$\mathbf{E} = (\hat{\mathbf{x}}a - \hat{\mathbf{y}}b)\, e^{j\omega t}. \tag{1.22}$$

For have $\sin\phi = 0$, the phase angles must satisfy $\alpha - \beta = 2\pi k$, $k \in \mathbb{Z}$. For this case eq. (1.17) reduces to

$$\frac{x}{a} = \frac{y}{b}, \tag{1.23}$$

also just a line.

Example 1.2: Elliptical polarization.

Let $\alpha = \beta = 0$, so that the phasor has the value

$$\mathbf{E} = (\hat{\mathbf{x}}a + \hat{\mathbf{y}}b)\, e^{j\omega t}. \tag{1.24}$$

Last is the circular and elliptically polarized case. The system is clearly elliptically polarized if $\cos(2\phi) = 0$, or $\alpha - \beta = (\pi/2)(1 + 2k), k \in \mathbb{Z}$. When that is the case and $a = b$ also holds, the ellipse is a circle. When the $\cos(2\phi) = 0$ condition does not hold, a rotation of coordinates

$$\begin{bmatrix} x \\ y \end{bmatrix} = \begin{bmatrix} \cos\mu & \sin\mu \\ -\sin\mu & \cos\mu \end{bmatrix} \begin{bmatrix} u \\ v \end{bmatrix}, \tag{1.25}$$

where

$$\mu = \frac{1}{2}\tan^{-1}\left(\frac{2\cos(\alpha - \beta)}{b - a}\right), \tag{1.26}$$

puts the trajectory into a standard (but messy) conic form

$$1 = \frac{u^2}{ab} \left(\frac{b}{a} \cos^2 \mu + \frac{a}{b} \sin^2 \mu + \frac{1}{2} \sin \left(2\mu + \alpha - \beta \right) \right) + \frac{v^2}{ab} \left(\frac{b}{a} \sin^2 \mu + \frac{a}{b} \cos^2 \mu - \frac{1}{2} \sin \left(2\mu + \alpha - \beta \right) \right). \tag{1.27}$$

It isn't obvious to me that the factors of the u^2, v^2 terms are necessarily positive, which is required for the conic to be an ellipse and not a hyperbola.

Example 1.3: Circular polarization.

With $a = b = E_0$, $\alpha = 0$, $\beta = \pm\pi/2$, all the circular polarization conditions are met, leaving the phasor with values

$$\mathbf{E} = E_0 \left(\hat{\mathbf{x}} \pm j \hat{\mathbf{y}} \right) e^{j\omega t}. \tag{1.28}$$

1.7 PHASOR POWER.

In §2.13 the phasor power is written as

$$I^2 R/2, \tag{1.29}$$

where I, R are the magnitudes of phasors in the circuit.

I vaguely recall this relation, but had to refer back to [15] for the details. This relation expresses average power over a period associated with the frequency of the phasor

$$
\begin{aligned}
P &= \frac{1}{T}\int_{t_0}^{t_0+T} p(t)dt \\
&= \frac{1}{T}\int_{t_0}^{t_0+T} |\mathbf{V}|\cos\left(\omega t + \phi_V\right)|\mathbf{I}|\cos\left(\omega t + \phi_I\right)dt \\
&= \frac{1}{T}\int_{t_0}^{t_0+T} |\mathbf{V}||\mathbf{I}|\left(\cos\left(\phi_V - \phi_I\right) + \cos\left(2\omega t + \phi_V + \phi_I\right)\right)dt \\
&= \frac{1}{2}|\mathbf{V}||\mathbf{I}|\cos\left(\phi_V - \phi_I\right).
\end{aligned}
\tag{1.30}
$$

Introducing the impedance for this circuit element

$$
\begin{aligned}
\mathbf{Z} &= \frac{|\mathbf{V}|e^{j\phi_V}}{|\mathbf{I}|e^{j\phi_I}} \\
&= \frac{|\mathbf{V}|}{|\mathbf{I}|}e^{j\left(\phi_V - \phi_I\right)},
\end{aligned}
\tag{1.31}
$$

this average power can be written in phasor form

$$
\mathbf{P} = \frac{1}{2}|\mathbf{I}|^2\mathbf{Z},
\tag{1.32}
$$

with

$$
P = \operatorname{Re}\mathbf{P}.
\tag{1.33}
$$

Observe that we have to be careful to use the absolute value of the current phasor $\mathbf{I}$, since $\mathbf{I}^2$ differs in phase from $|\mathbf{I}|^2$. This explains the conjugation in the [15] definition of complex power, which had the form

$$
\mathbf{S} = \mathbf{V}_{\text{rms}}\mathbf{I}^*_{\text{rms}}.
\tag{1.34}
$$

1.8 RADAR CROSS SECTION EXAMPLES.

Flat plate.

$$
\sigma_{\text{max}} = \frac{4\pi\left(LW\right)^2}{\lambda^2}.
\tag{1.35}
$$

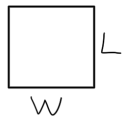

Figure 1.4: Square geometry for RCS example.

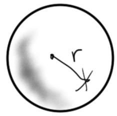

Figure 1.5: Sphere geometry for RCS example.

Sphere. In the optical limit the radar cross section for a sphere

$$\sigma_{\max} = \pi r^2. \tag{1.36}$$

Note that this is smaller than the physical area $4\pi r^2$.

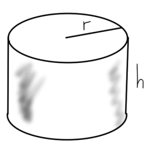

Figure 1.6: Cylinder geometry for RCS example.

Cylinder.

$$\sigma_{\max} = \frac{2\pi r h^2}{\lambda}. \tag{1.37}$$

Tridedral corner reflector.

$$\sigma_{\max} = \frac{4\pi L^4}{3\lambda^2}. \tag{1.38}$$

1.9 SCATTERING FROM A SPHERE VS FREQUENCY.

Frequency dependence of spherical scattering is sketched in fig. 1.8.

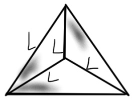

Figure 1.7: Trihedral corner reflector geometry for RCS example.

- Low frequency (or small particles): Rayleigh

$$\sigma = \left(\pi r^2\right) 7.11 \left(\kappa r\right)^4, \qquad \kappa = 2\pi/\lambda.. \tag{1.39}$$

- Mie scattering (resonance),

$$\sigma_{\text{max}}(A) = 4\pi r^2 \tag{1.40}$$

$$\sigma_{\text{max}}(B) = 0.26\pi r^2. \tag{1.41}$$

- optical limit ($r \gg \lambda$)

$$\sigma = \pi r^2. \tag{1.42}$$

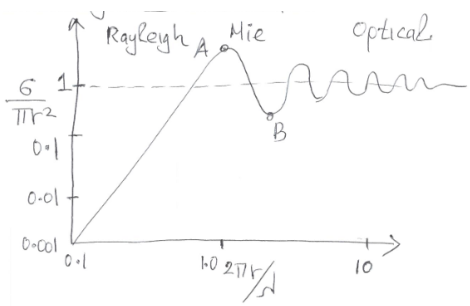

Figure 1.8: Scattering from a sphere vs frequency (from Prof. Eleftheriades' class notes).

FIXME: Do I have a derivation of this in my optics notes?

1.10 EIRP.

Prof. Eleftheriades introduces the term EIRP, the Effective Isotropic Receiving Power, the product of power and gain $P_t G_t$, measured in W.

1.11 FREE SPACE IMPEDANCE.

In class we've seen

$$\eta = \sqrt{\frac{\mu_0}{\epsilon_0}}. \tag{1.43}$$

expressed as $120\pi \approx 377$. It seemed curious to me that this was an exact value. With

- $\epsilon_0 = 8.85 \times 10^{-12}\, \mathrm{C}^2/\mathrm{Nm}^2$ (number from [11])
- $\mu_0 = 4\pi \times 10^{-7} \mathrm{N}/\mathrm{A}^2$ (exact),

the numeric value of η/π is 119.945 (eta.jl), which is close to 120. It's pointed out in [25] that this is just the consequence of using $c = 3 \times 10^8 \mathrm{m/s}$.

This can be seen by writing η in an alternate form

$$\begin{aligned}
\eta &= \frac{1}{c\epsilon_0} \\
&= \mu_0 c \\
&= (4\pi \times 10^{-7} \mathrm{N}/\mathrm{A}^2)(3 \times 10^8 \mathrm{m/s}) \\
&= 120\pi \mathrm{Nm}/\mathrm{A}^2\mathrm{s} \\
&= 120\pi\Omega.
\end{aligned} \tag{1.44}$$

1.12 NOTATION.

- Time average. Both Prof. Eleftheriades and the text [5] use square brackets $[\cdots]$ for time averages, not $\langle \cdots \rangle$. Was that an engineering convention?
- Bold vectors are usually phasors, with (bold) calligraphic script used for the time domain fields. Example: $\mathbf{E}(x, y, z, t) = \hat{\mathbf{e}} E(x, y) e^{j(\omega t - kz)}$, $\mathcal{E}(x, y, z, t) = \mathrm{Re}\, \mathbf{E}$.

1.13 PROBLEMS.

Exercise 1.1 **Max power density and directivity.** (*2015 ps1, p1*)

The power radiated by a lossless antenna is 10 W. The corresponding radiation intensity is given by,

$$U = B_0 \cos^3\theta, \qquad 0 \le \theta < \pi/2, 0 \le \phi < 2\pi. \tag{1.45}$$

Calculate

a. the maximum power density at a distance of 1 km.
b. the directivity of the antenna (dimensionless and dB).

Answer for Exercise 1.1

Part a. The radiated power density is

$$W_r(r,\theta) = \frac{U}{r^2} = \frac{B_0 \cos^3\theta}{r^2}, \qquad W/m^2, \tag{1.46}$$

with the maximum at $\theta = 0$ of

$$W_r(r)|_{\max} = \frac{B_0}{r^2}, \qquad W/m^2. \tag{1.47}$$

Since the average power density is

$$\begin{aligned} P_{av} &= \oiint U d\Omega \\ &= 2\pi B_0 \int_0^{\pi/2} \cos^3\theta \sin\theta d\theta \\ &= -2\pi B_0 \int_0^{\pi/2} \cos^3\theta d\cos\theta \\ &= 2\pi B_0 \left.\frac{\cos^4\theta}{4}\right|_{\pi/2}^{0} \\ &= \frac{\pi B_0}{2} \\ &= 10 \qquad (W), \end{aligned} \tag{1.48}$$

the constant $B_0 = 20/\pi \approx 6.37$W, so the maximum power density at 1 km is

$$W_r(1\,\text{km})|_{\max} = \frac{20}{\pi} \times 10^{-6} \approx 6.37 \times 10^{-6} \qquad (W/m^2). \tag{1.49}$$

Part b. The maximum directivity of the antenna is

$$\begin{aligned} D_0 &= 4\pi \frac{U_{\text{max}}}{P_{\text{rad}}} \\ &= 4\pi \frac{U_{\text{max}}}{P_{\text{av}}} \\ &= \frac{4\cancel{\pi B_0}}{\cancel{\pi B_0}/2} \\ &= 8, \end{aligned} \tag{1.50}$$

so the directivity is

$$D = 8\cos^3\theta. \tag{1.51}$$

In dB the maximum directivity is

$$D_0 = 10\log_{10} 8 = 9\,\text{dB}. \tag{1.52}$$

Exercise 1.2 Directivity and free space loss. (*2015 ps1, p2*)

A satellite dish has a diameter $d = 1.5$m and an aperture efficiency of 70%. Calculate the directivity of the dish at 12 GHz. If the distance from a geostationary satellite is 37,000 km calculate the corresponding free-space loss in dB.

Answer for Exercise 1.2

Ignoring any concavity in the dish (which is probably parabolic, with physical area somewhere between πr^2, and $2\pi^2$), the maximum effective area is

$$\begin{aligned} A_{\text{em}} &= \epsilon_{\text{em}} A_{\text{p}} \\ &= 0.7\pi 0.75^2 \\ &= 0.39\pi \\ &= 1.24\,(\text{m}^2). \end{aligned} \tag{1.53}$$

The maximum directivity is

$$\begin{aligned} D_0 &= \frac{4\pi A_{\text{em}}}{\lambda^2} \\ &= \frac{4\pi A_{\text{em}} \nu^2}{c^2} \\ &= 4\pi \times 1.24\,\text{m}^2 \times \left(12 \times 10^9\,\text{s}^{-1}\right)^2 / \left(3 \times 10^8\,\text{m/s}\right)^2 \\ &= 2.5 \times 10^4. \end{aligned} \tag{1.54}$$

The free-space loss factor at $R = 37 \times 10^6$ m is

$$
\begin{aligned}
\left(\frac{\lambda}{4\pi R}\right)^2 &= \left(\frac{c}{4\pi R\nu}\right)^2 \\
&= \left(\frac{3 \times 10^8\,\mathrm{m/s}}{4\pi\left(37 \times 10^6\,\mathrm{m}\right)\left(12 \times 10^9\,\mathrm{s}^{-1}\right)}\right)^2 \\
&= 2.9 \times 10^{-21} \\
&= -205\,\mathrm{dB}.
\end{aligned}
\tag{1.55}
$$

Exercise 1.3 Approximating directivity. (*2015 ps1, p3*)

A beam antenna has half-power beamwidths of 30° and 35° in orthogonal planes intersecting at the maximum of the mainbeam. Determine the approximate maximum directivity

Answer for Exercise 1.3

$$
\begin{aligned}
D_0 &\approx \frac{4\pi}{\Theta_{1r}\Theta_{2r}} \\
&= \frac{4 \times 180^2}{\pi(30)(35)} \\
&= 39.3.
\end{aligned}
\tag{1.56}
$$

Exercise 1.4 Polarization power loss. (*2015 ps1, p4*)

Transmitting and receiving antennas operating at 1 GHz have gains of 20 and 15 dB respectively and are separated by a distance of 1 km. Find the power delivered to a matched load when the input power is 150 W and when

a. both antennas are polarization matched.
b. One antenna is linearly polarized and the other is circularly polarized.

Answer for Exercise 1.4

Part a. Answering this requires an application of the Friis transmission equation. First note that the gains in non-dB units are

$$G_1 = 10^{20/10}, \tag{1.57a}$$

$$G_2 = 10^{15/10}. \tag{1.57b}$$

The wavelength is

$$\begin{aligned}\lambda &= \frac{c}{\nu} \\ &= \frac{3 \times 10^8\,\mathrm{m/s}}{10^9\,\mathrm{s}^{-1}} \\ &= 0.3\,\mathrm{m}.\end{aligned} \tag{1.58}$$

From the Friis equation, the receiving antenna has power

$$\begin{aligned}P_\mathrm{r} &= P_\mathrm{t} \left(\frac{\lambda}{4\pi R}\right)^2 G_1 G_2 \\ &= 150\,\mathrm{W} \left(\frac{0.3\,\mathrm{m}}{4\pi(10^3\,\mathrm{m})}\right)^2 10^{3.5} \\ &= 0.27\,\mathrm{mW}.\end{aligned} \tag{1.59}$$

Part b. Suppose that the linear polarization vector is

$$\hat{\boldsymbol{\rho}}_1 = \hat{\mathbf{x}}, \tag{1.60}$$

and the circular polarization vector is

$$\hat{\boldsymbol{\rho}}_2 = \frac{1}{\sqrt{2}} \left(\hat{\mathbf{x}} + j\hat{\mathbf{y}}\right). \tag{1.61}$$

The polarization factor is

$$\left|\hat{\boldsymbol{\rho}}_1 \cdot \hat{\boldsymbol{\rho}}_2\right|^2 = \frac{1}{2}, \tag{1.62}$$

so the power found in eq. (1.59) must be reduced by 50 % when there is a linear vs. circular polarization mismatch. Rotating one of these polarization vectors, say the linear polarization vector, does not change the result. For example, let

$$\hat{\boldsymbol{\rho}}_1 = \frac{1}{\sqrt{a^2 + b^2}} \left(a\hat{\mathbf{x}} + b\hat{\mathbf{y}}\right). \tag{1.63}$$

The polarization factor is now

$$\begin{aligned}\left|\hat{\boldsymbol{\rho}}_1 \cdot \hat{\boldsymbol{\rho}}_2\right|^2 &= \left|\frac{a}{\sqrt{2(a^2+b^2)}} + \frac{jb}{\sqrt{2(a^2+b^2)}}\right|^2 \\ &= \frac{1}{2(a^2+b^2)} \left(a^2 + b^2\right) \\ &= \frac{1}{2},\end{aligned} \tag{1.64}$$

yielding the same factor of two reduction in power.

Exercise 1.5 Transmission power determination. (*2015 ps1, p5*)

A repeater link consists of a transmitter and a receiver at 10 GHz in a line-of-sight arrangement of distance 10km. The transmitting and receiving antennas are identical horns with gain over isotropic equal to 15 dB. For acceptable signal-to-noise ratio, the power received must be greater than 10 nW. Loss due to polarization mismatch is not expected to exceed 3 dB. Determine the minimum transmitted power that should be used.

Answer for Exercise 1.5

This is another Friis equation application. Each of the respective gains (converted from dB) are

$$G = 10^{15/10}\,\mathrm{W}. \tag{1.65}$$

The polarization loss factor is

$$\left|\hat{\boldsymbol{\rho}}_\mathrm{r} \cdot \hat{\boldsymbol{\rho}}_\mathrm{t}\right|^2 \le 10^{-3/10}. \tag{1.66}$$

The wavelength is

$$\begin{aligned}\lambda &= \frac{3 \times 10^8\,\mathrm{m/s}}{10^{10}\,\mathrm{s}^{-1}} \\ &= 3 \times 10^{-2}\,\mathrm{m}.\end{aligned} \tag{1.67}$$

Put together we are looking for a value of P_t at least that of

$$\begin{aligned}\frac{P_\mathrm{r}}{P_\mathrm{t}} &= \frac{10^{-8}\,\mathrm{W}}{P_\mathrm{t}} \\ &= \left(\frac{0.03\,\mathrm{m}}{4\pi 10^4\,\mathrm{m}}\right)^2 \left(10^{3/2}\right)^2 10^{-0.3} \\ &= 2.9 \times 10^{-11},\end{aligned} \tag{1.68}$$

or

$$P_\mathrm{t} \ge 350\,\mathrm{W}. \tag{1.69}$$

Exercise 1.6 Radar cross section. (*2015 ps1, p6*)

A rectangular X-band horn, with aperture dimensions 5.5cm × 7.4cm and a gain of 16.3 dB at 10 GHz, transmits and receives power scattered by the objects specified below. In each case, determine the maximum scattered power delivered to the load when the distance between the horn and scattering object is $n\lambda$, where n is

1. 200
2. 500.

The scattering objects to consider are a perfectly conducting

a. sphere of radius $a = 5\lambda$,

b. plate of dimensions $10\lambda \times 10\lambda$.

Answer for Exercise 1.6

This is an application of the Radar Cross Section equation

$$\begin{aligned} \frac{P_\mathrm{r}}{P_\mathrm{t}} &= \sigma \frac{G^2}{4\pi} \left(\frac{\lambda}{4\pi n^2 \lambda^2} \right)^2 \\ &= \sigma \frac{G^2}{4\pi} \left(\frac{1}{4\pi n^2 \lambda} \right)^2 . \end{aligned} \tag{1.70}$$

The same gain is used for transmission and reception, since both are for the same horn. That gain (not in dB) is

$$\begin{aligned} G &= 10^{16.3/10} \\ &= 43. \end{aligned} \tag{1.71}$$

The wavelength is

$$\begin{aligned} \lambda &= \frac{3 \times 10^8 \,\mathrm{m/s}}{10^{10}\,\mathrm{m}} \\ &= 0.03\,\mathrm{m}. \end{aligned} \tag{1.72}$$

Part a. For the sphere the scattering area is

$$\begin{aligned} \sigma &= \pi r^2 \\ &= \pi (5\lambda)^2 \\ &= 25\pi\lambda^2, \end{aligned} \tag{1.73}$$

so the ratio of delivered power to the transmitted power is

$$\begin{aligned}\frac{P_r}{P_t} &= 25\pi\lambda^2 \frac{G^2}{4\pi}\left(\frac{1}{4\pi n^2 \lambda}\right)^2 \\ &= \frac{25(43)^2}{64\pi^2 n^4} \\ &= \frac{73}{n^4}.\end{aligned} \tag{1.74}$$

For the $n = 200, 500$ cases respectively, the delivered power ratio is

1. $n = 200$

$$\begin{aligned}\frac{P_r}{P_t} &= \frac{73}{200^4} \\ &= 4.6 \times 10^{-8}.\end{aligned} \tag{1.75}$$

2. $R = 500\lambda$

$$\begin{aligned}\frac{P_r}{P_t} &= \frac{73}{500^4} \\ &= 1.2 \times 10^{-9}.\end{aligned} \tag{1.76}$$

Part b. For the plate the scattering area is

$$\begin{aligned}\sigma &= 4\pi \frac{(LW)^2}{\lambda^2} \\ &= 4\pi \frac{\left(100\lambda^2\right)^2}{\lambda^2} \\ &= 4\pi\lambda^2 \times 10^4,\end{aligned} \tag{1.77}$$

so the ratio of delivered power to the transmitted power is

$$\begin{aligned}\frac{P_r}{P_t} &= 4\pi\lambda^2 \times 10^4 \frac{G^2}{4\pi}\left(\frac{1}{4\pi n^2 \lambda}\right)^2 \\ &= \frac{(43)^2 \times 10^4}{16\pi^2 n^4} \\ &= \frac{1.2 \times 10^5}{n^4}.\end{aligned} \tag{1.78}$$

For the $n = 200, 500$ cases respectively, the delivered power ratio is

1. $n = 200$

$$\frac{P_r}{P_t} = \frac{1.2 \times 10^5}{200^4} = 7.3 \times 10^{-5}. \tag{1.79}$$

2. $R = 500\lambda$

$$\frac{P_r}{P_t} = \frac{1.2 \times 10^5}{500^4} = 1.9 \times 10^{-6}. \tag{1.80}$$

Exercise 1.7 **Directivities for a short horizontal electrical dipole.**

In [24] a field for which directivities can be calculated exactly was used in comparisons of some directivity approximations

$$\mathbf{E} = E_0 \left(\cos\theta \cos\phi \hat{\boldsymbol{\theta}} - \sin\phi \hat{\boldsymbol{\phi}}\right). \tag{1.81}$$

(Observe that an inverse radial dependence in E_0 must be implied here for this to be a valid far-field representation of the field.)

Show that Tai & Pereira's formula gives $D_1 = 3$, and $D_2 = 1$ respectively for this field.

Calculate the exact directivity for this field.

Answer for Exercise 1.7

The field components are

$$E_\theta = E_0 \cos\theta \cos\phi, \tag{1.82a}$$

$$E_\phi = -E_0 \sin\phi. \tag{1.82b}$$

Using eq. (1.91) from the paper, the directivities are

$$\begin{aligned} D_1 &= \frac{2}{\int_0^\pi \cos^2\theta \sin\theta d\theta} \\ &= \frac{2}{-\frac{1}{3}\cos^3\theta\Big|_0^\pi} \\ &= 3, \end{aligned} \tag{1.83}$$

and

$$\begin{aligned} D_2 &= \frac{2}{\int_0^\pi \sin\theta d\theta} \\ &= \frac{2}{-\cos\theta|_0^\pi} \\ &= 1. \end{aligned} \tag{1.84}$$

To find the exact directivity, first the Poynting vector is required. That is

$$\begin{aligned} \mathbf{P} &= \frac{|E_0|^2}{2c\mu_0}\left(\cos\theta\cos\phi\hat{\boldsymbol{\theta}} - \sin\phi\hat{\boldsymbol{\phi}}\right) \times \left(\hat{\mathbf{r}} \times \left(\cos\theta\cos\phi\hat{\boldsymbol{\theta}} - \sin\phi\hat{\boldsymbol{\phi}}\right)\right) \\ &= \frac{|E_0|^2}{2c\mu_0}\left(\cos\theta\cos\phi\hat{\boldsymbol{\theta}} - \sin\phi\hat{\boldsymbol{\phi}}\right) \times \left(\cos\theta\cos\phi\hat{\boldsymbol{\phi}} + \sin\phi\hat{\boldsymbol{\theta}}\right) \\ &= \frac{|E_0|^2\hat{\mathbf{r}}}{2c\mu_0}\left(\cos^2\theta\cos^2\phi + \sin^2\phi\right), \end{aligned} \tag{1.85}$$

so the radiation intensity is

$$U(\theta,\phi) \propto \cos^2\theta\cos^2\phi + \sin^2\phi. \tag{1.86}$$

The $\hat{\boldsymbol{\theta}}$, and $\hat{\boldsymbol{\phi}}$ contributions to this intensity, and the total intensity are all plotted in fig. 1.9

FIXME: did I save these under the right paths? Recall thetacap and phicap reversed.

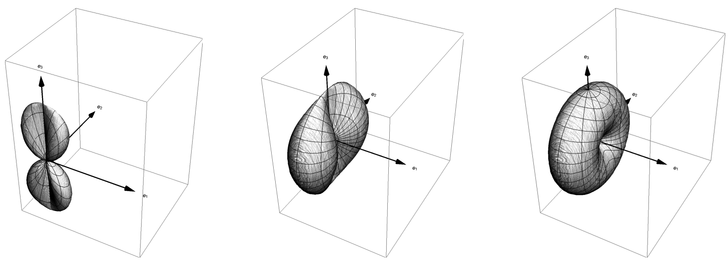

(a) (b) (c)

Figure 1.9: Radiation intensity.

Given this the total radiated power is

$$\begin{aligned} P_{\text{rad}} &= \int_0^{2\pi}\int_0^{\pi} \left(\cos^2\theta\cos^2\phi + \sin^2\phi\right)\sin\theta d\theta d\phi \\ &= \frac{8\pi}{3}. \end{aligned} \tag{1.87}$$

Observe that the radiation intensity U can also be decomposed into two components, one for each component of the original **E** phasor.

$$U_\theta = \cos^2\theta\cos^2\phi, \tag{1.88a}$$

$$U_\phi = \sin^2\phi. \tag{1.88b}$$

This decomposition allows for expression of the partial directivities in these respective (orthogonal) directions

$$D_\theta = \frac{4\pi U_\theta}{P_{\text{rad}}} = \frac{3}{2}\cos^2\theta\cos^2\phi, \tag{1.89a}$$

$$D_\phi = \frac{4\pi U_\phi}{P_{\text{rad}}} = \frac{3}{2}\sin^2\phi. \tag{1.89b}$$

The maximum of each of these partial directivities is both $3/2$, giving a maximum directivity of

$$D_0 = D_\theta\big|_{\text{max}} + D_\phi\big|_{\text{max}} = 3, \tag{1.90}$$

the exact value from the paper.

Exercise 1.8 E and H plane directivities.

In [24] directivities associated with the half power beamwidths are given as

$$D_1 = \frac{\left|E_\theta\right|^2_{\text{max}}}{\frac{1}{2}\int_0^\pi \left|E_\theta(\theta,0)\right|^2\sin\theta d\theta}, \tag{1.91a}$$

$$D_2 = \frac{\left|E_\phi\right|^2_{\text{max}}}{\frac{1}{2}\int_0^\pi \left|E_\phi(\theta,\pi/2)\right|^2\sin\theta d\theta}, \tag{1.91b}$$

whereas [5] lists these as

$$\frac{1}{D_1} = \frac{1}{2\ln 2}\int_0^{\Theta_{1r}/2} \sin\theta d\theta, \tag{1.92a}$$

$$\frac{1}{D_2} = \frac{1}{2\ln 2}\int_0^{\Theta_{2r}/2} \sin\theta d\theta. \tag{1.92b}$$

Reconcile these pairs of relations.

Answer for Exercise 1.8

TODO.

Exercise 1.9 Radar cross section. (*2015 ps2, p1*)

Consider a flat rectangular metallic plate of physical area A_p (m^2). The incident normal power density is W_i ($\mathrm{W/m}^2$). Now consider the plate as a receiving and re-transmitting antenna having an effective aperture equal to its physical area (the plate is electrically large). Based on this idea, show that approximately the radar scattering cross section (RCS) of the plate is given by

$$\sigma = \frac{4\pi A_\mathrm{p}^2}{\lambda^2}, \tag{1.93}$$

as we have seen in class.

Answer for Exercise 1.9

A few simplifying assumptions are required to show this result:

1. All the power received is re-radiated as if from a point source.
2. The plate is a perfectly efficient re-radiator.
3. The effective aperture A_eff is also the maximum effective aperture, so it (and the directivity) has no directional dependence.

The scattering geometry for this problem is sketched in fig. 1.10. First note that the definition of the radar cross section σ is

$$\sigma \equiv \lim_{R\to\infty} 4\pi R^2 \frac{W_s}{W_i}, \tag{1.94}$$

where W_s is the scattered power density, W_i is the incident power density, and R is the distance from the scattering object to the

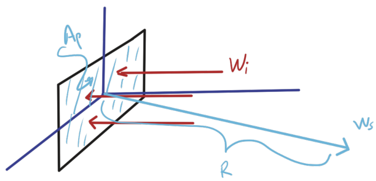

Figure 1.10: Scattering off of plane surface.

measurement point. Without the point source approximation for the re-radiation of the incident power, this quantity would depend on the orientation of the plate with respect to the observation.

With constant normal incident power density, the captured power is

$$P_c = W_i A_p, \tag{1.95}$$

where A_p is the area of the plate. Treating all the power as radiated as if from a point source, measured at distance R from the plate, and assuming a perfect radiator (i.e. $G = D_0$), the scattered power density at this point of observation is

$$W_s = \frac{P_c G}{4\pi R^2} = \frac{P_c D_0}{4\pi R^2}. \tag{1.96}$$

The directivity follows from the assumption that the effective area equals the physical area, since that means

$$A_{\text{eff}} \equiv \frac{\lambda^2 D_0}{4\pi} = A_p, \tag{1.97}$$

so

$$D_0 = \frac{4\pi A_p}{\lambda^2}. \tag{1.98}$$

The scattered power density at the receiver is

$$\begin{aligned} W_s &= \frac{P_c}{4\pi R^2} D_0 \\ &= \frac{W_i A_p}{4\pi R^2} \frac{4\pi A_p}{\lambda^2}. \end{aligned} \tag{1.99}$$

Plugging this into eq. (1.94), and dropping the limit that becomes irrelevant, gives

$$\begin{aligned}\sigma &= \cancel{4\pi R^2} \frac{\cancel{W_i} A_p}{\cancel{4\pi R^2}} \frac{4\pi A_p}{\lambda^2} \frac{1}{\cancel{W_i}} \\ &= \frac{4\pi A_p^2}{\lambda^2},\end{aligned} \tag{1.100}$$

as desired.

Exercise 1.10 Testing antenna gain. (*2015 ps2, p2*)

One way to measure the absolute gain of an antenna under test (AUT) is to use a "standard-gain" antenna (usually a horn) which has a known gain G_{sg}. Consider a two antenna setup, where port #1 is connected to a transmitting antenna G_{x}. First, the second antenna connected to port #2 is the standard-gain one. Then at port #2 we connect the unknown antenna under test G_{AUT}. Show that,

$$\frac{P_2^{\mathrm{AUT}}}{P_2^{\mathrm{sg}}} = \frac{G_{\mathrm{AUT}}}{G_{\mathrm{sg}}}, \tag{1.101}$$

where the left-hand side of the above equation represents the ratio of the powers received by the antenna under test and the standard-gain antenna.

Answer for Exercise 1.10

The Friis equation can be used for this measurement task. For the respective set of antenna configurations, and for fixed transmission power, there are two such equations

$$\frac{P_2^{\mathrm{AUT}}}{P_t} = \left(\frac{\lambda}{4\pi R}\right)^2 G_{\mathrm{AUT}} G_{\mathrm{t}}, \tag{1.102a}$$

$$\frac{P_2^{\mathrm{sg}}}{P_t} = \left(\frac{\lambda}{4\pi R}\right)^2 G_{\mathrm{sg}} G_{\mathrm{t}}, \tag{1.102b}$$

where the transmission power is P_t and transmission antenna gain is G_{t}. That transmit antenna power and gain need not be known, since dividing these equations cancels the common factors, including those, leaving

$$\frac{P_2^{\mathrm{AUT}}}{P_2^{\mathrm{sg}}} = \frac{G_{\mathrm{AUT}}}{G_{\mathrm{sg}}}, \tag{1.103}$$

as desired.

This procedure assumes that the standard gain antenna and the antenna under test have identical polarization, and that neither is orthogonally polarized with respect to the antenna at port #1.

2 MAXWELL'S EQUATIONS.

2.1 REVIEW.

For reasons that are yet to be seen (and justified), we work with a generalization of Maxwell's equations to include electric AND magnetic charge densities.

$$\boldsymbol{\nabla} \times \mathcal{E} = -\mathcal{M} - \frac{\partial \mathcal{B}}{\partial t} \tag{2.1a}$$

$$\boldsymbol{\nabla} \times \mathcal{H} = \mathcal{J} + \frac{\partial \mathcal{D}}{\partial t} \tag{2.1b}$$

$$\boldsymbol{\nabla} \cdot \mathcal{D} = q_{\mathrm{e}} \tag{2.1c}$$

$$\boldsymbol{\nabla} \cdot \mathcal{B} = q_{\mathrm{m}}. \tag{2.1d}$$

Assuming a phasor relationships of the form $\mathcal{E} = \operatorname{Re}\left(\mathbf{E}(\mathbf{r})e^{j\omega t}\right)$ for the fields and the currents, these reduce to

$$\boldsymbol{\nabla} \times \mathbf{E} = -\mathbf{M} - j\omega\mathbf{B} \tag{2.2a}$$

$$\boldsymbol{\nabla} \times \mathbf{H} = \mathbf{J} + j\omega\mathbf{D} \tag{2.2b}$$

$$\boldsymbol{\nabla} \cdot \mathbf{D} = \rho \tag{2.2c}$$

$$\boldsymbol{\nabla} \cdot \mathbf{B} = \rho_{\mathrm{m}}. \tag{2.2d}$$

In engineering the fields

- $\mathcal{E}(\mathbf{x}, t)$: Electric field intensity [V/m] (Volts/meter)
- $\mathcal{H}(\mathbf{x}, t)$: Magnetic field intensity [A/m] (Amperes/meter)

are designated the primary fields, whereas

- $\mathcal{D}(\mathbf{x}, t)$: Electric flux density (or displacement vector) [C/m] (Coulombs/meter)
- $\mathcal{B}(\mathbf{x}, t)$: Magnetic flux density [W/m^2] (Webers/square meter)

are designated the induced fields. The currents and charges are

- $\mathcal{J}(\mathbf{x}, t)$: Electric current density [A/m^2] (Amperes/square meter)
- $\mathcal{M}(\mathbf{x}, t)$: Magnetic current density [V/m^2] (Volts/square meter)
- $q_{\mathrm{e}}(\mathbf{x}, t)$: Electric charge density [C/m^3] (Coulombs/cubic meter)
- $q_{\mathrm{m}}(\mathbf{x}, t)$: Magnetic charge density [W/m^3] (Webers/cubic meter)

Because $\boldsymbol{\nabla} \cdot (\boldsymbol{\nabla} \times \mathbf{f}) = 0$ for any (sufficiently continuous) vector $\mathbf{f}$, divergence relations between the currents and the charges follow from eq. (2.2)

$$\begin{aligned} 0 &= -\boldsymbol{\nabla} \cdot \mathbf{M} - j\omega \boldsymbol{\nabla} \cdot \mathbf{B} \\ &= -\boldsymbol{\nabla} \cdot \mathbf{M} - j\omega \rho_{\mathrm{m}}, \end{aligned} \tag{2.3}$$

and

$$\begin{aligned} 0 &= \boldsymbol{\nabla} \cdot \mathbf{J} + j\omega \boldsymbol{\nabla} \cdot \mathbf{D} \\ &= \boldsymbol{\nabla} \cdot \mathbf{J} + j\omega \rho, \end{aligned} \tag{2.4}$$

These are the phasor forms of the continuity equations

$$\boldsymbol{\nabla} \cdot \mathbf{M} = -j\omega \rho_{\mathrm{m}} \tag{2.5a}$$

$$\boldsymbol{\nabla} \cdot \mathbf{J} = -j\omega \rho. \tag{2.5b}$$

Integral forms. The integral forms of Maxwell's equations follow from Stokes' theorem and the divergence theorems. Stokes' theorem is a relation between the integral of the curl and the outwards normal differential area element of a surface, to the boundary of that surface, and applies to any surface with that boundary

$$\iint d\mathbf{A} \cdot (\boldsymbol{\nabla} \times \mathbf{f}) = \oint \mathbf{f} \cdot d\mathbf{l}. \tag{2.6}$$

The divergence theorem, a special case of the general Stokes' theorem is

$$\iiint_V \boldsymbol{\nabla} \cdot \mathbf{f}\, dV = \iint_{\partial V} \mathbf{f} \cdot d\mathbf{A}, \tag{2.7}$$

where the integral is over the surface of the volume, and the area element of the bounding integral has an outwards normal orientation.

See [20] for a derivation of this and various generalizations. Applying these to eq. (2.2) gives

$$\oint d\mathbf{l} \cdot \mathbf{E} = -\iint d\mathbf{A} \cdot \left(\mathbf{M} + j\omega \mathbf{B} \right) \tag{2.8a}$$

$$\oint d\mathbf{l} \cdot \mathbf{H} = \iint d\mathbf{A} \cdot \left(\mathbf{J} + j\omega \mathbf{D} \right) \tag{2.8b}$$

$$\iint_{\partial V} d\mathbf{A} \cdot \mathbf{D} = \iiint \rho\, dV \tag{2.8c}$$

$$\iint_{\partial V} d\mathbf{A} \cdot \mathbf{B} = \iiint \rho_{\mathrm{m}}\, dV. \tag{2.8d}$$

2.2 CONSTITUTIVE RELATIONS.

For linear isotropic homogeneous materials, the following constitutive relations apply

- $\mathbf{D} = \epsilon \mathbf{E}$
- $\mathbf{B} = \mu \mathbf{H}$

- $\mathbf{J} = \sigma \mathbf{E}$, Ohm's law.

where

- $\epsilon = \epsilon_r \epsilon_0$, is the permittivity (F/m, Farads/meter).
- $\mu = \mu_r \mu_0$, is the permeability (H/m, Henries/meter), $\mu_0 = 4\pi \times 10^{-7}$.
- σ, is the conductivity ($\frac{1}{\Omega \mathrm{m}}$, where $1/\Omega$ is a Siemens.)

In AM radio, will see ferrite cores with the inductors, which introduces non-unit μ_r. This is to increase the radiation resistance.

2.3 BOUNDARY CONDITIONS.

For good electric conductor $\mathbf{E} = 0$. For good magnetic conductor $\mathbf{B} = 0$.

(more on class slides)

2.4 LINEAR TIME INVARIANT.

Linear time invariant meant that the impulse response $h(t, t')$ was a function of just the difference in times $h(t, t') = h(t - t')$.

2.5 GREEN'S FUNCTIONS.

For electromagnetic problems the impulse function sources $\delta(\mathbf{r} - \mathbf{r}')$ also has a direction, and can yield any of E_x, E_y, E_z. A tensor impulse response is required. Some overview of an approach that uses such tensor Green's functions is outlined on the slides. It gets really messy since we require four tensor Green's functions to handle electric and magnetic current and charges. Because of this complexity, we don't go down this path, and use potentials instead.

In §3.5 [5] and the class notes, a verification of the spherical wave form for the Helmholtz Green's function was developed. This was much simpler than the same verification I did in [19]. Part of the reason for that was that I worked in Cartesian coordinates, which made things much messier. The other part of the reason, for treating a neighbourhood of $|\mathbf{r} - \mathbf{r}'| \sim 0$, I verified the convolution, whereas Prof. Eleftheriades argues that a verification that $\int \left(\boldsymbol{\nabla}^2 + k^2\right) G(\mathbf{r}, \mathbf{r}') dV' = 1$ is sufficient. Balanis, on the other hand, argues that knowing the solution for $k \neq 0$ must just be the solution for $k = 0$ (i.e. the Poisson solution) provided it is multiplied by the e^{-jkr} factor. Note that back when I did that derivation, I used a different sign convention for the Green's function, and in QM we used a positive sign instead of the negative in e^{-jkr}.

2.6 TANGENTIAL AND NORMAL FIELD COMPONENTS.

The integral forms of Maxwell's equations can be used to derive relations for the tangential and normal field components to the sources. These relations were mentioned in class, but it is useful to go over the derivation. This isn't all review from first year electromagnetism since we are now using a magnetic source modifications of Maxwell's equations. The derivation below follows that of [3] closely, but I am trying it myself to ensure that I understand the assumptions.

The two infinitesimally thin pillboxes of fig. 2.1 are used in the argument. Maxwell's equations with both magnetic and electric

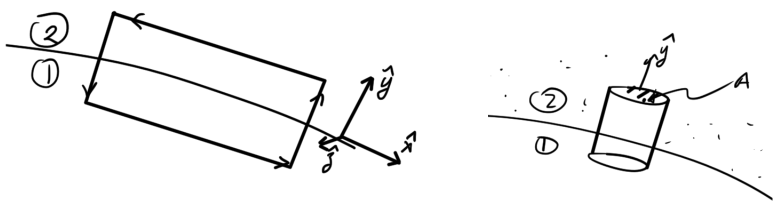

(a) (b)

Figure 2.1: Pillboxes for tangential and normal field relations

sources are

$$\boldsymbol{\nabla} \times \boldsymbol{\mathcal{E}} = -\frac{\partial \boldsymbol{\mathcal{B}}}{\partial t} - \boldsymbol{\mathcal{M}} \tag{2.9a}$$

$$\boldsymbol{\nabla} \times \boldsymbol{\mathcal{H}} = \boldsymbol{\mathcal{J}} + \frac{\partial \boldsymbol{\mathcal{D}}}{\partial t} \tag{2.9b}$$

$$\boldsymbol{\nabla} \cdot \mathcal{D} = \rho_{\mathrm{e}} \tag{2.9c}$$

$$\boldsymbol{\nabla} \cdot \mathcal{B} = \rho_{\mathrm{m}}. \tag{2.9d}$$

After application of Stokes' and the divergence theorems Maxwell's equations have the integral form

$$\oint \mathcal{E} \cdot d\mathbf{l} = -\int d\mathbf{A} \cdot \left(\frac{\partial \mathcal{B}}{\partial t} + \mathcal{m} \right) \tag{2.10a}$$

$$\oint \mathcal{H} \cdot d\mathbf{l} = \int d\mathbf{A} \cdot \left(\frac{\partial \mathcal{D}}{\partial t} + \mathcal{J} \right) \tag{2.10b}$$

$$\int_{\partial V} \mathcal{D} \cdot d\mathbf{A} = \int_V \rho_{\mathrm{e}} \, dV \tag{2.10c}$$

$$\int_{\partial V} \mathcal{B} \cdot d\mathbf{A} = \int_V \rho_{\mathrm{m}} \, dV. \tag{2.10d}$$

Maxwell-Faraday equation. First consider one of the loop integrals, like eq. (2.10a). For an infinitesimal loop, that integral is

$$\begin{aligned}\oint \mathcal{E} \cdot d\mathbf{l} &\approx \mathcal{E}_x^{(1)} \Delta x + \mathcal{E}^{(1)} \frac{\Delta y}{2} + \mathcal{E}^{(2)} \frac{\Delta y}{2} - \mathcal{E}_x^{(2)} \Delta x - \mathcal{E}^{(2)} \frac{\Delta y}{2} - \mathcal{E}^{(1)} \frac{\Delta y}{2} \\ &\approx \left(\mathcal{E}_x^{(1)} - \mathcal{E}_x^{(2)} \right) \Delta x + \frac{1}{2} \frac{\partial \mathcal{E}^{(2)}}{\partial x} \Delta x \Delta y + \frac{1}{2} \frac{\partial \mathcal{E}^{(1)}}{\partial x} \Delta x \Delta y.\end{aligned} \tag{2.11}$$

We let $\Delta y \rightarrow 0$ which kills off all but the first difference term.

The RHS of eq. (2.11) is approximately

$$-\int d\mathbf{A} \cdot \left(\frac{\partial \mathcal{B}}{\partial t} + \mathcal{m} \right) \approx -\Delta x \Delta y \left(\frac{\partial \mathcal{B}_z}{\partial t} + \mathcal{m}_z \right). \tag{2.12}$$

If the magnetic field contribution is assumed to be small in comparison to the magnetic current (i.e. infinite magnetic conductance), and if a linear magnetic current source of the form is also assumed

$$\mathcal{M}_s = \lim_{\Delta y \to 0} (\mathcal{M} \cdot \hat{\mathbf{z}})\, \hat{\mathbf{z}} \Delta y, \tag{2.13}$$

then the Maxwell-Faraday equation takes the form

$$\left(\mathcal{E}_x^{(1)} - \mathcal{E}_x^{(2)} \right) \Delta x \approx -\Delta x \mathcal{M}_s \cdot \hat{\mathbf{z}}. \tag{2.14}$$

While $\mathcal{M}$ may have components that are not normal to the interface, the surface current need only have a normal component, since only that component contributes to the surface integral.

The coordinate expression of eq. (2.14) can be written as

$$\begin{aligned} -\mathcal{M}_s \cdot \hat{\mathbf{z}} &= \left(\boldsymbol{\mathcal{E}}^{(1)} - \boldsymbol{\mathcal{E}}^{(2)} \right) \cdot (\hat{\mathbf{y}} \times \hat{\mathbf{z}}) \\ &= \left(\left(\boldsymbol{\mathcal{E}}^{(1)} - \boldsymbol{\mathcal{E}}^{(2)} \right) \times \hat{\mathbf{y}} \right) \cdot \hat{\mathbf{z}}. \end{aligned} \tag{2.15}$$

This is satisfied when

$$\boxed{\left(\boldsymbol{\mathcal{E}}^{(1)} - \boldsymbol{\mathcal{E}}^{(2)} \right) \times \hat{\mathbf{n}} = -\mathcal{M}_s,} \tag{2.16}$$

where $\hat{\mathbf{n}}$ is the normal between the interfaces. I'd failed to understand when reading this derivation initially, how the $\mathcal{B}$ contribution was killed off. i.e. If the vanishing area in the surface integral kills off the $\mathcal{B}$ contribution, why do we have a $\mathcal{M}$ contribution left. The key to this is understanding that this magnetic current is considered to be confined very closely to the surface getting larger as Δy gets smaller.

Also note that the units of $\mathcal{M}_s$ are volts/meter like the electric field (not volts/squared-meter like $\mathcal{M}$.)

Ampere's law. As above, assume a linear electric surface current density of the form

$$\mathcal{J}_s = \lim_{\Delta y \to 0} (\mathcal{J} \cdot \hat{\mathbf{n}})\, \hat{\mathbf{n}} \Delta y, \tag{2.17}$$

in units of amperes/meter (not amperes/meter-squared like $\mathcal{J}$.)

To apply the arguments above to Ampere's law, only the sign needs to be adjusted

$$\boxed{\left(\mathcal{H}^{(1)} - \mathcal{H}^{(2)}\right) \times \hat{\mathbf{n}} = \mathcal{J}_s.} \tag{2.18}$$

Gauss's law. Using the cylindrical pillbox surface with radius Δr, height Δy, and top and bottom surface areas $\Delta A = \pi \left(\Delta r\right)^2$, the LHS of Gauss's law eq. (2.10c) expands to

$$\begin{aligned}\int_{\partial V} \mathcal{D} \cdot d\mathbf{A} &\approx \mathcal{D}_y^{(2)} \Delta A + \mathcal{D}_\rho^{(2)} 2\pi \Delta r \frac{\Delta y}{2} + \mathcal{D}_\rho^{(1)} 2\pi \Delta r \frac{\Delta y}{2} - \mathcal{D}_y^{(1)} \Delta A \\ &\approx \left(\mathcal{D}_y^{(2)} - \mathcal{D}_y^{(1)}\right) \Delta A.\end{aligned} \tag{2.19}$$

As with the Stokes integrals above it is assumed that the height is infinitesimal with respect to the radial dimension. Letting that height $\Delta y \rightarrow 0$ kills off the radially directed contributions of the flux through the sidewalls.

The RHS expands to approximately

$$\int_V \rho_{\mathrm{e}} \, dV \approx \Delta A \Delta y \rho_{\mathrm{e}}. \tag{2.20}$$

Define a highly localized surface current density (coulombs/meter-squared) as

$$\sigma_{\mathrm{e}} = \lim_{\Delta y \rightarrow 0} \Delta y \rho_{\mathrm{e}}. \tag{2.21}$$

Equating eq. (2.20) with eq. (2.19) gives

$$\left(\mathcal{D}_y^{(2)} - \mathcal{D}_y^{(1)}\right) \Delta A = \Delta A \sigma_{\mathrm{e}}, \tag{2.22}$$

or

$$\boxed{\left(\mathcal{D}^{(2)} - \mathcal{D}^{(1)}\right) \cdot \hat{\mathbf{n}} = \sigma_{\mathrm{e}}.} \tag{2.23}$$

Gauss's law for magnetism. The same argument can be applied to the magnetic flux. Define a highly localized magnetic surface current density (webers/meter-squared) as

$$\sigma_{\mathrm{m}} = \lim_{\Delta y \rightarrow 0} \Delta y \rho_{\mathrm{m}}, \tag{2.24}$$

yielding the boundary relation

$$\boxed{\left(\mathcal{B}^{(2)} - \mathcal{B}^{(1)}\right) \cdot \hat{\mathbf{n}} = \sigma_{\mathrm{m}}.} \tag{2.25}$$

2.7 ENERGY MOMENTUM CONSERVATION.

Maxwell's equations with magnetic sources. In this section, the form of Maxwell's equations to be used are expressed in terms of $\mathcal{E}$ and $\mathcal{H}$, assume linear media, and do not assume a phasor representation

$$\boldsymbol{\nabla} \times \mathcal{E} = -\mathcal{M} - \mu_0 \frac{\partial \mathcal{H}}{\partial t} \tag{2.26a}$$

$$\boldsymbol{\nabla} \times \mathcal{H} = \mathcal{J} + \epsilon_0 \frac{\partial \mathcal{E}}{\partial t} \tag{2.26b}$$

$$\boldsymbol{\nabla} \cdot \mathcal{E} = \rho/\epsilon_0 \tag{2.26c}$$

$$\boldsymbol{\nabla} \cdot \mathcal{H} = \rho_{\mathrm{m}}/\mu_0. \tag{2.26d}$$

Energy momentum conservation. With magnetic sources the Poynting and energy conservation relationship has to be adjusted slightly. Let's derive that result, starting with the divergence of the Poynting vector

$$\begin{aligned}
\boldsymbol{\nabla} \cdot (\mathcal{E} \times \mathcal{H}) &= \mathcal{H} \cdot (\boldsymbol{\nabla} \times \mathcal{E}) - \mathcal{E} \cdot (\boldsymbol{\nabla} \times \mathcal{H}) \\
&= -\mathcal{H} \cdot \left(\mu_0 \partial_t \mathcal{H} + \mathcal{M}\right) - \mathcal{E} \cdot (\mathcal{J} + \epsilon_0 \partial_t \mathcal{E}) \\
&= -\mu_0 \mathcal{H} \cdot \partial_t \mathcal{H} - \mathcal{H} \cdot \mathcal{M} - \epsilon_0 \mathcal{E} \cdot \partial_t \mathcal{E} - \mathcal{E} \cdot \mathcal{J},
\end{aligned} \tag{2.27}$$

or

$$\boxed{\frac{1}{2} \frac{\partial}{\partial t} \left(\epsilon_0 \mathcal{E}^2 + \mu_0 \mathcal{H}^2\right) + \boldsymbol{\nabla} \cdot (\mathcal{E} \times \mathcal{H}) = -\mathcal{H} \cdot \mathcal{M} - \mathcal{E} \cdot \mathcal{J}.} \tag{2.28}$$

Momentum conservation. The usual relationship is only modified by one additional term. Recall from electrodynamics [18] that eq. (2.28) (when the magnetic current density $\mathcal{M}$ is omitted) is just one of four components of the energy momentum conservation equation

$$\partial_\mu T^{\mu\nu} = -\frac{1}{c} F^{\nu\lambda} j_\lambda. \tag{2.29}$$

Note that eq. (2.29) was likely not in SI units. The next task is to generalize this classical relationship to incorporate the magnetic sources used in antenna theory. With an eye towards the relativistic nature of the energy momentum tensor, it is natural to assume that the remainder of the energy momentum tensor conservation relation can be found by taking the time derivatives of the Poynting vector.

$$\begin{aligned} \frac{\partial}{\partial t}\left(\mathcal{E} \times \mathcal{H}\right) &= \frac{\partial \mathcal{E}}{\partial t} \times \mathcal{H} + \mathcal{E} \times \frac{\partial \mathcal{H}}{\partial t} \\ &= \frac{1}{\epsilon_0}\left(\boldsymbol{\nabla} \times \mathcal{H} - \mathcal{J}\right) \times \mathcal{H} + \frac{1}{\mu_0}\mathcal{E} \times \left(-\boldsymbol{\nabla} \times \mathcal{E} - \mathcal{M}\right), \end{aligned} \tag{2.30}$$

or

$$\begin{aligned} \frac{1}{c^2}\frac{\partial}{\partial t}\left(\mathcal{E} \times \mathcal{H}\right) + \mu_0 \mathcal{J} \times \mathcal{H} + \epsilon_0 \mathcal{E} \times \mathcal{M} \\ = -\mu_0 \mathcal{H} \times \left(\boldsymbol{\nabla} \times \mathcal{H}\right) \\ - \epsilon_0 \mathcal{E} \times \left(\boldsymbol{\nabla} \times \mathcal{E}\right). \end{aligned} \tag{2.31}$$

The $\mu_0 \mathcal{J} \times \mathcal{H} = \mathcal{J} \times \mathbf{B}$ is a portion of the Lorentz force equation in its density form. To put eq. (2.31) into the desired form, the remainder of the Lorentz force force equation $\rho \mathcal{E} = \epsilon_0 \mathcal{E} \boldsymbol{\nabla} \cdot \mathcal{E}$ must be added to both sides. To extend the magnetic current term to its full dual (magnetic) Lorentz force structure, the quantity to add to both sides is $\rho_{\mathrm{m}} \mathcal{H} = \mu_0 \mathcal{H} \boldsymbol{\nabla} \cdot \mathcal{H}$. Performing these manipulations gives

$$\begin{aligned} &\frac{1}{c^2}\frac{\partial}{\partial t}\left(\mathcal{E} \times \mathcal{H}\right) + \rho \mathbf{E} + \mu_0 \mathcal{J} \times \mathcal{H} + \rho_{\mathrm{m}} \mathcal{H} + \epsilon_0 \mathcal{E} \times \mathcal{M} \\ &= \mu_0 \left(\mathcal{H} \boldsymbol{\nabla} \cdot \mathcal{H} - \mathcal{H} \times \left(\boldsymbol{\nabla} \times \mathcal{H}\right)\right) + \epsilon_0 \left(\mathcal{E} \boldsymbol{\nabla} \cdot \mathcal{E} - \mathcal{E} \times \left(\boldsymbol{\nabla} \times \mathcal{E}\right)\right). \end{aligned} \tag{2.32}$$

It seems slightly surprising the sign of the magnetic equivalent of the Lorentz force terms have an alternation of sign. This is, however, consistent with the duality transformations outlined in ([5] table 3.2)

$$\rho \rightarrow \rho_{\mathrm{m}} \tag{2.33a}$$

$$\mathcal{J} \rightarrow \mathcal{M} \tag{2.33b}$$

$$\mu_0 \rightarrow \epsilon_0 \tag{2.33c}$$

$$\mathcal{E} \rightarrow \mathcal{H} \tag{2.33d}$$

$$\mathcal{H} \rightarrow -\mathcal{E}, \tag{2.33e}$$

for

$$\rho \mathbf{E} + \mu_0 \mathcal{J} \times \mathcal{H} \rightarrow \rho_{\mathrm{m}} \mathbf{H} + \epsilon_0 \mathcal{M} \times (-\mathcal{E}) = \rho_{\mathrm{m}} \mathbf{H} + \epsilon_0 \mathcal{E} \times \mathcal{M}. \tag{2.34}$$

Comfortable that the LHS has the desired structure, the RHS can expressed as a divergence. Just expanding one of the differences of vector products on the RHS does not obviously show that this is possible, for example

$$\begin{aligned}
\mathbf{e}_a \cdot (\mathcal{E} \boldsymbol{\nabla} \cdot \mathcal{E} - \mathcal{E} \times (\boldsymbol{\nabla} \times \mathcal{E})) &= E_a \partial_b E_b - \epsilon_{abc} E_b \epsilon_{crs} \partial_r E_s \\
&= E_a \partial_b E_b - \delta_{ab}^{[rs]} E_b \partial_r E_s \\
&= E_a \partial_b E_b - E_b \left(\partial_a E_b - \partial_b E_a \right) \\
&= E_a \partial_b E_b - E_b \partial_a E_b + E_b \partial_b E_a .
\end{aligned} \tag{2.35}$$

This happens to equal

$$\begin{aligned}
\boldsymbol{\nabla} \cdot \left(\left(E_a E_b - \frac{1}{2} \delta_{ab} \mathcal{E}^2 \right) \mathbf{e}_b \right) &= \partial_b \left(E_a E_b - \frac{1}{2} \delta_{ab} \mathcal{E}^2 \right) \\
&= E_b \partial_b E_a + E_a \partial_b E_b - \frac{1}{2} \delta_{ab} 2 E_c \partial_b E_c \\
&= E_b \partial_b E_a + E_a \partial_b E_b - E_b \partial_a E_b .
\end{aligned} \tag{2.36}$$

This allows a final formulation of the remaining energy momentum conservation equation in its divergence form. Let

$$T^{ab} = \epsilon_0 \left(E_a E_b - \frac{1}{2} \delta_{ab} \mathcal{E}^2 \right) + \mu_0 \left(H_a H_b - \frac{1}{2} \delta_{ab} \mathcal{H}^2 \right), \tag{2.37}$$

so that the remaining energy momentum conservation equation, extended to both electric and magnetic sources , is

$$\begin{aligned}\frac{1}{c^2}\frac{\partial}{\partial t}\left(\mathcal{E}\times\mathcal{H}\right)+\left(\rho\mathbf{E}+\mu_0\mathcal{J}\times\mathcal{H}\right)\\+\left(\rho_{\mathrm{m}}\mathcal{H}+\epsilon_0\mathcal{E}\times\mathcal{M}\right)=\mathbf{e}_a\boldsymbol{\nabla}\cdot\left(T^{ab}\mathbf{e}_b\right).\end{aligned}\tag{2.38}$$

On the LHS we have the rate of change of momentum density, the electric Lorentz force density terms, the dual (magnetic) Lorentz force density terms, and on the RHS the the momentum flux terms.

In the frequency domain. With frequency domain fields $\mathcal{E} = \mathrm{Re}\,\mathbf{E}e^{j\omega t}$ and $\mathcal{H} = \mathrm{Re}\,\mathbf{H}e^{j\omega t}$. Using the electric field dot product as an example, note that we can write

$$\mathcal{E}=\frac{1}{2}\left(\mathbf{E}e^{j\omega t}+\mathbf{E}^*e^{-j\omega t}\right),\tag{2.39}$$

so

$$\begin{aligned}\mathcal{E}^2&=\frac{1}{2}\left(\mathbf{E}e^{j\omega t}+\mathbf{E}^*e^{-j\omega t}\right)\cdot\frac{1}{2}\left(\mathbf{E}e^{j\omega t}+\mathbf{E}^*e^{-j\omega t}\right)\\&=\frac{1}{4}\left(\mathbf{E}^2e^{2j\omega t}+\mathbf{E}\cdot\mathbf{E}^*+\mathbf{E}^*\cdot\mathbf{E}+\left(\mathbf{E}^*\right)^2e^{-2j\omega t}\right)\\&=\frac{1}{2}\mathrm{Re}\left(\mathbf{E}\cdot\mathbf{E}^*+\mathbf{E}^2e^{2j\omega t}\right).\end{aligned}\tag{2.40}$$

Similarly, for the cross product

$$\begin{aligned}\mathcal{E}\times\mathcal{H}&=\frac{1}{4}\left(\mathbf{E}\times\mathbf{H}e^{2j\omega t}+\mathbf{E}\times\mathbf{H}^*+\mathbf{E}^*\times\mathbf{H}+\left(\mathbf{E}^*\times\mathbf{H}^*\right)e^{-2j\omega t}\right)\\&=\frac{1}{2}\mathrm{Re}\left(\mathbf{E}\times\mathbf{H}^*+\mathbf{E}\times\mathbf{H}e^{2j\omega t}\right).\end{aligned}\tag{2.41}$$

Given phasor representations of the sources $\mathcal{M} = \mathbf{M}e^{j\omega t}$, $\mathcal{J} = \mathbf{J}e^{j\omega t}$, eq. (2.28) can be recast into (a messy) phasor form

$$\begin{aligned}\frac{1}{2}\mathrm{Re}\,\frac{1}{2}\frac{\partial}{\partial t}\left(\epsilon_0\mathbf{E}\cdot\mathbf{E}^*+\mu_0\mathbf{H}\cdot\mathbf{H}^*+\epsilon_0\mathbf{E}^2e^{2j\omega t}+\mu_0\mathbf{H}^2e^{2j\omega t}\right)\\+\frac{1}{2}\mathrm{Re}\,\boldsymbol{\nabla}\cdot\left(\mathbf{E}\times\mathbf{H}^*+\mathbf{E}\times\mathbf{H}e^{2j\omega t}\right)\\=\frac{1}{2}\mathrm{Re}\left(-\mathbf{H}\cdot\mathbf{M}^*-\mathbf{E}\cdot\mathbf{J}^*-\mathbf{H}\cdot\mathbf{M}e^{2j\omega t}-\mathbf{E}\cdot\mathbf{J}e^{2j\omega t}\right).\end{aligned}\tag{2.42}$$

All the time dependence has been moved into the exponential factors, so the $\epsilon_0 \mathbf{E} \cdot \mathbf{E}^* + \mu_0 \mathbf{H} \cdot \mathbf{H}^*$ terms are killed by the time derivative operator. Averaging over one period kills the rest of the oscillatory terms, leaving just

$$\boxed{0 = \boldsymbol{\nabla} \cdot (\mathbf{E} \times \mathbf{H}^*) + \mathbf{H} \cdot \mathbf{M}^* + \mathbf{E} \cdot \mathbf{J}^*.} \tag{2.43}$$

Comparison to the reciprocity theorem result. The reciprocity theorem had a striking similarity to the Poynting theorem above, which isn't suprising since both were derived by calculating the divergence of a Poynting like quantity. Here's a repetition of the reciprocity divergence calculation without the single frequency (phasor) assumption

$$\begin{aligned}
\boldsymbol{\nabla} \cdot & \left(\mathcal{E}^{(a)} \times \mathcal{H}^{(b)} - \mathcal{E}^{(b)} \times \mathcal{H}^{(a)} \right) \\
&= \mathcal{H}^{(b)} \cdot \left(\boldsymbol{\nabla} \times \mathcal{E}^{(a)} \right) - \mathcal{E}^{(a)} \cdot \left(\boldsymbol{\nabla} \times \mathcal{H}^{(b)} \right) \\
&\quad - \mathcal{H}^{(a)} \cdot \left(\boldsymbol{\nabla} \times \mathcal{E}^{(b)} \right) + \mathcal{E}^{(b)} \cdot \left(\boldsymbol{\nabla} \times \mathcal{H}^{(a)} \right) \\
&= -\mathcal{H}^{(b)} \cdot \left(\mu_0 \partial_t \mathcal{H}^{(a)} + \mathcal{M}^{(a)} \right) - \mathcal{E}^{(a)} \cdot \left(\mathcal{J}^{(b)} + \epsilon_0 \partial_t \mathcal{E}^{(b)} \right) \\
&\quad + \mathcal{H}^{(a)} \cdot \left(\mu_0 \partial_t \mathcal{H}^{(b)} + \mathcal{M}^{(b)} \right) + \mathcal{E}^{(b)} \cdot \left(\mathcal{J}^{(a)} + \epsilon_0 \partial_t \mathcal{E}^{(a)} \right) \\
&= \epsilon_0 \left(\mathcal{E}^{(b)} \cdot \partial_t \mathcal{E}^{(a)} - \mathcal{E}^{(a)} \cdot \partial_t \mathcal{E}^{(b)} \right) + \mu_0 \left(\mathcal{H}^{(a)} \cdot \partial_t \mathcal{H}^{(b)} - \mathcal{H}^{(b)} \cdot \partial_t \mathcal{H}^{(a)} \right) \\
&+ \mathcal{H}^{(a)} \cdot \mathcal{M}^{(b)} - \mathcal{H}^{(b)} \cdot \mathcal{M}^{(a)} + \mathcal{E}^{(b)} \cdot \mathcal{J}^{(a)} - \mathcal{E}^{(a)} \cdot \mathcal{J}^{(b)}.
\end{aligned} \tag{2.44}$$

What do these time derivative terms look like in the frequency domain?

$$\begin{aligned}
\mathcal{E}^{(b)} \cdot \partial_t \mathcal{E}^{(a)} &= \frac{1}{4} \left(\mathbf{E}^{(b)} e^{j\omega t} + {\mathbf{E}^{(b)}}^* e^{-j\omega t} \right) \cdot \partial_t \left(\mathbf{E}^{(a)} e^{j\omega t} + {\mathbf{E}^{(a)}}^* e^{-j\omega t} \right) \\
&= \frac{j\omega}{4} \left(\mathbf{E}^{(b)} e^{j\omega t} + {\mathbf{E}^{(b)}}^* e^{-j\omega t} \right) \cdot \left(\mathbf{E}^{(a)} e^{j\omega t} - {\mathbf{E}^{(a)}}^* e^{-j\omega t} \right) \\
&= \frac{\omega}{4} \Big(j\mathbf{E}^{(a)} \cdot {\mathbf{E}^{(b)}}^* - j\mathbf{E}^{(b)} \cdot {\mathbf{E}^{(a)}}^* + j\mathbf{E}^{(a)} \cdot \mathbf{E}^{(b)} e^{2j\omega t} - j{\mathbf{E}^{(a)}}^* \\
&\qquad \cdot {\mathbf{E}^{(b)}}^* e^{-2j\omega t} \Big) \\
&= \frac{1}{2} \operatorname{Re} \left(j\omega \mathbf{E}^{(a)} \cdot {\mathbf{E}^{(b)}}^* + j\omega \mathbf{E}^{(a)} \cdot \mathbf{E}^{(b)} e^{2j\omega t} \right).
\end{aligned} \tag{2.45}$$

Permuting indexes and taking the difference kills all the time dependentent terms, even without averaging

$$\begin{aligned}
&\boldsymbol{\mathcal{E}}^{(b)} \cdot \partial_t \boldsymbol{\mathcal{E}}^{(a)} - \boldsymbol{\mathcal{E}}^{(a)} \cdot \partial_t \boldsymbol{\mathcal{E}}^{(b)} \\
&= \frac{1}{2} \operatorname{Re} \left(j\omega \left(\mathbf{E}^{(a)} \cdot \mathbf{E}^{(b)*} - \mathbf{E}^{(b)} \cdot \mathbf{E}^{(a)*} + \mathbf{E}^{(a)} \cdot \mathbf{E}^{(b)} e^{2j\omega t} - \mathbf{E}^{(b)} \cdot \mathbf{E}^{(a)} e^{2j\omega t} \right) \right) \\
&= -\omega \operatorname{Im} \left(\mathbf{E}^{(a)} \cdot \mathbf{E}^{(b)*} \right),
\end{aligned} \tag{2.46}$$

so we have

$$\begin{aligned}
0 = \boldsymbol{\nabla} \cdot \operatorname{Re} &\left(\mathbf{E}^{(a)} \times \mathbf{H}^{(b)*} - \mathbf{E}^{(b)} \times \mathbf{H}^{(a)*} \right) \\
&+ \omega \operatorname{Im} \left(\epsilon_0 \mathbf{E}^{(a)} \cdot \mathbf{E}^{(b)*} + \mu_0 \mathbf{H}^{(a)} \cdot \mathbf{H}^{(b)*} \right) \\
&+ \operatorname{Re} \left(-\mathbf{H}^{(a)} \cdot \mathbf{M}^{(b)*} + \mathbf{H}^{(b)} \cdot \mathbf{M}^{(a)*} - \mathbf{E}^{(b)} \cdot \mathbf{J}^{(a)*} + \mathbf{E}^{(a)} \cdot \mathbf{J}^{(b)*} \right).
\end{aligned} \tag{2.47}$$

Followup Questions. FIXME: TODO.

1. What do the energy momentum conservation equations look like in geometric algebra form with magnetic sources?

2. What do the energy momentum conservation equations look like in tensor form with magnetic sources?

2.8 DUALITY TRANSFORMATION.

In a discussion of Dirac's monopoles, [16] §6.12 introduces a duality transformation, forming electric and magnetic fields by forming a rotation that combines a different pair of electric and magnetic fields. In SI units that transformation becomes

$$\begin{bmatrix} \boldsymbol{\mathcal{E}} \\ \eta \boldsymbol{\mathcal{H}} \end{bmatrix} = \begin{bmatrix} \cos\theta & \sin\theta \\ -\sin\theta & \cos\theta \end{bmatrix} \begin{bmatrix} \boldsymbol{\mathcal{E}}' \\ \eta \boldsymbol{\mathcal{H}}' \end{bmatrix} \tag{2.48a}$$

$$\begin{bmatrix} \boldsymbol{\mathcal{D}} \\ \boldsymbol{\mathcal{B}}/\eta \end{bmatrix} = \begin{bmatrix} \cos\theta & \sin\theta \\ -\sin\theta & \cos\theta \end{bmatrix} \begin{bmatrix} \boldsymbol{\mathcal{D}}' \\ \boldsymbol{\mathcal{B}}'/\eta \end{bmatrix}, \tag{2.48b}$$

where $\eta = \sqrt{\mu_0/\epsilon_0}$. It is left as an exercise to the reader to show that application of these to Maxwell's equations

$$\boldsymbol{\nabla} \cdot \mathcal{E} = \rho_{\mathrm{e}}/\epsilon_0 \tag{2.49a}$$

$$\boldsymbol{\nabla} \cdot \mathcal{H} = \rho_{\mathrm{m}}/\mu_0 \tag{2.49b}$$

$$-\boldsymbol{\nabla} \times \mathcal{E} - \partial_t \mathcal{B} = \mathcal{J}_{\mathrm{m}} \tag{2.49c}$$

$$\boldsymbol{\nabla} \times \mathcal{H} - \partial_t \mathcal{D} = \mathcal{J}_{\mathrm{e}}, \tag{2.49d}$$

determine a similar relation between the sources. That transformation of Maxwell's equation is

$$\boldsymbol{\nabla} \cdot \left(\cos\theta \mathcal{E}' + \sin\theta \eta \mathcal{H}'\right) = \rho_{\mathrm{e}}/\epsilon_0 \tag{2.50a}$$

$$\boldsymbol{\nabla} \cdot \left(-\sin\theta \mathcal{E}'/\eta + \cos\theta \mathcal{H}'\right) = \rho_{\mathrm{m}}/\mu_0 \tag{2.50b}$$

$$-\boldsymbol{\nabla} \times \left(\cos\theta \mathcal{E}' + \sin\theta \eta \mathcal{H}'\right) - \partial_t \left(-\sin\theta \eta \mathcal{D}' + \cos\theta \mathcal{B}'\right) = \mathcal{J}_{\mathrm{m}} \tag{2.50c}$$

$$\boldsymbol{\nabla} \times \left(-\sin\theta \mathcal{E}'/\eta + \cos\theta \mathcal{H}'\right) - \partial_t \left(\cos\theta \mathcal{D}' + \sin\theta \mathcal{B}'/\eta\right) = \mathcal{J}_{\mathrm{e}}. \tag{2.50d}$$

A bit of rearranging gives

$$\begin{bmatrix} \eta \rho_{\mathrm{e}} \\ \rho_{\mathrm{m}} \end{bmatrix} = \begin{bmatrix} \cos\theta & \sin\theta \\ -\sin\theta & \cos\theta \end{bmatrix} \begin{bmatrix} \eta \rho'_{\mathrm{e}} \\ \rho'_{\mathrm{m}} \end{bmatrix} \tag{2.51a}$$

$$\begin{bmatrix} \eta \mathcal{J}_{\mathrm{e}} \\ \mathcal{J}_{\mathrm{m}} \end{bmatrix} = \begin{bmatrix} \cos\theta & \sin\theta \\ -\sin\theta & \cos\theta \end{bmatrix} \begin{bmatrix} \eta \mathcal{J}'_{\mathrm{e}} \\ \mathcal{J}'_{\mathrm{m}} \end{bmatrix}. \tag{2.51b}$$

For example, with $\rho_{\mathrm{m}} = \mathcal{J}_{\mathrm{m}} = 0$, and $\theta = \pi/2$, the transformation of sources is

$$\begin{aligned} \rho'_{\mathrm{e}} &= 0 \\ \mathcal{J}'_{\mathrm{e}} &= 0 \\ \rho'_{\mathrm{m}} &= \eta \rho_{\mathrm{e}} \\ \mathcal{J}'_{\mathrm{m}} &= \eta \mathcal{J}_{\mathrm{e}}, \end{aligned} \tag{2.52}$$

and Maxwell's equations then have only magnetic sources

$$\boldsymbol{\nabla} \cdot \boldsymbol{\mathcal{E}}' = 0 \tag{2.53a}$$

$$\boldsymbol{\nabla} \cdot \boldsymbol{\mathcal{H}}' = \rho'_{\mathrm{m}}/\mu_0 \tag{2.53b}$$

$$-\boldsymbol{\nabla} \times \boldsymbol{\mathcal{E}}' - \partial_t \boldsymbol{\mathcal{B}}' = \boldsymbol{\mathcal{J}}'_{\mathrm{m}} \tag{2.53c}$$

$$\boldsymbol{\nabla} \times \boldsymbol{\mathcal{H}}' - \partial_t \boldsymbol{\mathcal{D}}' = 0. \tag{2.53d}$$

Of this relation Jackson points out that "The invariance of the equations of electrodynamics under duality transformations shows that it is a matter of convention to speak of a particle possessing an electric charge, but not magnetic charge." This is an interesting comment, and worth some additional thought.

2.9 RECIPROCITY THEOREM.

The class slides presented a derivation of the reciprocity theorem, a theorem that contained the integral of

$$\int \left(\mathbf{E}^{(a)} \times \mathbf{H}^{(b)} - \mathbf{E}^{(b)} \times \mathbf{H}^{(a)} \right) \cdot d\mathbf{S} = \cdots \tag{2.54}$$

over a surface, where the RHS was a volume integral involving the fields and (electric and magnetic) current sources. The idea was to consider two different source loading configurations of the same system, and to show that the fields and sources in the two configurations can be related. To derive the result in question, a simple way to start is to look at the divergence of the difference of cross products above. This will require the phasor form of the two cross product Maxwell's equations

$$\boldsymbol{\nabla} \times \mathbf{E} = -(\mathbf{M} + j\omega\mu_0\mathbf{H}) \tag{2.55a}$$

$$\boldsymbol{\nabla} \times \mathbf{H} = \mathbf{J} + j\omega\epsilon_0\mathbf{E}, \tag{2.55b}$$

so the divergence is

$$\begin{aligned}
&\boldsymbol{\nabla} \cdot \left(\mathbf{E}^{(a)} \times \mathbf{H}^{(b)} - \mathbf{E}^{(b)} \times \mathbf{H}^{(a)}\right) \\
&\quad= \mathbf{H}^{(b)} \cdot \left(\boldsymbol{\nabla} \times \mathbf{E}^{(a)}\right) - \mathbf{E}^{(a)} \cdot \left(\boldsymbol{\nabla} \times \mathbf{H}^{(b)}\right) \\
&\quad- \mathbf{H}^{(a)} \cdot \left(\boldsymbol{\nabla} \times \mathbf{E}^{(b)}\right) + \mathbf{E}^{(b)} \cdot \left(\boldsymbol{\nabla} \times \mathbf{H}^{(a)}\right) \\
&\quad= -\mathbf{H}^{(b)} \cdot \left(\mathbf{M}^{(a)} + j\omega\mu_0\mathbf{H}^{(a)}\right) - \mathbf{E}^{(a)} \cdot \left(\mathbf{J}^{(b)} + j\omega\epsilon_0\mathbf{E}^{(b)}\right) \\
&\quad+ \mathbf{H}^{(a)} \cdot \left(\mathbf{M}^{(b)} + j\omega\mu_0\mathbf{H}^{(b)}\right) + \mathbf{E}^{(b)} \cdot \left(\mathbf{J}^{(a)} + j\omega\epsilon_0\mathbf{E}^{(a)}\right).
\end{aligned} \tag{2.56}$$

The non-source terms cancel, leaving

$$\begin{aligned}
&\boldsymbol{\nabla} \cdot \left(\mathbf{E}^{(a)} \times \mathbf{H}^{(b)} - \mathbf{E}^{(b)} \times \mathbf{H}^{(a)}\right) \\
&\quad= -\mathbf{H}^{(b)} \cdot \mathbf{M}^{(a)} - \mathbf{E}^{(a)} \cdot \mathbf{J}^{(b)} + \mathbf{H}^{(a)} \cdot \mathbf{M}^{(b)} + \mathbf{E}^{(b)} \cdot \mathbf{J}^{(a)}.
\end{aligned} \tag{2.57}$$

Should we be surprised to have a relation of this form? Probably not, given that the energy momentum relationship between the fields and currents of a single source has the form

$$\frac{\partial}{\partial t}\frac{\epsilon_0}{2}\left(\mathcal{E}^2 + c^2\mathcal{B}^2\right) + \boldsymbol{\nabla} \cdot \frac{1}{\mu_0}(\mathcal{E} \times \mathcal{B}) = -\mathcal{E} \cdot \mathcal{J}. \tag{2.58}$$

(this is without magnetic sources). This initially suggests that the reciprocity theorem can be expressed more generally in terms of the energy-momentum tensor. However, there are some subtle differences since the time domain products lead to averages in terms of the real parts of conjugate pairs such as $\mathcal{E} \times \mathcal{B} \rightarrow \mathbf{E} \times \mathbf{B}^*$, and $\mathcal{E} \cdot \mathcal{J} \rightarrow \mathbf{E} \cdot \mathbf{J}^*$.

Far field integral form. Employing the divergence theorem over a sphere the identity above takes the form

$$\begin{aligned}&\int_S \left(\mathbf{E}^{(a)} \times \mathbf{H}^{(b)} - \mathbf{E}^{(b)} \times \mathbf{H}^{(a)}\right) \cdot \hat{\mathbf{r}} dS \\ &= \int_V \left(-\mathbf{H}^{(b)} \cdot \mathbf{M}^{(a)} - \mathbf{E}^{(a)} \cdot \mathbf{J}^{(b)} + \mathbf{H}^{(a)} \cdot \mathbf{M}^{(b)} + \mathbf{E}^{(b)} \cdot \mathbf{J}^{(a)}\right) dV\end{aligned} \tag{2.59}$$

In the far field, the cross products are strictly radial. That surface integral can be written as

$$\begin{aligned}&\int_S \left(\mathbf{E}^{(a)} \times \mathbf{H}^{(b)} - \mathbf{E}^{(b)} \times \mathbf{H}^{(a)}\right) \cdot \hat{\mathbf{r}} dS \\ &= \frac{1}{\mu_0} \int_S \left(\mathbf{E}^{(a)} \times \left(\hat{\mathbf{r}} \times \mathbf{E}^{(b)}\right) - \mathbf{E}^{(b)} \times \left(\hat{\mathbf{r}} \times \mathbf{E}^{(a)}\right)\right) \cdot \hat{\mathbf{r}} dS \\ &= \frac{1}{\mu_0} \int_S \left(\mathbf{E}^{(a)} \cdot \mathbf{E}^{(b)} - \mathbf{E}^{(b)} \cdot \mathbf{E}^{(a)}\right) dS \\ &= 0.\end{aligned} \tag{2.60}$$

The above expansions used eq. (2.64) to expand the terms of the form

$$(\mathbf{A} \times (\hat{\mathbf{r}} \times \mathbf{C})) \cdot \hat{\mathbf{r}} = \mathbf{A} \cdot \mathbf{C} - (\mathbf{A} \cdot \hat{\mathbf{r}}) (\mathbf{C} \cdot \hat{\mathbf{r}}), \tag{2.61}$$

in which only the first dot product survives due to the transverse nature of the fields. So in the far field we have a direct relation between the fields and sources of two source configurations of the same system of the form

$$\int_V \left(\mathbf{H}^{(a)} \cdot \mathbf{M}^{(b)} + \mathbf{E}^{(b)} \cdot \mathbf{J}^{(a)}\right) dV = \int_V \left(\mathbf{H}^{(b)} \cdot \mathbf{M}^{(a)} + \mathbf{E}^{(a)} \cdot \mathbf{J}^{(b)}\right) dV. \tag{2.62}$$

Application to antenna theory. This is the underlying reason that we are able to pose the problem of what an antenna can receive, in terms of what the antenna can transmit. Prof. Eleftheriades explained the the send-receive equivalence using the concepts of a two-port network ([15], [22]). An alternate, and very intuitive, explanation can be found in appendix A.1 [6], that directly related the current density sources and scalar current to the voltages in those regions using an integral representation of the reciprocity theorem.

Identities.

Lemma 2.1: Divergence of a cross product

$$\boldsymbol{\nabla} \cdot (\mathbf{A} \times \mathbf{B}) = \mathbf{B} (\boldsymbol{\nabla} \times \mathbf{A}) - \mathbf{A} (\boldsymbol{\nabla} \times \mathbf{B}).$$

Proof.

$$\begin{aligned}\boldsymbol{\nabla} \cdot (\mathbf{A} \times \mathbf{B}) &= \partial_a \epsilon_{abc} A_b B_c \\ &= \epsilon_{abc} (\partial_a A_b) B_c - \epsilon_{bac} A_b (\partial_a B_c) \\ &= \mathbf{B} \cdot (\boldsymbol{\nabla} \times \mathbf{A}) - \mathbf{B} \cdot (\boldsymbol{\nabla} \times \mathbf{A}).\end{aligned} \tag{2.63}$$

Lemma 2.2: Triple cross product dotted

$$(\mathbf{A} \times (\mathbf{B} \times \mathbf{C})) \cdot \mathbf{D} = (\mathbf{A} \cdot \mathbf{C}) (\mathbf{B} \cdot \mathbf{D}) - (\mathbf{A} \cdot \mathbf{B}) (\mathbf{C} \cdot \mathbf{D}).$$

Proof.

$$\begin{aligned}(\mathbf{A} \times (\mathbf{B} \times \mathbf{C})) \cdot \mathbf{D} &= \epsilon_{abc} A_b \epsilon_{rsc} B_r C_s D_a \\ &= \delta^{rs}_{[ab]} A_b B_r C_s D_a \\ &= A_s B_r C_s D_r - A_r B_r C_s D_s \\ &= (\mathbf{A} \cdot \mathbf{C}) (\mathbf{B} \cdot \mathbf{D}) - (\mathbf{A} \cdot \mathbf{B}) (\mathbf{C} \cdot \mathbf{D}).\end{aligned} \tag{2.64}$$

2.10 NOTATION.

Some notes on notation for this chapter and the coverage of this material in class:

- Phasor frequency terms are written as $e^{j\omega t}$, not $e^{-j\omega t}$, as done in physics. I didn't recall that this was always the case in physics, and wouldn't have assumed it. This is the case in both [17] and [12]. The latter however, also uses $\cos(\omega t - kr)$

for spherical waves possibly implying an alternate phasor sign convention in that content, so I'd be wary about trusting any absolute "engineering" vs. physics sign convention without checking carefully.

- In Green's functions $G(\mathbf{r}, \mathbf{r}')$, $\mathbf{r}$ is the point of observation, and $\mathbf{r}'$ is the point in the convolution integration space.
- Both $\mathbf{M}$ and $\mathbf{J}_m$ are used for magnetic current sources in the class notes.

2.11 PROBLEMS.

Exercise 2.1 Far field electric field. (*2015 ps2, p3*)

Show that in a region of space where there are no sources, the electric field derived from the magnetic vector potential is given by the expression:

$$\mathbf{E} = \frac{1}{j\omega\epsilon_0\mu_0} \boldsymbol{\nabla} \times (\boldsymbol{\nabla} \times \mathbf{A}) . \tag{2.65}$$

Answer for Exercise 2.1

First consider the expansion of the curls

$$\begin{aligned} \boldsymbol{\nabla} \times (\boldsymbol{\nabla} \times \mathbf{A}) &= \epsilon_{rst} \mathbf{e}_r \partial_s \epsilon_{tbc} \partial_b A_c \\ &= \delta_{rs}^{[bc]} \mathbf{e}_r \partial_s \partial_b A_c \\ &= \mathbf{e}_r \partial_s (\partial_r A_s - \partial_s A_r) , \end{aligned} \tag{2.66}$$

so

$$\boldsymbol{\nabla} \times (\boldsymbol{\nabla} \times \mathbf{A}) = \boldsymbol{\nabla} (\boldsymbol{\nabla} \cdot A) - \boldsymbol{\nabla}^2 \mathbf{A}. \tag{2.67}$$

This supplies a strong hint of how to proceed. The electric field can be expanded utilizing this relation and the Helmholtz equation relating $\mathbf{A}$ and $\mathbf{J}$

$$\begin{aligned} \mathbf{E} &= -j\omega\mathbf{A} - j\frac{1}{\omega\epsilon_0\mu_0} \boldsymbol{\nabla} (\boldsymbol{\nabla} \cdot \mathbf{A}) \\ &= -j\omega\mathbf{A} - j\frac{1}{\omega\epsilon_0\mu_0} \left(\boldsymbol{\nabla} \times (\boldsymbol{\nabla} \times \mathbf{A}) + \boldsymbol{\nabla}^2 \mathbf{A} \right) \\ &= -j\omega\mathbf{A} - j\frac{1}{\omega\epsilon_0\mu_0} \left(\boldsymbol{\nabla} \times (\boldsymbol{\nabla} \times \mathbf{A}) - \left(k^2 \mathbf{A} + \mu_0 \mathbf{J} \right) \right) . \end{aligned} \tag{2.68}$$

However,

$$\frac{k^2}{\omega\epsilon_0\mu_0} = \frac{\omega^2/c^2}{\omega(1/c^2)} = \omega, \tag{2.69}$$

leaving

$$\mathbf{E} = -j\frac{1}{\omega\epsilon_0\mu_0}\boldsymbol{\nabla} \times (\boldsymbol{\nabla} \times \mathbf{A}) + j\frac{1}{\omega\epsilon_0}\mathbf{J}. \tag{2.70}$$

Since $\mathbf{J} = 0$ in a region of space where there are no sources, the electric field in such a region is given by eq. (2.65) as stated.

3 LINEAR WIRE ANTENNAS.

3.1 MAGNETIC VECTOR POTENTIAL.

The symbol **A** has been referred to as the Magnetic Vector Potential in class and in the problem set. My recollection was that we called this the Vector Potential. Prefixing this with magnetic seemed counter intuitive to me since it is generated by electric sources (charges and currents). This terminology can be justified due to the fact that **A** generates the magnetic field by its curl. Some mention of this can be found in [26], which also points out that the Electric Potential refers to the scalar ϕ. Prof. Eleftheriades points out that Electric Vector Potential refers to the vector potential **F** generated by magnetic sources (because in that case the electric field is generated by the curl of **F**.)

3.2 PLOTS OF INFINITESIMAL DIPOLE RADIAL DEPENDENCE.

In §4.2 of [5] are some discussions of the $kr < 1$, $kr = 1$, and $kr > 1$ radial dependence of the fields and power of a solution to an infinitesimal dipole system. Here are some plots of those kr dependence, along with the $kr = 1$ contour as a reference. All the θ dependence and any scaling is left out.

The CDF notebook visualizeDipoleFields.cdf is available to interactively plot these, rotate the plots and change the ranges of what is plotted.

Plots of the real and imaginary parts of

$$\begin{aligned} H_\phi &= \frac{jk}{r} e^{-jkr} \left(1 - \frac{j}{kr} \right) \\ E_r &= \frac{1}{r^2} \left(1 - \frac{j}{kr} \right) e^{-jkr} \\ E_\theta &= \frac{jk}{r} \left(1 - \frac{j}{kr} - \frac{1}{k^2 r^2} \right) e^{-jkr}, \end{aligned} \tag{3.1}$$

can be found in fig. 3.1, fig. 3.2, and fig. 3.3 respectively.

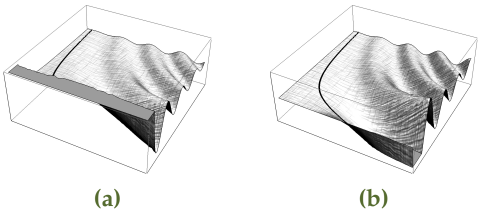

Figure 3.1: Radial dependence of Re H_ϕ and Im H_ϕ.

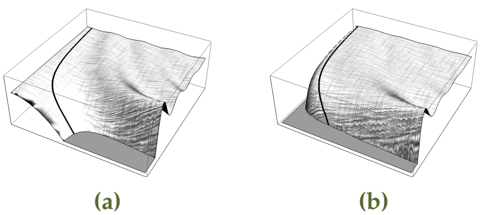

Figure 3.2: Radial dependence of Re E_r and Im E_r.

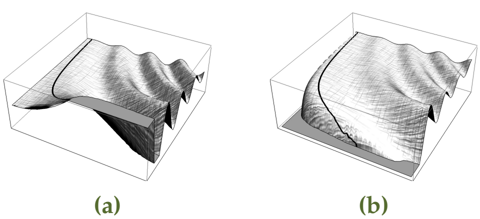

Figure 3.3: Radial dependence of Re E_θ and Im E_θ.

3.3 ELECTRIC FAR FIELD FOR A SPHERICAL POTENTIAL.

It is interesting to look at the far electric field associated with an arbitrary spherical magnetic vector potential, assuming all of the radial dependence is in the spherical envelope. That is

$$\mathbf{A} = \frac{e^{-jkr}}{r} \left(\hat{\mathbf{r}} a_r \left(\theta, \phi\right) + \hat{\boldsymbol{\theta}} a_\theta \left(\theta, \phi\right) + \hat{\boldsymbol{\phi}} a_\phi \left(\theta, \phi\right) \right). \tag{3.2}$$

The electric field is

$$\mathbf{E} = -j\omega \mathbf{A} - j \frac{1}{\omega \mu_0 \epsilon_0} \boldsymbol{\nabla} \left(\boldsymbol{\nabla} \cdot \mathbf{A} \right). \tag{3.3}$$

The divergence and gradient in spherical coordinates are

$$\boldsymbol{\nabla} \cdot \mathbf{A} = \frac{1}{r^2} \frac{\partial}{\partial r} \left(r^2 A_r \right) + \frac{1}{r \sin\theta} \frac{\partial}{\partial \theta} \left(A_\theta \sin\theta \right) + \frac{1}{r \sin\theta} \frac{\partial A_\phi}{\partial \phi} \tag{3.4a}$$

$$\boldsymbol{\nabla} \psi = \hat{\mathbf{r}} \frac{\partial \psi}{\partial r} + \frac{\hat{\boldsymbol{\theta}}}{r} \frac{\partial \psi}{\partial \theta} + \frac{\hat{\boldsymbol{\phi}}}{r \sin\theta} \frac{\partial \psi}{\partial \phi}. \tag{3.4b}$$

For the assumed potential, the divergence is

$$\begin{aligned}
\boldsymbol{\nabla} \cdot \mathbf{A} &= \frac{a_r}{r^2} \frac{\partial}{\partial r} \left(r^2 \frac{e^{-jkr}}{r} \right) + \frac{1}{r \sin\theta} \frac{e^{-jkr}}{r} \frac{\partial}{\partial \theta} \left(\sin\theta a_\theta \right) + \frac{1}{r \sin\theta} \frac{e^{-jkr}}{r} \frac{\partial a_\phi}{\partial \phi} \\
&= a_r e^{-jkr} \left(\frac{1}{r^2} - jk \frac{1}{r} \right) + \frac{1}{r^2 \sin\theta} e^{-jkr} \frac{\partial}{\partial \theta} \left(\sin\theta a_\theta \right) \\
&\quad + \frac{1}{r^2 \sin\theta} e^{-jkr} \frac{\partial a_\phi}{\partial \phi} \\
&\approx -jk \frac{a_r}{r} e^{-jkr}.
\end{aligned} \tag{3.5}$$

The last approximation dropped all the $1/r^2$ terms that will be small compared to $1/r$ contribution that dominates when $r \rightarrow \infty$, the far field.

The gradient can now be computed

$$\begin{aligned}
\boldsymbol{\nabla}\left(\boldsymbol{\nabla}\cdot\mathbf{A}\right) &\approx -jk\boldsymbol{\nabla}\left(\frac{a_r}{r}e^{-jkr}\right) \\
&= -jk\left(\hat{\mathbf{r}}\frac{\partial}{\partial r}+\frac{\hat{\boldsymbol{\theta}}}{r}\frac{\partial}{\partial\theta}+\frac{\hat{\boldsymbol{\phi}}}{r\sin\theta}\frac{\partial}{\partial\phi}\right)\frac{a_r}{r}e^{-jkr} \\
&= -jk\left(\hat{\mathbf{r}}a_r\frac{\partial}{\partial r}\left(\frac{1}{r}e^{-jkr}\right)+\frac{\hat{\boldsymbol{\theta}}}{r^2}e^{-jkr}\frac{\partial a_r}{\partial\theta}+e^{-jkr}\frac{\hat{\boldsymbol{\phi}}}{r^2\sin\theta}\frac{\partial a_r}{\partial\phi}\right) \\
&= -jk\left(-\hat{\mathbf{r}}\frac{a_r}{r^2}\left(1+jkr\right)+\frac{\hat{\boldsymbol{\theta}}}{r^2}\frac{\partial a_r}{\partial\theta}+\frac{\hat{\boldsymbol{\phi}}}{r^2\sin\theta}\frac{\partial a_r}{\partial\phi}\right)e^{-jkr} \\
&\approx -k^2\hat{\mathbf{r}}\frac{a_r}{r}e^{-jkr}.
\end{aligned} \tag{3.6}$$

Again, a far field approximation has been used to kill all the $1/r^2$ terms. The far field approximation of the electric field is now possible

$$\begin{aligned}
\mathbf{E} &= -j\omega\mathbf{A}-j\frac{1}{\omega\mu_0\epsilon_0}\boldsymbol{\nabla}\left(\boldsymbol{\nabla}\cdot\mathbf{A}\right) \\
&= -j\omega\frac{e^{-jkr}}{r}\left(\hat{\mathbf{r}}a_r\left(\theta,\phi\right)+\hat{\boldsymbol{\theta}}a_\theta\left(\theta,\phi\right)+\hat{\boldsymbol{\phi}}a_\phi\left(\theta,\phi\right)\right)+j\frac{1}{\omega\mu_0\epsilon_0}k^2\hat{\mathbf{r}}\frac{a_r}{r}e^{-jkr} \\
&= -j\omega\frac{e^{-jkr}}{r}\left(\cancel{\hat{\mathbf{r}}a_r\left(\theta,\phi\right)}+\hat{\boldsymbol{\theta}}a_\theta\left(\theta,\phi\right)+\hat{\boldsymbol{\phi}}a_\phi\left(\theta,\phi\right)\right)+\cancel{j\frac{c^2}{\omega}\left(\frac{\omega}{c}\right)^2\hat{\mathbf{r}}\frac{a_r}{r}e^{-jkr}} \\
&= -j\omega\frac{e^{-jkr}}{r}\left(\hat{\boldsymbol{\theta}}a_\theta\left(\theta,\phi\right)+\hat{\boldsymbol{\phi}}a_\phi\left(\theta,\phi\right)\right).
\end{aligned} \tag{3.7}$$

Observe the perfect, somewhat miraculous seeming, cancellation of all the radial components of the field. If $\mathbf{A}_\mathrm{T}$ is the non-radial projection of $\mathbf{A}$, the electric far field is just

$$\boxed{\mathbf{E}_{\mathrm{ff}} = -j\omega\mathbf{A}_\mathrm{T}.} \tag{3.8}$$

3.4 MAGNETIC FAR FIELD FOR A SPHERICAL POTENTIAL.

Application of the same assumed representation for the magnetic field gives

$$\begin{aligned}
\mathbf{B} &= \boldsymbol{\nabla} \times \mathbf{A} \\
&= \frac{\hat{\mathbf{r}}}{r\sin\theta}\partial_\theta \left(A_\phi \sin\theta\right) + \frac{\hat{\boldsymbol{\theta}}}{r}\left(\frac{1}{\sin\theta}\partial_\phi A_r - \partial_r \left(r A_\phi\right)\right) \\
&\quad + \frac{\hat{\boldsymbol{\phi}}}{r}\left(\partial_r \left(r A_\theta\right) - \partial_\theta A_r\right) \\
&= \frac{\hat{\mathbf{r}}}{r\sin\theta}\partial_\theta \left(\frac{e^{-jkr}}{r} a_\phi \sin\theta\right) \\
&\quad + \frac{\hat{\boldsymbol{\theta}}}{r}\left(\frac{1}{\sin\theta}\partial_\phi \left(\frac{e^{-jkr}}{r} a_r\right) - \partial_r \left(r\frac{e^{-jkr}}{r} a_\phi\right)\right) \\
&\quad + \frac{\hat{\boldsymbol{\phi}}}{r}\left(\partial_r \left(r\frac{e^{-jkr}}{r} a_\theta\right) - \partial_\theta \left(\frac{e^{-jkr}}{r} a_r\right)\right) \\
&= \frac{\hat{\mathbf{r}}}{r\sin\theta}\frac{e^{-jkr}}{r}\partial_\theta \left(a_\phi \sin\theta\right) + \frac{\hat{\boldsymbol{\theta}}}{r}\left(\frac{1}{\sin\theta}\frac{e^{-jkr}}{r}\partial_\phi a_r - \partial_r \left(e^{-jkr}\right) a_\phi\right) \\
&\quad + \frac{\hat{\boldsymbol{\phi}}}{r}\left(\partial_r \left(e^{-jkr}\right) a_\theta - \frac{e^{-jkr}}{r}\partial_\theta a_r\right) \\
&\approx jk \left(\hat{\boldsymbol{\theta}} a_\phi - \hat{\boldsymbol{\phi}} a_\theta\right) \frac{e^{-jkr}}{r} \\
&= -jk\hat{\mathbf{r}} \times \left(\hat{\boldsymbol{\theta}} a_\theta + \hat{\boldsymbol{\phi}} a_\phi\right) \frac{e^{-jkr}}{r} \\
&= \frac{1}{c}\mathbf{E}_{\mathrm{ff}}.
\end{aligned} \tag{3.9}$$

The approximation above drops the $1/r^2$ terms. Since

$$\frac{1}{\mu_0 c} = \frac{1}{\mu_0}\sqrt{\mu_0 \epsilon_0} = \sqrt{\frac{\epsilon_0}{\mu_0}} = \frac{1}{\eta}, \tag{3.10}$$

the magnetic far field can be expressed in terms of the electric far field as

$$\boxed{\mathbf{H} = \frac{1}{\eta}\hat{\mathbf{r}} \times \mathbf{E}.} \tag{3.11}$$

3.5 PLANE WAVE RELATIONS BETWEEN ELECTRIC AND MAGNETIC FIELDS.

I recalled an identity of the form eq. (3.11) in [16], but didn't think that it required a far field approximation. The reason for this was because the Jackson identity assumed a plane wave representation of the field, something that the far field assumptions also locally require.

Assuming a plane wave representation for both fields

$$\mathcal{E}(\mathbf{x}, t) = \mathbf{E} e^{j(\omega t - \mathbf{k}\cdot\mathbf{x})} \tag{3.12a}$$

$$\mathcal{B}(\mathbf{x}, t) = \mathbf{B} e^{j(\omega t - \mathbf{k}\cdot\mathbf{x})}. \tag{3.12b}$$

The cross product relation between the fields follows from the Maxwell-Faraday law of induction

$$0 = \boldsymbol{\nabla} \times \mathcal{E} + \frac{\partial \mathcal{B}}{\partial t}, \tag{3.13}$$

or

$$\begin{aligned}
0 &= \mathbf{e}_r \times \mathbf{E} \partial_r e^{j(\omega t - \mathbf{k}\cdot\mathbf{x})} + j\omega \mathbf{B} e^{j(\omega t - \mathbf{k}\cdot\mathbf{x})} \\
&= -j \mathbf{e}_r k_r \times \mathbf{E} e^{j(\omega t - \mathbf{k}\cdot\mathbf{x})} + j\omega \mathbf{B} e^{j(\omega t - \mathbf{k}\cdot\mathbf{x})} \\
&= \left(-\mathbf{k} \times \mathbf{E} + \omega \mathbf{B}\right) j e^{j(\omega t - \mathbf{k}\cdot\mathbf{x})},
\end{aligned} \tag{3.14}$$

or

$$\begin{aligned}
\mathbf{H} &= \frac{k}{k c \mu_0} \hat{\mathbf{k}} \times \mathbf{E} \\
&= \frac{1}{\eta} \hat{\mathbf{k}} \times \mathbf{E},
\end{aligned} \tag{3.15}$$

which also finds eq. (3.11), but with much less work and less mess.

3.6 TRANSVERSE ONLY NATURE OF THE FAR-FIELD FIELDS.

Also observe that its possible to tell that the far field fields have only transverse components using the same argument that they are locally plane waves at that distance. The plane waves must satisfy the zero divergence Maxwell's equations

$$\boldsymbol{\nabla} \cdot \mathcal{E} = 0 \tag{3.16a}$$

$$\boldsymbol{\nabla} \cdot \mathcal{B} = 0, \tag{3.16b}$$

so by the same logic

$$\mathbf{k} \cdot \mathbf{E} = 0 \tag{3.17a}$$

$$\mathbf{k} \cdot \mathbf{B} = 0. \tag{3.17b}$$

In the far field the electric field must equal its transverse projection

$$\mathbf{E} = \mathrm{Proj}_{\mathrm{T}} \left(-j\omega \mathbf{A} - j\frac{1}{\omega \mu_0 \epsilon_0} \boldsymbol{\nabla} \left(\boldsymbol{\nabla} \cdot \mathbf{A} \right) \right). \tag{3.18}$$

Since by eq. (3.6) the scalar potential term has only a radial component, that leaves

$$\mathbf{E} = -j\omega \, \mathrm{Proj}_{\mathrm{T}} \, \mathbf{A}, \tag{3.19}$$

which provides eq. (3.8) with slightly less work.

3.7 DUALITY TRANSFORMATION OF THE FAR FIELD FIELDS.

We've seen that the far field electric and magnetic fields associated with a magnetic vector potential were

$$\mathbf{E} = -j\omega \, \mathrm{Proj}_{\mathrm{T}} \, \mathbf{A}, \tag{3.20a}$$

$$\mathbf{H} = \frac{1}{\eta} \hat{\mathbf{k}} \times \mathbf{E}. \tag{3.20b}$$

What does **H** look like in terms of **A**? Expanding the rejection of the radial component answers that

$$\mathbf{H} = -\frac{j\omega}{\eta} \hat{\mathbf{k}} \times \left(\mathbf{A} - \left(\mathbf{A} \cdot \hat{\mathbf{k}} \right) \hat{\mathbf{k}} \right). \tag{3.21}$$

The $\hat{\mathbf{k}}$ crossed terms are killed, leaving

$$\mathbf{H} = -\frac{j\omega}{\eta}\hat{\mathbf{k}} \times \mathbf{A}. \tag{3.22}$$

It's worth a quick note that the duality transformation for this, referring to [5] tab. 3.2, is

$$\mathbf{H} = -j\omega \operatorname{Proj}_{\mathrm{T}} \mathbf{F} \tag{3.23a}$$

$$\mathbf{E} = \eta\hat{\mathbf{k}} \times \mathbf{H} = j\omega\eta\hat{\mathbf{k}} \times \mathbf{F}. \tag{3.23b}$$

These show explicitly that neither the electric or magnetic far field have any radial component, matching with intuition for transverse propagation of the fields.

3.8 VERTICAL DIPOLE REFLECTION COEFFICIENT.

In class a ground reflection scenario was covered for a horizontal dipole. Reading the text I was surprised to see what looked like the same sort of treatment §4.7.2, but ending up with a quite different result. It turns out the difference is because the text was treating the vertical dipole configuration, whereas Prof. Eleftheriades was treating a horizontal dipole configuration, which have different reflection coefficients. These differing reflection coefficients are due to differences in the polarization of the field.

To understand these differences in reflection coefficients, consider first the field due to a vertical dipole as sketched in fig. 3.4, with a wave vector directed from the transmission point downwards in the z-y plane. The wave vector has direction

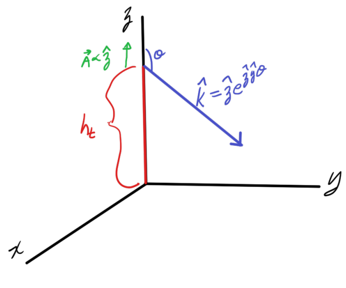

Figure 3.4: Vertical dipole configuration.

$$\hat{\mathbf{k}} = \hat{\mathbf{z}} e^{\hat{\mathbf{z}}\hat{\mathbf{x}}\theta} = \hat{\mathbf{z}} \cos\theta + \hat{\mathbf{y}} \sin\theta. \tag{3.24}$$

Suppose that the (magnetic) vector potential is that of an infinitesimal dipole

$$\mathbf{A} = \hat{\mathbf{z}} \frac{\mu_0 I_0 l}{4\pi r} e^{-jkr}. \tag{3.25}$$

The electric field, in the far field, can be computed by computing the normal projection to the wave vector direction

$$\begin{aligned}
\mathbf{E} &= -j\omega \left(\mathbf{A} \wedge \hat{\mathbf{k}} \right) \cdot \hat{\mathbf{k}} \\
&= -j\omega \frac{\mu_0 I_0 l}{4\pi r} \left(\hat{\mathbf{z}} \wedge \left(\hat{\mathbf{z}} \cos\theta + \hat{\mathbf{y}} \sin\theta \right) \right) \left(\hat{\mathbf{z}} \cos\theta + \hat{\mathbf{y}} \sin\theta \right) \\
&= -j\omega \frac{\mu_0 I_0 l}{4\pi r} \left(\hat{\mathbf{z}}\hat{\mathbf{y}} \sin\theta \right) \left(\hat{\mathbf{z}} \cos\theta + \hat{\mathbf{y}} \sin\theta \right) \\
&= -j\omega \frac{\mu_0 I_0 l}{4\pi r} \sin\theta \left(-\hat{\mathbf{y}} \cos\theta + \hat{\mathbf{z}} \sin\theta \right) \\
&= j\omega \frac{\mu_0 I_0 l}{4\pi r} \sin\theta \hat{\mathbf{y}} e^{\hat{\mathbf{z}}\hat{\mathbf{y}}\theta}.
\end{aligned} \tag{3.26}$$

This is directed in the z-y plane rotated an additional $\pi/2$ past $\hat{\mathbf{k}}$. The magnetic field must then be directed into the page, along the x axis. This is sketched in fig. 3.5. Referring to [13] (eq. 4.40) for the

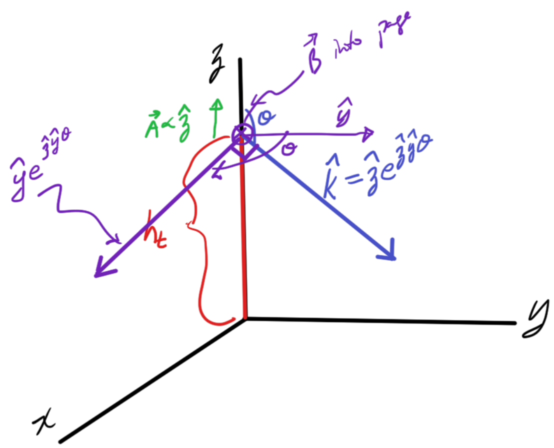

Figure 3.5: Electric and magnetic field directions.

coefficient of reflection component

$$R = \frac{n_t \cos\theta_i - n_i \cos\theta_t}{n_i \cos\theta_i + n_t \cos\theta_t}. \tag{3.27}$$

This is the Fresnel equation for the case when that corresponds to **E** lies in the plane of incidence, and the magnetic field is completely parallel to the plane of reflection). For the no transmission case, allowing $v_t \rightarrow 0$, the index of refraction is $n_t = c/v_t \rightarrow \infty$, and the reflection coefficient is 1 as claimed in §4.7.2 of [5]. Because of the symmetry of this dipole configuration, the azimuthal angle that the wave vector is directed along does not matter.

3.9 HORIZONTAL DIPOLE REFLECTION COEFFICIENT.

In the class notes, a horizontal dipole coming out of the page is indicated. With the page representing the z-y plane, this is a magnetic vector potential directed along the x-axis direction

$$\mathbf{A} = \hat{\mathbf{x}} \frac{\mu_0 I_0 l}{4\pi r} e^{-jkr}. \tag{3.28}$$

For a wave vector directed in the z-y plane as in eq. (3.24), the electric far field is directed along

$$\begin{aligned} \left(\hat{\mathbf{x}} \wedge \hat{\mathbf{k}}\right) \cdot \hat{\mathbf{k}} &= \hat{\mathbf{x}} - \left(\hat{\mathbf{x}} \cdot \hat{\mathbf{k}}\right) \hat{\mathbf{k}} \\ &= \hat{\mathbf{x}} - \left(\hat{\mathbf{x}} \cdot (\hat{\mathbf{z}} \cos\theta + \hat{\mathbf{y}} \sin\theta)\right) \hat{\mathbf{k}} \\ &= \hat{\mathbf{x}}. \end{aligned} \tag{3.29}$$

The electric far field lies completely in the plane of reflection. From [13] (eq. 4.34), the Fresnel reflection coefficients is

$$R = \frac{n_i \cos\theta_i - n_t \cos\theta_t}{n_i \cos\theta_i + n_t \cos\theta_t}, \tag{3.30}$$

which approaches -1 when $n_t \rightarrow \infty$. This is consistent with the image theorem summation that Prof. Eleftheriades used in class.

Azimuthal angle dependency of the reflection coefficient. Now consider a horizontal dipole directed along the y-axis. For the same wave vector direction as above, the electric far field is now directed along

$$\begin{aligned}\left(\hat{\mathbf{y}} \wedge \hat{\mathbf{k}}\right) \cdot \hat{\mathbf{k}} &= \hat{\mathbf{y}} - \left(\hat{\mathbf{y}} \cdot \hat{\mathbf{k}}\right) \hat{\mathbf{k}} \\ &= \hat{\mathbf{y}} - \left(\hat{\mathbf{y}} \cdot \left(\hat{\mathbf{z}} \cos\theta + \hat{\mathbf{y}} \sin\theta\right)\right) \hat{\mathbf{k}} \\ &= \hat{\mathbf{y}} - \hat{\mathbf{k}} \sin\theta \\ &= \hat{\mathbf{y}} - \sin\theta \left(\hat{\mathbf{z}} \cos\theta + \hat{\mathbf{y}} \sin\theta\right) \\ &= \hat{\mathbf{y}} \cos^2\theta - \sin\theta \cos\theta \hat{\mathbf{z}} \\ &= \cos\theta \left(\hat{\mathbf{y}} \cos\theta - \sin\theta \hat{\mathbf{z}}\right) \\ &= \cos\theta \hat{\mathbf{y}} e^{\hat{\mathbf{z}}\hat{\mathbf{y}}\theta}.\end{aligned} \tag{3.31}$$

That is

$$\mathbf{E} = -j\omega \frac{\mu_0 I_0 l}{4\pi r} e^{-jkr} \cos\theta \hat{\mathbf{y}} e^{\hat{\mathbf{z}}\hat{\mathbf{y}}\theta}. \tag{3.32}$$

This far field electric field lies in the plane of incidence (a direction of $\hat{\boldsymbol{\theta}}$ rotated by $\pi/2$), not in the plane of reflection. The corresponding magnetic field should be directed along the plane of reflection, which is easily confirmed by calculation

$$\begin{aligned}\hat{\mathbf{k}} \times \left(\hat{\mathbf{y}} \cos\theta - \sin\theta \hat{\mathbf{z}}\right) &= \left(\hat{\mathbf{z}} \cos\theta + \hat{\mathbf{y}} \sin\theta\right) \times \left(\hat{\mathbf{y}} \cos\theta - \sin\theta \hat{\mathbf{z}}\right) \\ &= -\hat{\mathbf{x}} \cos^2\theta - \hat{\mathbf{x}} \sin^2\theta \\ &= -\hat{\mathbf{x}}.\end{aligned} \tag{3.33}$$

The far field magnetic field is seen to be

$$\mathbf{H} = j\omega \frac{I_0 l}{4\pi r} e^{-jkr} \cos\theta \hat{\mathbf{x}}, \tag{3.34}$$

so a reflection coefficient of 1 is required to calculate the power loss after a single ground reflection signal bounce for this relative orientation of antenna to the target. I fail to see how the horizontal dipole treatment in §4.7.5 can use a single reflection coefficient without taking into account the azimuthal dependency of that reflection coefficient.

Reflecting on this (no pun intended), made me realize that the no transmission case has some interesting aspects. One of these is that radiation momentum must be transferred to the reflecting surface in some fashion since the direction of the incident radiation changes. Perhaps this is why the use of Image theory seems to be careful to state that the reflecting plane is a perfect electrical conductor. Study of reflection off of conducting surfaces is clearly in order to understand how this differs from normal reflection in transmitting media.

3.10 FIELD RESOLUTION W.R.T THE REFLECTING PLANE.

In order to apply the Fresnel equations, the field components have to be resolved into components where either the electric field or the magnetic field is parallel to the plane of reflection. The geometry of this, with the wave vector direction $\hat{\mathbf{k}}$ and the electric and magnetic field phasors perpendicular to that direction is sketched in fig. 3.6. If the incident wave is a plane wave, or equivalently a far field

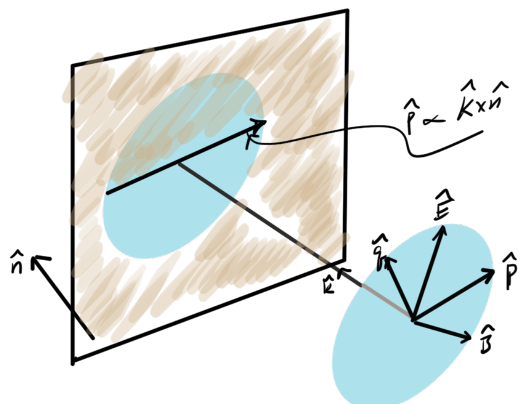

Figure 3.6: Field components relative to reflecting plane.

spherical wave, it will have the form

$$\mathbf{H} = \frac{1}{\mu_0} \hat{\mathbf{k}} \times \mathbf{E}, \tag{3.35}$$

with the field directions and wave vector directions satisfying

$$\hat{\mathbf{E}} \times \hat{\mathbf{H}} = \hat{\mathbf{k}} \tag{3.36a}$$

$$\hat{\mathbf{E}} \cdot \hat{\mathbf{k}} = 0 \tag{3.36b}$$

$$\hat{\mathbf{H}} \cdot \hat{\mathbf{k}} = 0. \tag{3.36c}$$

The key to resolving the fields into components parallel to the plane of reflection lies in the observation that the cross product of the plane normal $\hat{\mathbf{n}}$ and the incident wave vector direction $\hat{\mathbf{k}}$ lies in that plane. With

$$\hat{\mathbf{p}} = \frac{\hat{\mathbf{k}} \times \hat{\mathbf{n}}}{\left|\hat{\mathbf{k}} \times \hat{\mathbf{n}}\right|} \tag{3.37a}$$

$$\hat{\mathbf{q}} = \hat{\mathbf{k}} \times \hat{\mathbf{p}}, \tag{3.37b}$$

the field directions can be resolved into components

$$\mathbf{E} = (\mathbf{E} \cdot \hat{\mathbf{p}})\,\hat{\mathbf{p}} + (\mathbf{E} \cdot \hat{\mathbf{q}})\,\hat{\mathbf{q}} = E_{\parallel}\hat{\mathbf{p}} + E_{\perp}\hat{\mathbf{q}} \tag{3.38a}$$

$$\mathbf{H} = (\mathbf{H} \cdot \hat{\mathbf{p}})\,\hat{\mathbf{p}} + (\mathbf{H} \cdot \hat{\mathbf{q}})\,\hat{\mathbf{q}} = H_{\parallel}\hat{\mathbf{p}} + H_{\perp}\hat{\mathbf{q}}. \tag{3.38b}$$

This subdivides the fields into two pairs, one with the electric field parallel to the reflection plane

$$\begin{aligned} \mathbf{E}_1 &= (\mathbf{E} \cdot \hat{\mathbf{p}})\,\hat{\mathbf{p}} = E_{\parallel}\hat{\mathbf{p}} \\ \mathbf{H}_1 &= (\mathbf{H} \cdot \hat{\mathbf{q}})\,\hat{\mathbf{q}} = H_{\perp}\hat{\mathbf{q}}, \end{aligned} \tag{3.39}$$

and one with the magnetic field parallel to the reflection plane

$$\begin{aligned} \mathbf{H}_2 &= (\mathbf{H} \cdot \hat{\mathbf{p}})\,\hat{\mathbf{p}} = H_{\parallel}\hat{\mathbf{p}} \\ \mathbf{E}_2 &= (\mathbf{E} \cdot \hat{\mathbf{q}})\,\hat{\mathbf{q}} = E_{\perp}\hat{\mathbf{q}}. \end{aligned} \tag{3.40}$$

This is most of what we need to proceed with the reflection and transmission analysis. The only task remaining is to determine the reflection angle. Using a pencil with the tip on the table I was able to convince myself by observation that there is always a normal plane of incidence regardless of any oblique angle that the ray hits the reflecting surface. This was, for some reason, not intuitively obvious to me. Having done that, the geometry must be reduced to

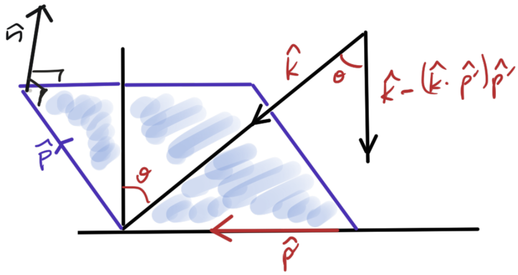

Figure 3.7: Angle of incidence determination.

what is sketched in fig. 3.7. Once a $\hat{\mathbf{p}}' = \hat{\mathbf{p}} \times \hat{\mathbf{n}}$ has been determined, regardless of it's orientation in the reflection plane, the component of $\hat{\mathbf{k}}$ that is normal, directed towards, the plane of reflection is

$$\hat{\mathbf{k}} - \left(\hat{\mathbf{k}} \cdot \hat{\mathbf{p}}'\right) \hat{\mathbf{p}}', \tag{3.41}$$

with (squared) length

$$\begin{aligned} \left(\hat{\mathbf{k}} - \left(\hat{\mathbf{k}} \cdot \hat{\mathbf{p}}'\right) \hat{\mathbf{p}}'\right)^2 &= 1 + \left(\hat{\mathbf{k}} \cdot \hat{\mathbf{p}}'\right)^2 - 2\left(\hat{\mathbf{k}} \cdot \hat{\mathbf{p}}'\right)^2 \\ &= 1 - \left(\hat{\mathbf{k}} \cdot \hat{\mathbf{p}}'\right)^2 . \end{aligned} \tag{3.42}$$

The angle of incidence, relative to the normal to the reflection plane, follows from

$$\begin{aligned} \cos\theta &= \hat{\mathbf{k}} \cdot \frac{\hat{\mathbf{k}} - \left(\hat{\mathbf{k}} \cdot \hat{\mathbf{p}}'\right) \hat{\mathbf{p}}'}{\sqrt{1 - \left(\hat{\mathbf{k}} \cdot \hat{\mathbf{p}}'\right)^2}} \\ &= \sqrt{1 - \left(\hat{\mathbf{k}} \cdot \hat{\mathbf{p}}'\right)^2}. \end{aligned} \tag{3.43}$$

Expanding the dot product above gives

$$\begin{aligned} \hat{\mathbf{k}} \cdot \hat{\mathbf{p}}' &= \hat{\mathbf{k}} \cdot (\hat{\mathbf{p}} \times \hat{\mathbf{n}}) \\ &= \frac{1}{\left|\hat{\mathbf{k}} \times \hat{\mathbf{n}}\right|} \hat{\mathbf{k}} \cdot \left(\left(\hat{\mathbf{k}} \times \hat{\mathbf{n}}\right) \times \hat{\mathbf{n}}\right), \end{aligned} \tag{3.44}$$

where

$$\begin{aligned}
\hat{\mathbf{k}} \cdot \left(\left(\hat{\mathbf{k}} \times \hat{\mathbf{n}} \right) \times \hat{\mathbf{n}} \right) &= k_r \epsilon_{rst} \left(\hat{\mathbf{k}} \times \hat{\mathbf{n}} \right)_s n_t \\
&= k_r \epsilon_{rst} \epsilon_{sab} k_a n_b n_t \\
&= -k_r \delta_{rt}^{[ab]} k_a n_b n_t \\
&= -k_r n_t \left(k_r n_t - k_t n_r \right) \\
&= -1 + \left(\hat{\mathbf{k}} \cdot \hat{\mathbf{n}} \right)^2 .
\end{aligned} \tag{3.45}$$

That gives

$$\begin{aligned}
\hat{\mathbf{k}} \cdot \hat{\mathbf{p}}' &= \frac{-1 + \left(\hat{\mathbf{k}} \cdot \hat{\mathbf{n}} \right)^2}{\sqrt{1 - \left(\hat{\mathbf{k}} \cdot \hat{\mathbf{n}} \right)^2}} \\
&= -\sqrt{1 - \left(\hat{\mathbf{k}} \cdot \hat{\mathbf{n}} \right)^2},
\end{aligned} \tag{3.46}$$

or

$$\begin{aligned}
\cos\theta &= \sqrt{1 - \left(-\sqrt{1 - \left(\hat{\mathbf{k}} \cdot \hat{\mathbf{n}} \right)^2} \right)^2} \\
&= \sqrt{\left(\hat{\mathbf{k}} \cdot \hat{\mathbf{n}} \right)^2} \\
&= \hat{\mathbf{k}} \cdot \hat{\mathbf{n}}.
\end{aligned} \tag{3.47}$$

This surprisingly simple result makes so much sense, it is an awful admission of stupidity that I went through all the vector algebra to get it instead of just writing it down directly.

The end result is the reflection angle is given by

$$\boxed{\theta = \cos^{-1} \hat{\mathbf{k}} \cdot \hat{\mathbf{n}},} \tag{3.48}$$

where the reflection plane normal should off the back surface to get the sign right. The only detail left is the vector direction of the reflected ray (as well as the direction for the transmitted ray if that is of interest). The reflected ray direction flips the sign of the normal component of the ray

$$\begin{aligned} \hat{\mathbf{k}}' &= -\left(\hat{\mathbf{k}} \cdot \hat{\mathbf{n}}\right)\hat{\mathbf{n}} + \left(\hat{\mathbf{k}} \wedge \hat{\mathbf{n}}\right)\hat{\mathbf{n}} \\ &= -\left(\hat{\mathbf{k}} \cdot \hat{\mathbf{n}}\right)\hat{\mathbf{n}} + \hat{\mathbf{k}} - \left(\hat{\mathbf{n}}\hat{\mathbf{k}}\right) \cdot \hat{\mathbf{n}} \\ &= \hat{\mathbf{k}} - 2\left(\hat{\mathbf{k}} \cdot \hat{\mathbf{n}}\right)\hat{\mathbf{n}}. \end{aligned} \tag{3.49}$$

Here the sign of the normal doesn't matter since it only occurs quadratically. This now supplies everything needed for the application of the Fresnel equations to determine the reflected ray characteristics of an arbitrarily polarized incident field.

3.11 IMAGE THEOREM.

In the last problem set we examined the array factor for a corner cube configuration, shown in fig. 3.8.

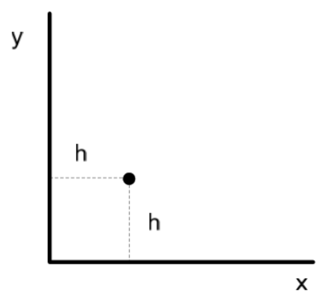

Figure 3.8: A corner-cube antenna.

Motivation. This is a horizontal dipole antenna placed next to a metallic corner. The radiation at points in the interior of the cube have contributions due to the line of sight field from the antenna as well as reflections. We looked at an approximation of ground reflections using the Image Theorem, modeling the ground as a perfectly conducting surface. I completely misunderstood that theorem and how it should be applied. As presented it seemed like a simple way to figure out the reflection characteristics. This confused me since it did not seem consistent with Fresnel reflection theory. I did try to reconcile to the two, but that reconciliation only appeared to work for certain dipole orientations, and that orientation dependence remained an open question. It turns out that the idea of the Image Theorem is to find a source configuration that contains the specified source, but contains enough other sources that the tangential component of the electric field superposition is zero on the conducting surface, as required by Maxwell's equations. This allows the boundary to be completely removed from the problem. Thinking of the corner cube configuration as a reflection problem, I positioned sources as in fig. 3.9. Because of the horizon-

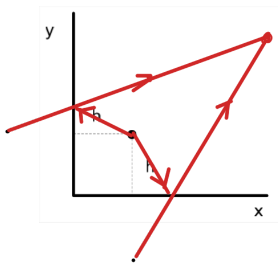

Figure 3.9: Incorrect Image Theorem source placement for corner cube.

tal orientation of the dipole, I argued that the reflection coefficient should be -1. The reflection point is a bit messy to calculate, and it turns out to zeroth order in h/r the $\sin\theta$ magnitude scaling of the reflected (far-field) field is present for both reflected rays. I though that this was probably because the observation point lays at the same altitude for both the line of sight ray and the reflected ray. Attempting this problem as a reflection problem makes it much more difficult than it needs to be. It turns out that the correct image source placement for this problem is that of fig. 3.10. This wasn't at all obvious to me. The key is understanding that the goal of the image source placement isn't to figure out how the reflection will occur, but to manufacture a source configuration for which the tangential component of the electric field is zero on the conducting surface.

Image placement for infinite conducting plane. Before thinking about the corner cube configuration, consider a horizontal dipole next to an infinite conducting plane. This, and the correct image source

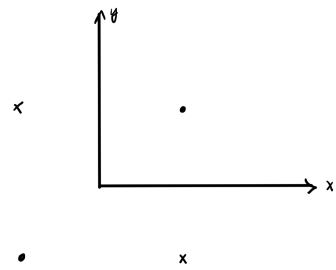

Figure 3.10: Correct image source placement for the corner cube.

placement is illustrated in fig. 3.11. I'll now verify that this is

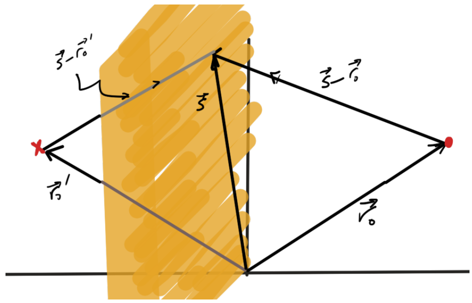

Figure 3.11: Image source placement for horizontal dipole.

the correct image source. This is basically a calculation that the tangential components of the electric fields from both sources sum to zero.

Let,

$$r = \left|\mathbf{s} - \mathbf{r}_0\right|, \tag{3.50}$$

so that the magnetic vector potential for the first quadrant dipole has the form

$$\mathbf{A} = \frac{A_0}{4\pi r} e^{-jkr} \hat{\mathbf{z}}. \tag{3.51}$$

With

$$\begin{aligned}\hat{\mathbf{k}} &= \frac{\mathbf{s} - \mathbf{r}_0}{s} \\ \tilde{\mathbf{E}} &= \hat{\mathbf{z}} - \left(\hat{\mathbf{z}} \cdot \hat{\mathbf{k}}\right)\hat{\mathbf{k}},\end{aligned} \tag{3.52}$$

the far-field electric field at the point $\mathbf{s}$ on the plane is

$$\mathbf{E} = -j\omega \frac{A_0}{4\pi r} e^{-jkr} \tilde{\mathbf{E}}. \tag{3.53}$$

If the normal to the plane is $\hat{\mathbf{n}}$ the tangential component of this field is the projection of $\mathbf{E}$ on the direction

$$\hat{\mathbf{p}} = \frac{\hat{\mathbf{k}} \times \hat{\mathbf{n}}}{\left|\hat{\mathbf{k}} \times \hat{\mathbf{n}}\right|}. \tag{3.54}$$

That tangential component is directed along

$$\left(\tilde{\mathbf{E}} \cdot \hat{\mathbf{p}}\right) \hat{\mathbf{p}} = \left(\left(\hat{\mathbf{z}} - \left(\hat{\mathbf{z}} \cdot \hat{\mathbf{k}}\right) \hat{\mathbf{k}}\right) \cdot \left(\hat{\mathbf{k}} \times \hat{\mathbf{n}}\right)\right) \frac{\hat{\mathbf{k}} \times \hat{\mathbf{n}}}{\left|\hat{\mathbf{k}} \times \hat{\mathbf{n}}\right|^2}. \tag{3.55}$$

Because the triple product $\hat{\mathbf{k}} \cdot \left(\hat{\mathbf{k}} \times \hat{\mathbf{n}}\right) = 0$, the tangential component of the electric field, provided $\hat{\mathbf{k}} \cdot \hat{\mathbf{n}} \neq 0$, is

$$\mathbf{E}_{\parallel} = -j\omega \frac{A_0}{4\pi r} e^{-jkr} \hat{\mathbf{z}} \cdot \left(\hat{\mathbf{k}} \times \hat{\mathbf{n}}\right) \frac{\hat{\mathbf{k}} \times \hat{\mathbf{n}}}{1 - \left(\hat{\mathbf{n}} \cdot \hat{\mathbf{k}}\right)^2}. \tag{3.56}$$

Now the wave vector direction for the second quadrant ray on the plane is required. Both $\hat{\mathbf{k}}'$ and $\mathbf{s}'$ are reflections across the plane. Any such reflection has the value

$$\begin{aligned} \mathbf{x}' &= (\mathbf{x} \wedge \hat{\mathbf{n}}) \hat{\mathbf{n}} - (\mathbf{x} \cdot \hat{\mathbf{n}}) \hat{\mathbf{n}} \\ &= -(\hat{\mathbf{n}} \wedge \mathbf{x} + \hat{\mathbf{n}} \cdot \mathbf{x}) \hat{\mathbf{n}} \\ &= -\hat{\mathbf{n}}\mathbf{x}\hat{\mathbf{n}}. \end{aligned} \tag{3.57}$$

This multivector product nicely encapsulates the reflection operation. Consider a reflection against the y-z plane with normal $\mathbf{e}_1$ to verify that this works

$$\begin{aligned} -\mathbf{e}_1\mathbf{x}\mathbf{e}_1 &= -\mathbf{e}_1 \left(x\mathbf{e}_1 + y\mathbf{e}_2 + z\mathbf{e}_3\right) \mathbf{e}_1 \\ &= -\left(x - y\mathbf{e}_2\mathbf{e}_1 + z\mathbf{e}_3\mathbf{e}_1\right) \mathbf{e}_1 \\ &= -\left(x\mathbf{e}_1 - y\mathbf{e}_2 + z\mathbf{e}_3\right) \\ &= -x\mathbf{e}_1 + y\mathbf{e}_2 + z\mathbf{e}_3. \end{aligned} \tag{3.58}$$

This has the x component flipped in sign and the rest left untouched as desired for a reflection in the y-z plane.

The second quadrant field will have $\hat{\mathbf{k}}' \times \hat{\mathbf{n}}$ terms in place of all the $\hat{\mathbf{k}} \times \hat{\mathbf{n}}$ terms of eq. (3.56). We want to know how the two compare. This calculation is simply done using the dual form of the cross product temporarily

$$\begin{aligned}
\hat{\mathbf{k}}' \times \hat{\mathbf{n}} &= -I\left(\hat{\mathbf{k}}' \wedge \hat{\mathbf{n}}\right) \\
&= -I\left\langle \hat{\mathbf{k}}'\hat{\mathbf{n}} \right\rangle_2 \\
&= -I\left\langle -\hat{\mathbf{n}}\hat{\mathbf{k}}\hat{\mathbf{n}}\hat{\mathbf{n}} \right\rangle_2 \\
&= I\left\langle \hat{\mathbf{n}}\hat{\mathbf{k}} \right\rangle_2 \\
&= I\hat{\mathbf{n}} \wedge \hat{\mathbf{k}} \\
&= -\hat{\mathbf{n}} \times \hat{\mathbf{k}} \\
&= \hat{\mathbf{k}} \times \hat{\mathbf{n}}.
\end{aligned} \tag{3.59}$$

So, provided the image source in the second quadrant is oppositely oriented (sign inversion), the tangential components of the two will sum to zero on that surface.

Thinking back to the corner cube, it is clear that an image source opposite to the source across from one of the walls will result in a zero tangential electric field along this boundary as is the case here (say the y-z plane). A second pair of sources opposite from each other anywhere else also about the y-z plane will not change that zero tangential electric field on this surface, but if the signs of the sources is alternated as in fig. 3.10 it will also result in zero tangential electric field on the z-x plane, which has the desired boundary value effects for both surfaces of the corner cube. Once the image sources are placed, the problem can be tackled with the boundary removed.

3.12 PROBLEMS.

Exercise 3.1 Infinitesimal electric dipole. (*2015 ps2, p4*)

Show that in the near field $kr \rightarrow 0$, the electric field of an infinitesimal electrical dipole of length l and current $\mathbf{I} = I\hat{\mathbf{z}}$ can be derived from the field of an electric dipole moment $\mathbf{p} = ql\hat{\mathbf{z}}$. The electrostatic field of a dipole moment is given by,

$$\mathbf{E} = \frac{3(\mathbf{p} \cdot \hat{\mathbf{r}})\hat{\mathbf{r}} - \mathbf{p}}{4\pi\epsilon_0 r^3}. \tag{3.60}$$

Answer for Exercise 3.1

To write the electrostatic field in spherical coordinates, first note that

$$\begin{aligned}\mathbf{p} \cdot \hat{\mathbf{r}} &= ql\hat{\mathbf{z}} \cdot \left(\cos\phi\sin\theta, \sin\phi\sin\theta, \cos\theta\right) \\ &= ql\cos\theta,\end{aligned} \tag{3.61}$$

so the electrostatic dipole field is

$$\mathbf{E} = ql\frac{3\cos\theta\hat{\mathbf{r}} - \hat{\mathbf{z}}}{4\pi\epsilon_0 r^3}. \tag{3.62}$$

To calculate the radial component of this field, note that

$$\begin{aligned}(3\cos\theta\hat{\mathbf{r}} - \hat{\mathbf{z}}) \cdot \hat{\mathbf{r}} &= 3\cos\theta - \hat{\mathbf{z}} \cdot \hat{\mathbf{r}} \\ &= 2\cos\theta,\end{aligned} \tag{3.63}$$

so

$$E_r = ql\frac{\cos\theta}{2\pi\epsilon_0 r^3}. \tag{3.64}$$

For the θ component, noting that $\hat{\boldsymbol{\theta}} = \left(\cos\theta\cos\phi, \cos\theta\sin\phi, -\sin\theta\right)$,

$$\begin{aligned}(3\cos\theta\hat{\mathbf{r}} - \hat{\mathbf{z}}) \cdot \hat{\boldsymbol{\theta}} &= -\hat{\mathbf{z}} \cdot \hat{\boldsymbol{\theta}} \\ &= \sin\theta,\end{aligned} \tag{3.65}$$

so

$$E_\theta = ql\frac{\sin\theta}{4\pi\epsilon_0 r^3}. \tag{3.66}$$

Finally the E_ϕ component of this electrostatic field is zero since

$$(3\cos\theta\hat{\mathbf{r}} - \hat{\mathbf{z}}) \cdot \hat{\boldsymbol{\phi}} = 0, \tag{3.67}$$

because $\hat{\mathbf{r}}$ and $\hat{\boldsymbol{\phi}}$ are orthonormal, and $\hat{\boldsymbol{\phi}}$ lies in the x-y plane, always perpendicular to $\hat{\mathbf{z}}$.

Current for the dipole configuration. A set of equal magnitude oscillating charges $\pm q(t)$ separated by distance l, have the phasor representation

$$q(t) = q e^{j\omega t}. \tag{3.68}$$

The dipole moment associated with such a charge distribution is

$$\begin{aligned} \mathbf{p}(t) &= \left(+q \frac{l}{2} + (-q) \left(\frac{-l}{2} \right) \right) e^{j\omega t} \hat{\mathbf{z}} \\ &= q l e^{j\omega t} \hat{\mathbf{z}}. \end{aligned} \tag{3.69}$$

This has the desired dipole moment magnitude $\mathbf{p} = q l \hat{\mathbf{z}}$. The current for this dipole configuration is

$$\begin{aligned} I(t) &= \frac{dq(t)}{dt} \\ &= j\omega q e^{j\omega t}, \end{aligned} \tag{3.70}$$

allowing a phasor identification for the current magnitude

$$I_0 = j\omega q. \tag{3.71}$$

Near field equivalence. The near field electric field equations derived from the magnetic vector potential are expressed in terms of I_0, not q. Since the ratio of charge to permittivity is

$$\begin{aligned} \frac{q}{\epsilon_0} &= \frac{I_0}{j\omega\epsilon_0} \\ &= -j I_0 \frac{1}{k c \epsilon_0} \\ &= -j I_0 \frac{\sqrt{\mu_0 \epsilon_0}}{k \epsilon_0} \\ &= -j I_0 \frac{\eta}{k}, \end{aligned} \tag{3.72}$$

the electric field components eq. (3.64) and eq. (3.66) calculated from the dipole moment take the form

$$E_r = -j \eta I_0 l \frac{\cos\theta}{2\pi k r^3} \tag{3.73a}$$

$$E_\theta = -j\eta I_0 l \frac{\sin\theta}{4\pi k r^3} \tag{3.73b}$$

$$E_\phi = 0. \tag{3.73c}$$

This reproduces the near field electric field equations for a vertical infinitesimal dipole (4.20a,b) from the text [5] in the limit $kr \to 0$.

Exercise 3.2 Mobile power reception. (*2015 ps2, p5*)

A mobile is located 5 km from a base station and uses a vertical wire antenna of gain 2.55 dB to receive cellular radio signals. The carrier frequency used is 900 MHz and the EIRP of the base station is 30 mW. If the base station and mobile are located 50 m and 1.5 m above ground respectively, calculate the power level received at the mobile.

Answer for Exercise 3.2

The mobile in a transmitting geometry is sketched in fig. 3.12. For a vertical dipole the magnetic vector potential has the form

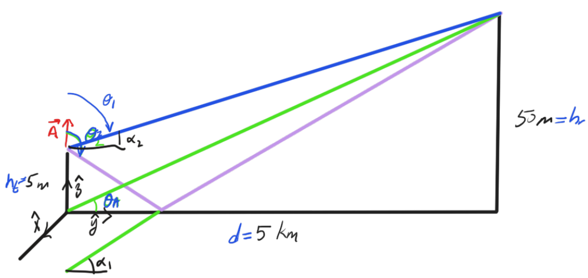

Figure 3.12: Vertical dipole reflection geometry.

$$\mathbf{A} = \hat{\mathbf{z}} \frac{A_0}{r} e^{-jkr}, \tag{3.74}$$

where $A_0 = \mu_0 I_0 l / 4\pi$. The far field electric field is

$$\begin{aligned} \mathbf{E} &= -j\omega \mathbf{A}_\mathrm{T} \\ &= -j\omega \frac{A_0}{r} e^{-jkr} \left(\hat{\mathbf{z}} - \left(\hat{\mathbf{z}} \cdot \hat{\mathbf{k}} \right) \hat{\mathbf{k}} \right), \end{aligned} \tag{3.75}$$

where all the radial (non-transverse) components of the magnetic vector potential have been subtracted out.

Reflection coefficient. To determine the sign of the reflection coefficient for a vertical dipole configuration, consider a wave vector directed in the z-y plane at an angle θ from the pole

$$\hat{\mathbf{k}} = \hat{\mathbf{z}} e^{\hat{\mathbf{z}}\hat{\mathbf{y}}\theta} = \hat{\mathbf{z}} \cos\theta + \hat{\mathbf{y}} \sin\theta. \tag{3.76}$$

The far field electric field that propagates along this direction, has direction

$$\begin{aligned}
\hat{\mathbf{z}} - \left(\hat{\mathbf{z}} \cdot \hat{\mathbf{k}}\right) \hat{\mathbf{k}} &= \hat{\mathbf{z}} - (\hat{\mathbf{z}} \cdot (\hat{\mathbf{z}} \cos\theta + \hat{\mathbf{y}} \sin\theta)) \hat{\mathbf{k}} \\
&= \hat{\mathbf{z}} - \cos\theta \hat{\mathbf{k}} \\
&= \hat{\mathbf{z}} - \cos\theta \left(\hat{\mathbf{z}} \cos\theta + \hat{\mathbf{y}} \sin\theta\right) \\
&= \hat{\mathbf{z}} \sin^2\theta - \sin\theta \cos\theta \hat{\mathbf{y}} \\
&= -\sin\theta \left(\cos\theta \hat{\mathbf{y}} - \sin\theta \hat{\mathbf{z}}\right).
\end{aligned} \tag{3.77}$$

When there is reflection, the electric (far) field is directed entirely in the plane of incidence (with the magnetic field entirely parallel to the reflecting interface). The Fresnel reflection coefficient ([13] eq. 4.40) for such a polarization is

$$R = \frac{n_t \cos\theta_i - n_i \cos\theta_t}{n_i \cos\theta_i + n_t \cos\theta_t}. \tag{3.78}$$

For no transmission the transmitted speed of the radiation $v_t \rightarrow 0$, and the the index of refraction of the ground approaches $n_t = c/v_t \rightarrow \infty$. This shows that the reflection coefficient for the vertical dipole configuration is +1. Because of the symmetry of this dipole's orientation the sign of the reflection coefficient has no azimuthal dependency.

Effects of ground reflection. Let

$$\alpha_{ref} = \arctan 55/5000 \tag{3.79a}$$

$$\alpha_{los} = \arctan 45/5000 \tag{3.79b}$$

$$r_{ref} = \sqrt{55^2 + 5000^2} \tag{3.79c}$$

$$r_{los} = \sqrt{45^2 + 5000^2} \tag{3.79d}$$

$$\hat{\mathbf{k}}_{\text{ref}} = \hat{\mathbf{y}} \cos \alpha_{\text{ref}} + \hat{\mathbf{z}} \sin \alpha_{\text{ref}} \tag{3.79e}$$

$$\hat{\mathbf{k}}_{\text{los}} = \hat{\mathbf{y}} \cos \alpha_{\text{los}} + \hat{\mathbf{z}} \sin \alpha_{\text{los}}. \tag{3.79f}$$

Summing the line of sight and reflected (image source contribution) gives

$$\begin{aligned}\mathbf{E} &= j\omega A_0 \sum_{i \in \{\text{los,ref}\}} \frac{1}{r_i} e^{-jkr_i} \cos \alpha_i \left(\sin \alpha_i \hat{\mathbf{y}} - \cos \alpha_i \hat{\mathbf{z}}\right) \\ &\approx j\omega A_0 \cos \theta_{\text{A}} \left(\sin \theta_{\text{A}} \hat{\mathbf{y}} - \cos \theta_{\text{A}} \hat{\mathbf{z}}\right) \frac{1}{r} \sum_{i \in \{\text{los,ref}\}} e^{-jkr_i},\end{aligned} \tag{3.80}$$

where an average distance $r = \sqrt{h_{\text{t}}^2 + d^2} = \sqrt{50^2 + 5000^2}$, the distance from the origin to the base station has been factored out in the denominator.

The sum of the phase terms is

$$\begin{aligned}e^{-jk\sqrt{r^2+2h_{\text{t}}h_{\text{r}}+h_{\text{r}}^2}} + e^{-jk\sqrt{r^2-2h_{\text{t}}h_{\text{r}}+h_{\text{r}}^2}} &\approx e^{-jk\sqrt{r^2+2h_{\text{t}}h_{\text{r}}}} + e^{-jk\sqrt{r^2-2h_{\text{t}}h_{\text{r}}}} \\ &= e^{-jkr\sqrt{1+2h_{\text{t}}h_{\text{r}}/r^2}} + e^{-jkr\sqrt{1-2h_{\text{t}}h_{\text{r}}/r^2}} \\ &\approx e^{-jkr} \left(e^{-jkh_{\text{t}}h_{\text{r}}/r} + e^{jkh_{\text{t}}h_{\text{r}}/r} \right) \\ &= 2e^{-jkr} \cos \left(\frac{kh_{\text{t}}h_{\text{r}}}{r} \right),\end{aligned} \tag{3.81}$$

so after reflection the far field electric field has the form

$$\mathbf{E} = j\omega A_0 \cos \theta_{\text{A}} \left(\sin \theta_{\text{A}} \hat{\mathbf{y}} - \cos \theta_{\text{A}} \hat{\mathbf{z}}\right) \frac{1}{r} 2e^{-jkr} \cos \left(\frac{kh_{\text{t}}h_{\text{r}}}{r} \right). \tag{3.82}$$

This differs from the line of sight field by a factor of $2 \cos \left(kh_{\text{t}}h_{\text{r}}/r\right)$.

Numerical results. The wavelength is

$$\lambda = c/\nu = \frac{3 \times 10^8 \text{m/s}}{900 \times 10^6 \text{s}^{-1}} = 0.33 \text{m}, \tag{3.83}$$

so the cosine argument is

$$kh_{\text{t}}h_{\text{r}}/r = \frac{2\pi \times 50 \times 1.5}{0.33 \times 5000.25} = 0.28, \tag{3.84}$$

and the cosine adjustment to the field strength is

$$2 \cos 0.28 = 1.92. \tag{3.85}$$

The mobile gain is

$$G = 10^{2.55\text{dB}/10} = 1.8. \tag{3.86}$$

Noting that EIRP $= P_t G_t$, the Friis transmission equation, after adjusting for the reflection effects, provides the power at the mobile

$$\begin{aligned} P_r &= \left(\frac{\lambda}{4\pi r}\right)^2 (P_t G_t)\, G_r (1.92)^2 \\ &= \left(\frac{0.33}{4\pi\, 5000.25}\right)^2 \left(30 \times 10^{-3}\right) \times 1.8 \times (1.92)^2 \text{W} \\ &= 5.6 \times 10^{-12}\, \text{W}. \end{aligned} \tag{3.87}$$

The total power received is just 5.6 pW, assuming no polarization losses (we know the polarization at the mobile, but not for the base station.) In an attempt to avoid calculator errors for this problem I scripted the numerical calculations in ps2p5.jl. That wasn't entirely successful on submission, since I used 5 m instead of 1.5 m!

Exercise 3.3 Dipole superposition. (*2015 ps3, p1*)

An infinitesimal electric dipole of electric current strength I_{eo} is oriented along the x-axis. With this there is also an infinitesimal magnetic dipole of magnetic current strength I_{mo} but oriented along the y-axis.

a. Write down an expression for the total electric field radiated in the far zone.
b. Assume now that $I_{eo}/I_{mo} = \eta_o = 120\pi\Omega$. Simplify the electric field expression found part a.
c. Plot in polar co-ordinates the normalized magnitude of the electric field in the zy plane and for $0 < \theta \leq 2\pi$ (far zone).

Answer for Exercise 3.3

Part a. The far field electric field induced by the electric current can be calculated with the transverse projection

$$\begin{aligned} \mathbf{E}_\mathrm{e} &= -j\omega \operatorname{Proj}_\mathrm{T} \mathbf{A} \\ &= -j\omega \left(\mathbf{A} - (\mathbf{A} \cdot \hat{\mathbf{k}})\hat{\mathbf{k}} \right), \end{aligned} \tag{3.88}$$

where

$$\mathbf{A} = \hat{\mathbf{x}} \frac{\mu_0 I_\mathrm{eo} l}{4\pi r} e^{-jkr}. \tag{3.89}$$

To simplify this, note that the Cartesian to spherical coordinates mapping is

$$\hat{\mathbf{x}} = \sin\theta\cos\phi\hat{\mathbf{k}} + \cos\theta\cos\phi\hat{\boldsymbol{\theta}} - \sin\phi\hat{\boldsymbol{\phi}} \tag{3.90a}$$

$$\hat{\mathbf{y}} = \sin\theta\sin\phi\hat{\mathbf{k}} + \cos\theta\sin\phi\hat{\boldsymbol{\theta}} + \cos\phi\hat{\boldsymbol{\phi}} \tag{3.90b}$$

$$\hat{\mathbf{z}} = \cos\theta\hat{\mathbf{k}} - \sin\theta\hat{\boldsymbol{\theta}}, \tag{3.90c}$$

so

$$\mathbf{E}_\mathrm{e} = -j\omega \left(\cos\theta\cos\phi\hat{\boldsymbol{\theta}} - \sin\phi\hat{\boldsymbol{\phi}} \right) \frac{\mu_0 I_\mathrm{eo} l}{4\pi r} e^{-jkr}. \tag{3.91}$$

For the magnetic current, first note that the far field magnetic field for an electric current can also be expressed in terms of the magnetic vector potential

$$\begin{aligned} \mathbf{H} &= \frac{1}{\eta} \hat{\mathbf{k}} \times \mathbf{E} \\ &= -j\frac{\omega}{\eta} \hat{\mathbf{k}} \times \left(\mathbf{A} - (\mathbf{A} \cdot \hat{\mathbf{k}})\hat{\mathbf{k}} \right) \\ &= -j\frac{\omega}{\eta} \hat{\mathbf{k}} \times \mathbf{A}. \end{aligned} \tag{3.92}$$

Duality provides the far field electric field given an electric vector potential

$$\mathbf{E}_\mathrm{m} = j\omega\eta\hat{\mathbf{k}} \times \mathbf{F}. \tag{3.93}$$

For the y-axis oriented magnetic current, the vector potential is

$$\mathbf{F} = \hat{\mathbf{y}} \frac{\epsilon_0 I_\mathrm{mo} l}{4\pi r} e^{-jkr}. \tag{3.94}$$

The electric field will be directed along

$$\begin{aligned}\hat{\mathbf{k}} \times \hat{\mathbf{y}} &= \hat{\mathbf{k}} \times \left(\sin\theta\sin\phi\hat{\mathbf{k}} + \cos\theta\sin\phi\hat{\boldsymbol{\theta}} + \cos\phi\hat{\boldsymbol{\phi}}\right) \\ &= \cos\theta\sin\phi\hat{\boldsymbol{\phi}} - \cos\phi\hat{\boldsymbol{\theta}},\end{aligned} \tag{3.95}$$

so

$$\mathbf{E}_\mathrm{m} = j\omega\eta\left(\cos\theta\sin\phi\hat{\boldsymbol{\phi}} - \cos\phi\hat{\boldsymbol{\theta}}\right)\frac{\epsilon_0 I_\mathrm{mo} l}{4\pi r} e^{-jkr}. \tag{3.96}$$

Summing eq. (3.91), and eq. (3.96) gives

$$\begin{aligned}\mathbf{E} = j\omega \frac{l}{4\pi r} e^{-jkr}\eta\epsilon_0 \big(&\left(-\cos\theta\cos\phi\hat{\boldsymbol{\theta}} + \sin\phi\hat{\boldsymbol{\phi}}\right)\eta I_\mathrm{eo} \\ &+ \left(\cos\theta\sin\phi\hat{\boldsymbol{\phi}} - \cos\phi\hat{\boldsymbol{\theta}}\right) I_\mathrm{mo}\big).\end{aligned} \tag{3.97}$$

Part b. When $\eta I_\mathrm{eo} = I_\mathrm{mo}$, this reduces to

$$\mathbf{E} = j\omega\frac{\mu_0 I_\mathrm{eo} l}{4\pi r} e^{-jkr}\left(1 + \cos\theta\right)\left(-\cos\phi\hat{\boldsymbol{\theta}} + \sin\phi\hat{\boldsymbol{\phi}}\right). \tag{3.98}$$

A view of this vector function are plotted in fig. 3.13 showing the electric and magnetic far field vector directions on the surface of the electric field magnitude. See electricAndMagneticDipoleSuperpositionStandalone.cdf for an interactive view of these plots, with θ, ϕ controls available for the wave vector position.

Part c. In the zy plane, $\phi = \pi/2$, and the electric field has only a $\hat{\boldsymbol{\phi}}$ component

$$\mathbf{E} = j\omega\frac{\mu_0 I_\mathrm{eo} l}{4\pi r} e^{-jkr}\left(1 + \cos\theta\right)\hat{\boldsymbol{\phi}}. \tag{3.99}$$

The magnitude of the θ variation in the $[0, 2\pi]$ interval is plotted in fig. 3.14.

Exercise 3.4 Long thin wire dipoles. (*2015 ps3, p2*)

a. On a single diagram, plot the polar patterns for $l = 0.5\lambda, l = 1.0\lambda, l = 1.25\lambda$ and $l = 2.0\lambda$ long thin wire dipole antennas.
b. Use numerical integration to calculate the maximum directivity for each dipole. Make a table with your results. Which length corresponds to the highest directivity?

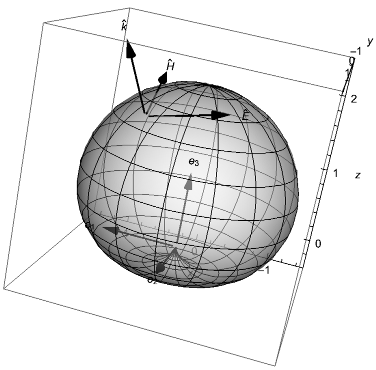

Figure 3.13: Electric and magnetic infinitesimal dipole superposition, view from above.

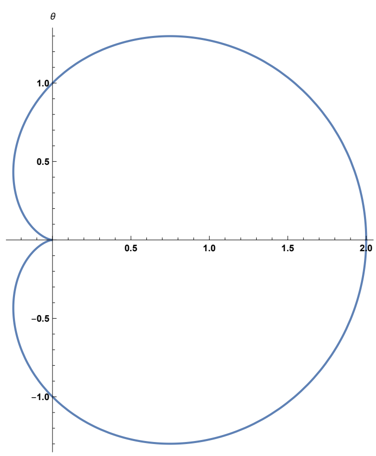

Figure 3.14: Electric and magnetic infinitesimal dipole superposition, polar plot in ZY plane.

c. Use numerical integration to calculate the radiation resisistance of the $l = 1.25\lambda$ dipole. Do you expect this dipole to be capacitive or inductive?

Answer for Exercise 3.4

Part a. Assuming a $\hat{\mathbf{z}}$ oriented dipole, in the far field, the electric field is

$$E_\theta \approx j\eta \frac{I_0 e^{-jkr}}{2\pi r} \left(\frac{\cos\left(\frac{kl}{2}\cos\theta\right) - \cos\left(\frac{kl}{2}\right)}{\sin\theta} \right). \tag{3.100}$$

Writing $l = \alpha\lambda$, and noting that the magnetic field is $H_\phi \approx E_\theta/\eta$, the radiation intensity $U = r^2 W_{\text{av}}$ is

$$U = \eta \frac{|I_0|^2}{8\pi^2} \left(\frac{\cos(\pi\alpha\cos\theta) - \cos(\pi\alpha)}{\sin\theta} \right)^2. \tag{3.101}$$

In fig. 3.15 $F(\theta) = 8\pi^2 U/\eta|I_0|^2$ is plotted for $\alpha \in \{0.5, 1, 1.25, 2.0\}$. For $\alpha = 1.25$ some very small side lobes are just barely visible. For $\alpha = 2$ the single lobe directivity is lost, and a significant split of the radiation field along two different directions can be observed. These individual features can be explored more easily in longDipolesWithLengthControl.cdf which provides a Manipulate based interactive control for varying the l/λ ratio. It is much more satisfactory to view these in a three dimensional plot as in ps3:longDipoleInteractiveLength.nb, and fig. 3.16, but such a visualization does not work well for overlaid intensity patterns. The side lobes for the $\alpha = 1.25$ case do not show up very well in the plot above. The log polar plot of fig. 3.17 shows this detail better.

Part b. The directivity is given by

$$D_0 = \frac{4\pi F(\theta)|_{\max}}{2\pi \int_0^\pi F(\theta)\sin\theta d\theta}. \tag{3.102}$$

These values, calculated in ps3:directivityLongDipole.nb using the Mathematica functions NMaximize and NIntegrate, are The largest directivity for these specific values of l is found at $l = 1.25\lambda$.

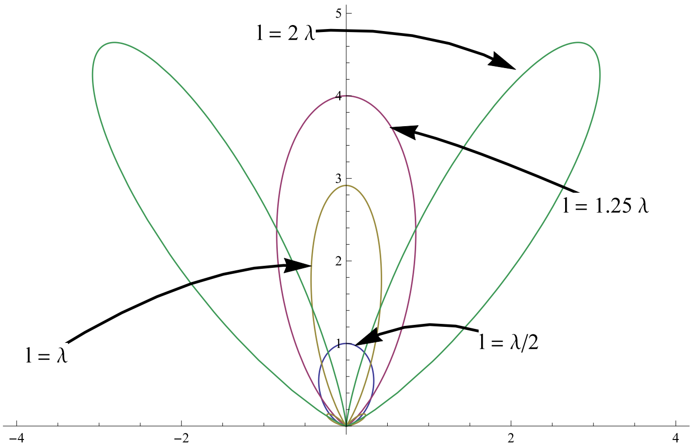

Figure 3.15: Polar plot of radiation intensities for some electric z-axis oriented dipoles.

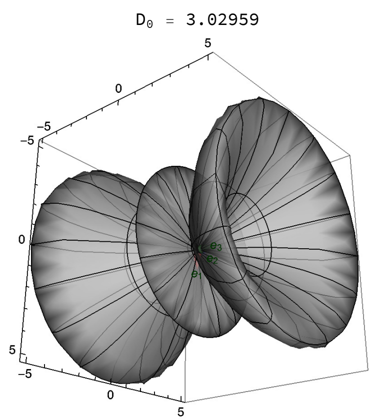

Figure 3.16: Double wavelength radiation intensity.

Table 3.1: Directivities.

α	0.5	1	1.25	2
D_0	1.64092	2.411	3.28248	2.52856

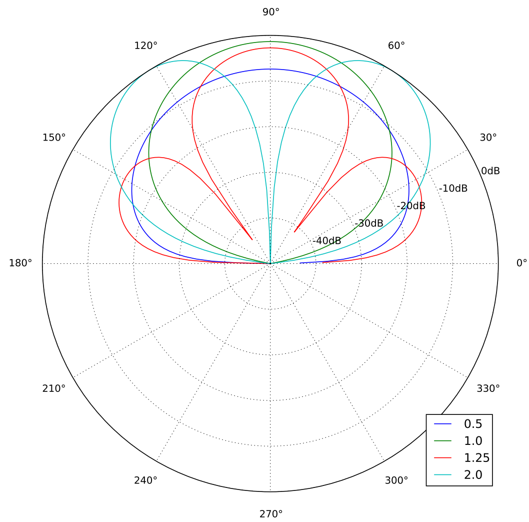

Figure 3.17: Log polar plot of radiation intensities for some electric z-axis oriented dipoles.

Part c. The radiation resistance is implicitly defined by

$$P_{\text{rad}} = \int U d\Omega = \frac{1}{2} |I_0|^2 R_{\text{r}}, \tag{3.103}$$

or, with $\eta = 120\pi\Omega$,

$$\begin{aligned} R_{\text{r}} &= \frac{2}{|I_0|^2} \int U d\Omega \\ &= 120\pi \frac{1}{4\pi^2} \int_0^{2\pi} d\phi \int_0^{\pi} \left(\frac{\cos(\pi\alpha\cos\theta) - \cos(\pi\alpha)}{\sin\theta} \right)^2 \sin\theta d\theta \\ &= 60 \int_0^{\pi} \frac{(\cos(\pi\alpha\cos\theta) - \cos(\pi\alpha))^2}{\sin\theta} d\theta. \end{aligned} \tag{3.104}$$

See ps3:longDipolesSelectedLengths.nb for the numerical integration using the the lengths in this problem. The half-wavelength number calculated matches the value quoted in [5] eq. 4-93.

For the reactance, without calculating, I don't know an intuitive way to determine whether it would be positive or negative for any given length. The graph of [5] fig. 8.17 appears to show that the

Table 3.2: Radiation resistances.

α	0.5	1	1.25	2
R_r	73.1296	199.088	106.537	259.634

reactance is roughly positive (inductive) in the $[0.5, 1]\lambda$ interval and negative (capacitive) in the $[1, 1.5]\lambda$ interval.

4 ANTENNA ARRAYS.

4.1 CHEBYSCHEFF POLYNOMIALS.

In ancient times (i.e. 2nd year undergrad) I recall being very impressed with Chebyscheff polynomials for designing lowpass filters. I'd used Chebyscheff filters for the hardware we used for a speech recognition system our group built in the design lab. One of the benefits of these polynomials is that the oscillation in the $|x| < 1$ interval is strictly bounded. This same property, as well as the unbounded nature outside of the $[-1, 1]$ interval turns out to have applications to antenna array design.

The Chebyscheff polynomials are defined by

$$T_m(x) = \cos\left(m \cos^{-1} x\right), \quad |x| < 1 \tag{4.1a}$$

$$T_m(x) = \cosh\left(m \cosh^{-1} x\right), \quad |x| > 1. \tag{4.1b}$$

Range restrictions and hyperbolic form. Prof. Eleftheriades's notes made a point to point out the definition in the $|x| > 1$ interval, but that can also be viewed as a consequence instead of a definition if the range restriction is removed. For example, suppose $x = 7$, and let

$$\cos^{-1} 7 = \theta, \tag{4.2}$$

so

$$\begin{aligned} 7 &= \cos\theta \\ &= \frac{e^{j\theta} + e^{-j\theta}}{2} \\ &= \cosh(\pm j\theta), \end{aligned} \tag{4.3}$$

or

$$\mp j \cosh^{-1} 7 = \theta. \tag{4.4}$$

$$\begin{aligned} T_m(7) &= \cos(\mp mj \cosh^{-1} 7) \\ &= \cosh(m \cosh^{-1} 7). \end{aligned} \tag{4.5}$$

The same argument clearly applies to any other value outside of the $|x| < 1$ range, so without any restrictions, these polynomials can be defined as just

$$\boxed{T_m(x) = \cos\left(m \cos^{-1} x\right).} \tag{4.6}$$

Polynomial nature. Equation (4.6) does not obviously look like a polynomial. Let's proceed to verify the polynomial nature for the first couple values of m.

- $m = 0$.

$$\begin{aligned} T_0(x) &= \cos(0 \cos^{-1} x) \\ &= \cos(0) \\ &= 1. \end{aligned} \tag{4.7}$$

- $m = 1$.

$$\begin{aligned} T_1(x) &= \cos(1 \cos^{-1} x) \\ &= x. \end{aligned} \tag{4.8}$$

- $m = 2$.

$$\begin{aligned} T_2(x) &= \cos(2 \cos^{-1} x) \\ &= 2\cos^2 \cos^{-1}(x) - 1 \\ &= 2x^2 - 1. \end{aligned} \tag{4.9}$$

To examine the general case

$$
\begin{aligned}
T_m(x) &= \cos(m \cos^{-1} x) \\
&= \operatorname{Re} e^{jm \cos^{-1} x} \\
&= \operatorname{Re} \left(e^{j \cos^{-1} x}\right)^m \\
&= \operatorname{Re} \left(\cos \cos^{-1} x + j \sin \cos^{-1} x\right)^m \\
&= \operatorname{Re} \left(x + j\sqrt{1 - x^2}\right)^m \\
&= \operatorname{Re} \left(x^m + \binom{m}{1} j x^{m-1} \left(1 - x^2\right)^{1/2} - \binom{m}{2} x^{m-2} \left(1 - x^2\right)^{2/2} \right. \\
&\qquad \left. - \binom{m}{3} j x^{m-3} \left(1 - x^2\right)^{3/2} + \binom{m}{4} x^{m-4} \left(1 - x^2\right)^{4/2} + \cdots \right) \\
&= x^m - \binom{m}{2} x^{m-2} \left(1 - x^2\right) + \binom{m}{4} x^{m-4} \left(1 - x^2\right)^2 - \cdots
\end{aligned}
\tag{4.10}
$$

This expansion was a bit cavalier with the signs of the $\sin \cos^{-1} x = \sqrt{1 - x^2}$ terms, since the negative sign should be picked for the root when $x \in [-1, 0]$. However, that doesn't matter in the end since the real part operation selects only powers of two of this root.

The final result of the expansion above can be written

$$
T_m(x) = \sum_{k=0}^{\lfloor m/2 \rfloor} \binom{m}{2k} (-1)^k x^{m-2k} \left(1 - x^2\right)^k . \tag{4.11}
$$

This clearly shows the polynomial nature of these functions, and is also perfectly well defined for any value of x. The even and odd alternation with m is also clear in this explicit expansion.

Some plots. The first couple polynomials are plotted in fig. 4.1.

Properties. In [1] a few properties can be found for these polynomials

$$
T_m(x) = 2x T_{m-1} - T_{m-2}, \tag{4.12a}
$$

$$
0 = \left(1 - x^2\right) \frac{dT_m(x)}{dx} + m x T_m(x) - m T_{m-1}(x), \tag{4.12b}
$$

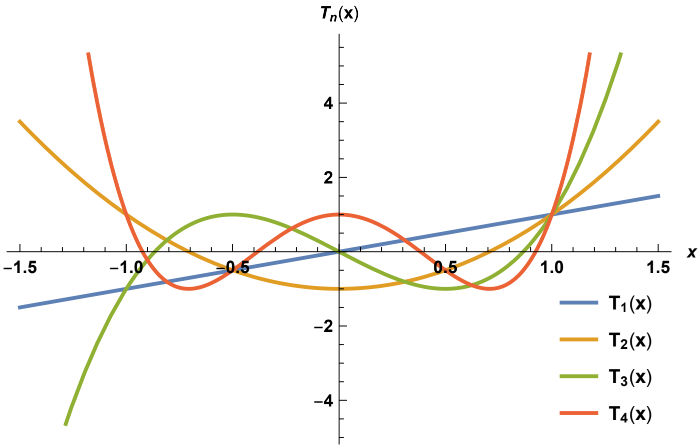

Figure 4.1: A couple Cheybshev plots.

$$0 = \left(1 - x^2\right) \frac{d^2 T_m(x)}{dx^2} - x \frac{dT_m(x)}{dx} + m^2 T_m(x), \tag{4.12c}$$

$$\int_{-1}^{1} \frac{1}{\sqrt{1-x^2}} T_m(x) T_n(x) dx = \begin{cases} 0 & \text{if } m \neq n \\ \pi & \text{if } m = n = 0 \\ \pi/2 & \text{if } m = n, m \neq 0. \end{cases} \tag{4.12d}$$

Example 4.1: Cheybshev antenna design.

In our text [5] is a design procedure that applies Cheybshev polynomials to the selection of current magnitudes for an evenly spaced array of identical antennas placed along the z-axis.

For an even number $2M$ of identical antennas placed at positions $\mathbf{r}_m = (d/2)\,(2m-1)\,\mathbf{e}_3$, the array factor is

$$\text{AF} = \sum_{m=-N}^{N} I_m e^{jk\hat{\mathbf{r}}\cdot\mathbf{r}_m}. \tag{4.13}$$

Assuming the currents are symmetric $I_{-m} = I_m$, with $\hat{\mathbf{r}} = (\sin\theta\cos\phi, \sin\theta\sin\phi, \cos\theta)$, and $u = \frac{\pi d}{\lambda}\cos\theta$, this is

$$\begin{aligned}
\text{AF} &= \sum_{m=-N}^{N} I_m e^{jk(d/2)(2m-1)\cos\theta} \\
&= 2\sum_{m=1}^{N} I_m \cos\left(k(d/2)(2m-1)\cos\theta\right) \\
&= 2\sum_{m=1}^{N} I_m \cos\left((2m-1)u\right).
\end{aligned} \tag{4.14}$$

This is a sum of only odd cosines, and can be expanded as a sum that includes all the odd powers of $\cos u$. Suppose for example that this is a four element array with $N = 2$. In this case the array factor has the form

$$\begin{aligned}
\text{AF} &= 2\left(I_1\cos u + I_2\left(4\cos^3 u - 3\cos u\right)\right) \\
&= 2\left((I_1 - 3I_2)\cos u + 4I_2\cos^3 u\right).
\end{aligned} \tag{4.15}$$

The design procedure in the text sets $\cos u = z/z_0$, and then equates this to $T_3(z) = 4z^3 - 3z$ to determine the current amplitudes I_m. That is

$$\frac{2I_1 - 6I_2}{z_0} z + \frac{8I_2}{z_0^3} z^3 = -3z + 4z^3, \tag{4.16}$$

or

$$\begin{aligned}
\begin{bmatrix} I_1 \\ I_2 \end{bmatrix} &= \begin{bmatrix} 2/z_0 & -6/z_0 \\ 0 & 8/z_0^3 \end{bmatrix}^{-1} \begin{bmatrix} -3 \\ 4 \end{bmatrix} \\
&= \frac{z_0}{2}\begin{bmatrix} 3(z_0^2 - 1) \\ z_0^2 \end{bmatrix}.
\end{aligned} \tag{4.17}$$

The currents in the array factor are fully determined up to a scale factor, reducing the array factor to

$$\text{AF} = 4z_0^3\cos^3 u - 3z_0\cos u. \tag{4.18}$$

The zeros of this array factor are located at the zeros of

$$T_3(z_0 \cos u) = \cos(3 \cos^{-1}(z_0 \cos u)), \tag{4.19}$$

which are at $3 \cos^{-1}(z_0 \cos u) = \pi/2 + m\pi = \pi\left(m + \frac{1}{2}\right)$

$$\begin{aligned} \cos u &= \frac{1}{z_0} \cos\left(\frac{\pi}{3}\left(m + \frac{1}{2}\right)\right) \\ &= \left\{0, \pm\frac{\sqrt{3}}{2z_0}\right\}. \end{aligned} \tag{4.20}$$

showing that the scaling factor z_0 effects the locations of the zeros. It also allows the values at the extremes $\cos u = \pm 1$, to increase past the ± 1 non-scaled limit values. These effects can be explored in `http://goo.gl/KPqcjX`, but can also be seen in fig. 4.2.

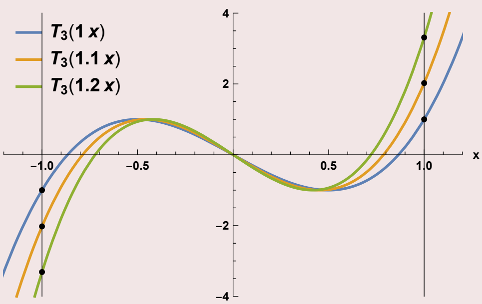

Figure 4.2: $T_3(z_0 x)$ for a few different scale factors z_0.

The scale factor can be fixed for a desired maximum power gain. For RdB, that will be when

$$20 \log_{10} \cosh(3 \cosh^{-1} z_0) = R\text{dB}, \tag{4.21}$$

or

$$z_0 = \cosh\left(\frac{1}{3} \cosh^{-1}\left(10^{\frac{R}{20}}\right)\right). \tag{4.22}$$

For $R = 30$ dB (say), we have $z_0 = 2.1$, and

$$\text{AF} = 40\cos^3\left(\frac{\pi d}{\lambda}\cos\theta\right) - 6.4\cos\left(\frac{\pi d}{\lambda}\cos\theta\right). \qquad (4.23)$$

These are plotted in fig. 4.3 for a couple values of d/λ.

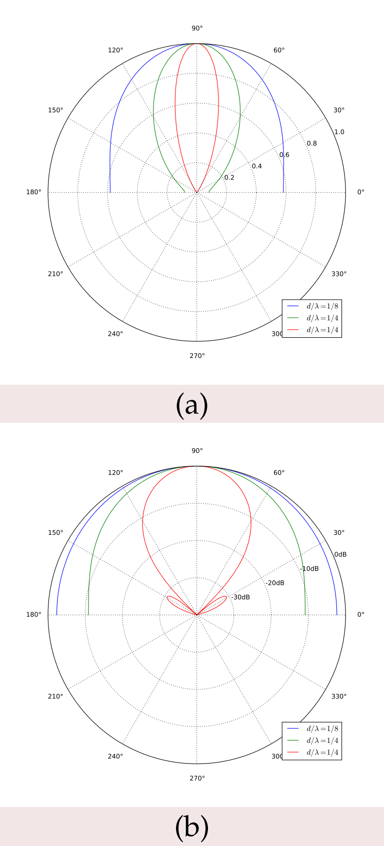

Figure 4.3: T_3 fitting of $N = 4$ array in linear and dB scales.

A Manipulate for exploring the d/λ dependence is available in `http://goo.gl/8FhUwC`.

Dolph-Cheybshev design procedure from class notes. Prof. Eleftheriades described a Cheybshev antenna array design method that looks different than the one of the text [5]. Portions of that procedure are like that of the text. For example, if a side lobe level of $20 \log_{10} R$ is desired, a scaling factor

$$x_0 = \cosh\left(\frac{1}{m}\cosh^{-1} R\right), \tag{4.24}$$

is used. Given N elements in the array, a Cheybshev polynomial of degree $m = N - 1$ is used. That is

$$T_m(x) = \cos\left(m \cos^{-1} x\right). \tag{4.25}$$

Observe that the roots x'_n of this polynomial lie where

$$m \cos^{-1} x'_n = \frac{\pi}{2} \pm \pi n, \tag{4.26}$$

or

$$x'_n = \cos\left(\frac{\pi}{2m}(2n \pm 1)\right). \tag{4.27}$$

The class notes use the negative sign, and number $n = 1, 2, \cdots, m$. It is noted that the roots are symmetric with $x'_1 = -x'_m$, which can be seen by direct expansion

$$\begin{aligned}
x'_{m-r} &= \cos\left(\frac{\pi}{2m}(2(m-r)-1)\right) \\
&= \cos\left(\pi - \frac{\pi}{2m}(2r+1)\right) \\
&= -\cos\left(\frac{\pi}{2m}(2r+1)\right) \\
&= -\cos\left(\frac{\pi}{2m}(2(r+1)-1)\right) \\
&= -x'_{r+1}. \qquad \square
\end{aligned} \tag{4.28}$$

The next step in the procedure is the identification

$$\begin{aligned}
u'_n &= 2\cos^{-1}\left(\frac{x'_n}{x_0}\right) \\
z_n &= e^{j u'_n}.
\end{aligned} \tag{4.29}$$

This has a factor of two that does not appear in the Balanis design method. It seems plausible that this factor of two was introduced so that the roots of the array factor z_n are conjugate pairs. Since $\cos^{-1}(-z) = \pi - \cos^{-1} z$, this choice leads to such conjugate pairs

$$\begin{aligned}\exp\left(ju'_{m-r}\right) &= \exp\left(j2\cos^{-1}\left(\frac{x'_{m-r}}{x_0}\right)\right) \\ &= \exp\left(j2\cos^{-1}\left(-\frac{x'_{r+1}}{x_0}\right)\right) \\ &= \exp\left(j2\left(\pi - \cos^{-1}\left(\frac{x'_{r+1}}{x_0}\right)\right)\right) \\ &= \exp\left(-ju_{r+1}\right).\end{aligned} \tag{4.30}$$

Because of this, the array factor can be written

$$\begin{aligned}\text{AF} &= (z - z_1)(z - z_2)\cdots(z - z_{m-1})(z - z_m) \\ &= (z - z_1)(z - z_1^*)(z - z_2)(z - z_2^*)\cdots \\ &= \left(z^2 - z(z_1 + z_1^*) + 1\right)\left(z^2 - z(z_2 + z_2^*) + 1\right)\cdots \\ &= \left(z^2 - 2z\cos\left(2\cos^{-1}\left(\frac{x'_1}{x_0}\right)\right) + 1\right) \times \\ &\quad \left(z^2 - 2z\cos\left(2\cos^{-1}\left(\frac{x'_2}{x_0}\right)\right) + 1\right)\cdots \\ &= \left(z^2 - 2z\left(2\left(\frac{x'_1}{x_0}\right)^2 - 1\right) + 1\right) \\ &\quad \left(z^2 - 2z\left(2\left(\frac{x'_2}{x_0}\right)^2 - 1\right) + 1\right)\cdots\end{aligned} \tag{4.31}$$

When m is even, there will only be such conjugate pairs of roots. When m is odd, the remaining factor will be

$$z - e^{2j\cos^{-1}(0/x_0)} = z - e^{2j\pi/2} = z - e^{j\pi} = z + 1. \tag{4.32}$$

However, with this factor of two included, the connection between the final array factor polynomial eq. (4.31), and the Cheybshev polynomial T_m is not clear to me. How does this scaling impact the roots?

Example 4.2: Expand AF for $N = 4$.

The roots of $T_3(x)$ are

$$x'_n \in \left\{ 0, \pm\frac{\sqrt{3}}{2} \right\}, \tag{4.33}$$

so the array factor is

$$\begin{aligned} \text{AF} &= \left(z^2 + z\left(2 - \frac{3}{x_0^2}\right) + 1 \right)(z+1) \\ &= z^3 + 3z^2\left(1 - \frac{1}{x_0^2}\right) + 3z\left(1 - \frac{1}{x_0^2}\right) + 1. \end{aligned} \tag{4.34}$$

With $20\log_{10} R = 30\text{dB}$, $x_0 = 2.1$, so this is

$$\text{AF} = z^3 + 2.33089z^2 + 2.33089z + 1. \tag{4.35}$$

With

$$\begin{aligned} z &= e^{j(u+u_0)} \\ &= e^{jkd\cos\theta + jku_0}, \end{aligned} \tag{4.36}$$

the array factor takes the form

$$\begin{aligned} \text{AF} = e^{j3kd\cos\theta + j3ku_0} &+ 2.33089e^{j2kd\cos\theta + j2ku_0} \\ &+ 2.33089e^{jkd\cos\theta + jku_0} + 1. \end{aligned} \tag{4.37}$$

This array function is highly phase dependent, plotted for $u_0 = 0$ in fig. 4.4.

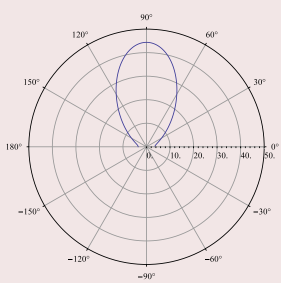

Figure 4.4: Plot with $u_0 = 0, d = \lambda/4$.

This can be directed along a single direction (z-axis) with higher phase choices as illustrated in fig. 4.5.

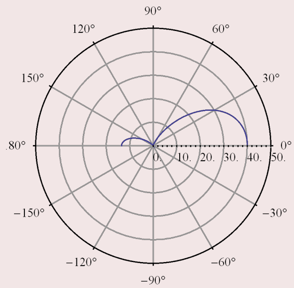

Figure 4.5: Plot with $u_0 = 3.5, d = 0.4\lambda$.

See ChebychevSecondMethod.nb for an interactive exploration of the parameters.

4.2 PROBLEMS.

Exercise 4.1 Corner cube antenna. (*2015 ps3, p3*)

Consider the symmetrically placed horizontal dipole antenna of fig. 3.80.2 , next to a metallic corner cube.

a. Calculate the array factor of the antenna in fig. 3.8.
b. Estimate the directivity enhancement of the antenna in fig. 3.8 compared to the isolated antenna.
c. Estimate the radiation resistance of the antenna in fig. 3.8 compared to the isolated antenna.
d. Plot the array-factor directivity pattern in the x-y plane for $0 < \phi \le 2\pi$.
e. By using numerical integration calculate the directivity of the array factor for $h = (1/8)\lambda, h = (1/4)\lambda$ and $h = (1/2)\lambda$.

Answer for Exercise 4.1

Part a. This problem can be tackled with the image theorem, which requires placement of sources as in fig. 3.10. The sources are located one in each quadrant

$$\begin{aligned}
\mathbf{s}_1 &= h\,(1,1,0) \\
\mathbf{s}_2 &= h\,(-1,1,0) \\
\mathbf{s}_3 &= h\,(-1,-1,0) \\
\mathbf{s}_4 &= h\,(1,-1,0)\,,
\end{aligned} \tag{4.38}$$

and the point of measurement at $\mathbf{r} = r\hat{\mathbf{r}} = r(\sin\theta\cos\phi, \sin\theta\sin\phi, \cos\theta)$. If $\mathbf{r}_m = \mathbf{r} - \mathbf{s}_m$ is the distance from the mth source to the observation point, then the squared distance is

$$\begin{aligned}
r_m &= \left|\mathbf{r} - \mathbf{s}_m\right| \\
&= \left(r^2 + \mathbf{s}_m^2 - 2\mathbf{r}\cdot\mathbf{s}_m\right)^{1/2} \\
&= r\left(1 + \frac{\mathbf{s}_m^2}{r^2} - 2\frac{\hat{\mathbf{r}}}{r}\cdot\mathbf{s}_m\right)^{1/2} \\
&\approx r\left(1 + \frac{1}{2}\frac{\mathbf{s}_m^2}{r^2} - \frac{\hat{\mathbf{r}}}{r}\cdot\mathbf{s}_m\right) \\
&= r + \frac{1}{2}\frac{\mathbf{s}_m^2}{r} - \hat{\mathbf{r}}\cdot\mathbf{s}_m \\
&\approx r - \hat{\mathbf{r}}\cdot\mathbf{s}_m.
\end{aligned} \tag{4.39}$$

Those distances are

$$\hat{\mathbf{r}}\cdot\mathbf{s}_1 = h\sin\theta\,(\cos\phi + \sin\phi) = \sqrt{2}h\sin\theta\cos\left(\phi - \pi/4\right) \tag{4.40a}$$

$$\hat{\mathbf{r}}\cdot\mathbf{s}_2 = h\sin\theta\,(-\cos\phi + \sin\phi) = -\sqrt{2}h\sin\theta\cos\left(\phi + \pi/4\right) \tag{4.40b}$$

$$\hat{\mathbf{r}}\cdot\mathbf{s}_3 = -h\sin\theta\,(\cos\phi + \sin\phi) = -\sqrt{2}h\sin\theta\cos\left(\phi - \pi/4\right) \tag{4.40c}$$

$$\hat{\mathbf{r}}\cdot\mathbf{s}_4 = h\sin\theta\,(\cos\phi - \sin\phi) = \sqrt{2}h\sin\theta\cos\left(\phi + \pi/4\right). \tag{4.40d}$$

Suppose the magnetic vector potential has the structure of an infinitesimal dipole

$$\mathbf{A}_m = \frac{\mu_0 I_0}{4\pi r_m} e^{-jkr_m}\hat{\mathbf{z}}. \tag{4.41}$$

In the far field, the direction vectors for all the fields will be approximately

$$\begin{aligned}\hat{\mathbf{z}} - (\hat{\mathbf{z}} \cdot \hat{\mathbf{r}})\,\hat{\mathbf{r}} &= \cos\theta\hat{\mathbf{r}} - \sin\theta\hat{\boldsymbol{\theta}} - \cos\theta\hat{\mathbf{r}} \\ &= -\sin\theta\hat{\boldsymbol{\theta}}.\end{aligned} \tag{4.42}$$

The far field electric field for each image source is approximately

$$\begin{aligned}\mathbf{E}_m &= -j\omega\mathbf{A}_T \\ &= j\omega\frac{\mu_0 I_0}{4\pi r}e^{-jkr_m}\sin\theta\hat{\boldsymbol{\theta}} \\ &= j\eta k\frac{I_0}{4\pi r}e^{-jkr_m}\sin\theta\hat{\boldsymbol{\theta}}.\end{aligned} \tag{4.43}$$

Writing $s = \sqrt{2}h$ for the distance from the origin to each of the image sources, the superposition of all the image sources is

$$\begin{aligned}\mathbf{E} = j\eta k\frac{I_0}{4\pi r}e^{-jkr}\sin\theta\Bigg(&e^{jks\sin\theta\cos(\phi-\pi/4)} - e^{-jks\sin\theta\cos(\phi+\pi/4)} \\ &+ e^{-jks\sin\theta\cos(\phi-\pi/4)} - e^{jks\sin\theta\cos(\phi+\pi/4)}\Bigg)\hat{\boldsymbol{\theta}},\end{aligned} \tag{4.44}$$

or

$$\begin{aligned}\mathbf{E} = 2j\eta k\frac{I_0}{4\pi r}e^{-jkr}\sin\theta\,&\left(\cos\left(ks\sin\theta\cos\left(\phi-\pi/4\right)\right)\right. \\ &\left.-\cos\left(ks\sin\theta\cos\left(\phi+\pi/4\right)\right)\right).\end{aligned} \tag{4.45}$$

The array factor can be picked off by inspection

$$\mathrm{AF} = 2I_0\left(\cos\left(ks\sin\theta\cos\left(\phi-\pi/4\right)\right) - \cos\left(ks\sin\theta\cos\left(\phi+\pi/4\right)\right)\right). \tag{4.46}$$

Part b. The radiation intensity is

$$U = \frac{1}{2}\eta\left(\frac{kI_0}{4\pi}\right)^2\sin^2\theta|\mathrm{AF}|^2 = B_0\sin^2\theta|\mathrm{AF}|^2. \tag{4.47}$$

This holds for both isolated antenna with AF = 1, and the corner cube with $|\mathrm{AF}|^2$ given by eq. (4.46).

For the isolated antenna, the radiation intensity is maximized at $\theta = \pi/2$, so

$$\begin{aligned} D_{0,\text{iso}} &= \frac{4\pi \times 1}{2\pi \int_0^\pi \sin^3\theta d\theta} \\ &= \frac{2}{4/3} \\ &= \frac{3}{2}. \end{aligned} \tag{4.48}$$

For the corner cube the maximization problem is trickier. As a first approximation, if ks is assumed to be small, then all the cosines in eq. (4.46) are close to unity, and the array factor is zero. The next order in ks expansion of the cosines is required

$$\begin{aligned} \text{AF} &= 2I_0 \left(1 - \frac{(ks\sin\theta)^2}{2}\cos^2(\phi - \pi/4) - 1 + \frac{(ks\sin\theta)^2}{2}\cos^2(\phi + \pi/4)\right) \\ &= 2I_0 \frac{(ks\sin\theta)^2}{2}\left(-\cos^2(\phi - \pi/4) + \cos^2(\phi + \pi/4)\right) \\ &= -I_0(ks\sin\theta)^2\sin(2\phi), \end{aligned} \tag{4.49}$$

so for small ks

$$U = B_0(ks)^4 \sin^6\theta \sin^2(2\phi). \tag{4.50}$$

The radiation intensity is clearly maximized at $\phi = \pi/4, \theta = \pi/2$, so

$$U_0 = B_0(ks)^4. \tag{4.51}$$

The radiated power, again for small ks, is

$$\begin{aligned} P_{\text{rad}} &= B_0 \int_0^{\pi/2} d\phi \int_0^\pi d\theta \sin\theta U(\theta,\phi) \\ &\approx B_0(ks)^4 \int_0^{\pi/2} d\phi \sin^2(2\phi) \int_0^\pi d\theta \sin^7\theta \\ &= B_0(ks)^4 \left(\frac{\pi}{4}\right) \times \left(\frac{32}{35}\right) \\ &= B_0(ks)^4 4\pi \frac{2}{35}. \end{aligned} \tag{4.52}$$

The approximate directivity of the corner cube is

$$D_{0,\text{ccube}} \approx \frac{4\pi \times B_0(ks)^4}{B_0(ks)^4 4\pi \frac{2}{35}} = \frac{35}{2} \approx 17.5. \tag{4.53}$$

almost 12 times greater than the directivity of the isolated radiator.

The posted solution omits the $\sin^2\theta$ contribution from the element factor. That results in

$$\begin{aligned} P_{\text{rad}} &\approx B_0(ks)^4 \int_0^{\pi/2} d\phi \sin^2(2\phi) \int_0^{\pi} d\theta \sin^5\theta \\ &= B_0(ks)^4 \left(\frac{\pi}{4}\right) \times \left(\frac{16}{15}\right) \\ &= B_0(ks)^4 4\pi \frac{1}{15}, \end{aligned} \tag{4.54}$$

and

$$D_{0,\text{ccube}} \approx \frac{4\pi \times B_0(ks)^4}{B_0(ks)^4 4\pi \frac{1}{15}} = 15. \tag{4.55}$$

Note that the baseline directivity without the $\sin^2\theta$ element factor is unity, since

$$4\pi/2\pi \int_0^{\pi} \sin\theta d\theta = 1, \tag{4.56}$$

so such a relative approximation is still correct for the dipole up to an order of magnitude.

Part c. The radiation resistance was defined implicitly by the relation

$$P_{\text{rad}} = \frac{1}{2}|I_0|^2 R_{\text{r}}, \tag{4.57}$$

so the ratio of radiation resistance will just be the ratio of the radiated powers

$$\frac{R_{\text{r,ccube}}}{R_{\text{r,iso}}} = \frac{P_{\text{rad,ccube}}}{P_{\text{rad,iso}}} = \frac{8\pi(ks)^4/35}{8\pi/3} = \frac{3(ks)^4}{35}. \tag{4.58}$$

Part d. The x-y plane is found at $\theta = \pi/2$ where the array factor is

$$\mathrm{AF} = 2\left(\cos\left(2\pi\frac{s}{\lambda}\cos\left(\phi - \pi/4\right)\right) - \cos\left(2\pi\frac{s}{\lambda}\cos\left(\phi + \pi/4\right)\right)\right). \tag{4.59}$$

This is plotted against both $\alpha = s/\lambda = \sqrt{2}h/\lambda$, and ϕ in fig. 4.6, which shows that there are generally four lobes for any value of s, except for the smallest values where the pattern is near zero. This is also plotted in fig. 4.7 for a few selected values of α. To

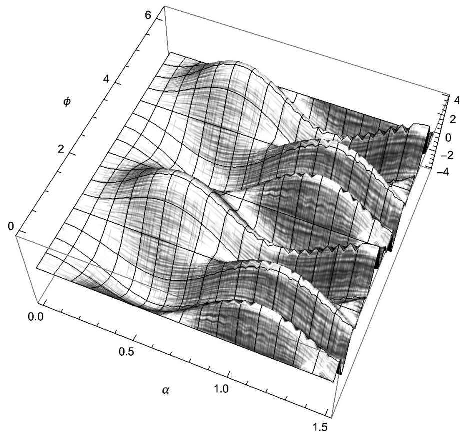

Figure 4.6: Plot of $|\mathrm{AF}|^2$ in XY plane with $\alpha = h/\lambda$.

plot the squared array factor, the physically significant range $\phi \in [0, \pi/2]$ can be used, because all of the negative sign contributions from quadrant III will be flipped into quadrant I. It's more fun to visualize this in 3D as in, and a manipulate control for visualizing $|\mathrm{AF}|^2$ is available at cornerCubeArrayFactorSq.cdf . This is plotted in fig. 4.9 for $\alpha = 0.69$.

Part e. The code for the numerical calculations can be found in ps3:ps3Q3plotsCorrected.nb. The results are

$$\begin{aligned} D_0[h = \lambda/8] &= 17.1 \\ D_0[h = \lambda/4] &= 15.9 \\ D_0[h = \lambda/2] &= 14.3. \end{aligned} \tag{4.60}$$

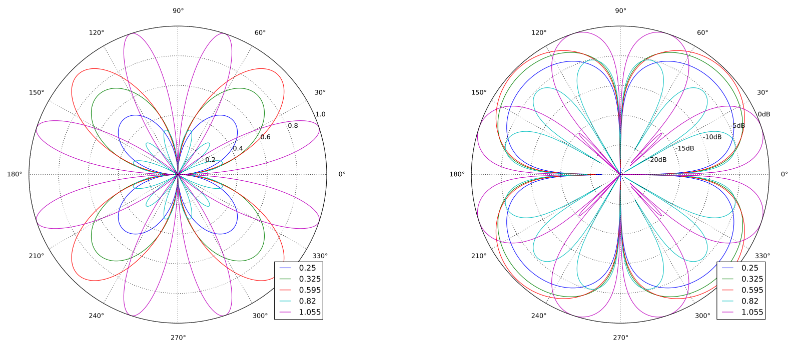

(a) (b)

Figure 4.7: Polar plot of AF in XY plane for various values of $\alpha = s/\lambda$.

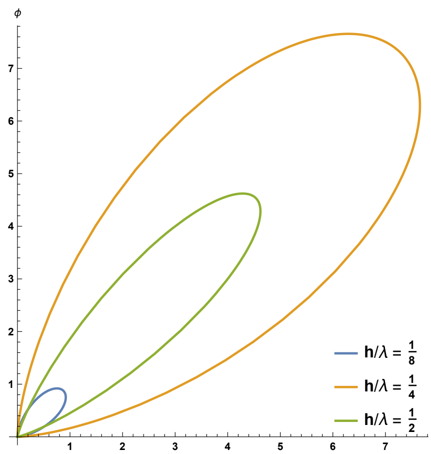

Figure 4.8: Polar plot of $|AF|^2$ for $\theta = 0$.

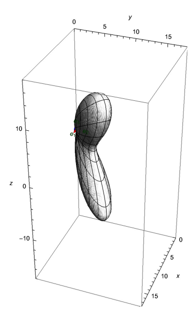

Figure 4.9: Spherical plot of $|AF|^2$ for $\alpha = 0.69$.

If the $\sin^2\theta$ contribution of the element factor is omitted (as the posted solution does in the directivity approximation), the directivities are all slightly less

$$\begin{aligned} D_0[h = \lambda/8] &= 14.6 \\ D_0[h = \lambda/4] &= 13.2 \\ D_0[h = \lambda/2] &= 15.1. \end{aligned} \tag{4.61}$$

Exercise 4.2 Chebyscheff Recurrence relation.

Prove eq. (4.12a).

Answer for Exercise 4.2

To show this, let

$$x = \cos\theta, \tag{4.62}$$

$$2xT_{m-1} - T_{m-2} = 2\cos\theta\cos((m-1)\theta) - \cos((m-2)\theta). \tag{4.63}$$

Recall the cosine addition formulas

$$\begin{aligned} \cos(a+b) &= \operatorname{Re} e^{j(a+b)} \\ &= \operatorname{Re} e^{ja} e^{jb} \\ &= \operatorname{Re} \left(\cos a + j\sin a\right)\left(\cos b + j\sin b\right) \\ &= \cos a\cos b - \sin a\sin b. \end{aligned} \tag{4.64}$$

Applying this gives

$$\begin{aligned} 2xT_{m-1} - T_{m-2} &= 2\cos\theta\left(\cos(m\theta)\cos\theta + \sin(m\theta)\sin\theta\right) \\ &\quad - \left(\cos(m\theta)\cos(2\theta) + \sin(m\theta)\sin(2\theta)\right) \\ &= 2\cos\theta\left(\cos(m\theta)\cos\theta + \sin(m\theta)\sin\theta)\right) \\ &\quad - \left(\cos(m\theta)(\cos^2\theta - \sin^2\theta) \right. \\ &\quad \left. + 2\sin(m\theta)\sin\theta\cos\theta\right) \\ &= \cos(m\theta)\left(\cos^2\theta + \sin^2\theta\right) \\ &= T_m(x). \qquad \square \end{aligned} \tag{4.65}$$

Exercise 4.3 Chebyscheff first order LDE relation.

Prove eq. (4.12b).

Answer for Exercise 4.3

To show this, again, let

$$x = \cos\theta. \tag{4.66}$$

Observe that

$$1 = -\sin\theta \frac{d\theta}{dx}, \tag{4.67}$$

so

$$\begin{aligned}\frac{d}{dx} &= \frac{d\theta}{dx}\frac{d}{d\theta} \\ &= -\frac{1}{\sin\theta}\frac{d}{d\theta}.\end{aligned} \tag{4.68}$$

Plugging this in gives

$$\begin{aligned}&\left(1 - x^2\right)\frac{d}{dx}T_m(x) + mxT_m(x) - mT_{m-1}(x) \\ &\quad = \sin^2\theta \left(-\frac{1}{\sin\theta}\frac{d}{d\theta}\right) \\ &\qquad \left(\cos(m\theta) + m\cos\theta\cos(m\theta) - m\cos((m-1)\theta)\right) \\ &\quad = -\sin\theta(-m\sin(m\theta)) + m\cos\theta\cos(m\theta) - m\cos((m-1)\theta).\end{aligned} \tag{4.69}$$

Applying the cosine addition formula eq. (4.64) gives

$$\begin{aligned}&m\left(\sin\theta\sin(m\theta) + \cos\theta\cos(m\theta)\right) \\ &\quad - m\left(\cos(m\theta)\cos\theta + \sin(m\theta)\sin\theta\right) = 0. \qquad \square\end{aligned} \tag{4.70}$$

Exercise 4.4 Chebyscheff second order LDE relation.

Prove eq. (4.12c).

Answer for Exercise 4.4

This follows the same way. The first derivative was

$$\begin{aligned}\frac{dT_m(x)}{dx} &= -\frac{1}{\sin\theta}\frac{d}{d\theta}\cos(m\theta) \\ &= -\frac{1}{\sin\theta}(-m)\sin(m\theta) \\ &= m\frac{1}{\sin\theta}\sin(m\theta),\end{aligned} \tag{4.71}$$

so the second derivative is

$$\begin{aligned}\frac{d^2T_m(x)}{dx^2} &= -m\frac{1}{\sin\theta}\frac{d}{d\theta}\frac{1}{\sin\theta}\sin(m\theta) \\ &= -m\frac{1}{\sin\theta}\left(-\frac{\cos\theta}{\sin^2\theta}\sin(m\theta) + \frac{1}{\sin\theta}m\cos(m\theta)\right).\end{aligned} \tag{4.72}$$

Putting all the pieces together gives

$$\begin{aligned}&\left(1-x^2\right)\frac{d^2T_m(x)}{dx^2} - x\frac{dT_m(x)}{dx} + m^2T_m(x) \\ &\quad= m\left(\frac{\cos\theta}{\sin\theta}\sin(m\theta) - m\cos(m\theta)\right) \\ &\qquad - \cos\theta m\frac{1}{\sin\theta}\sin(m\theta) + m^2\cos(m\theta) \\ &\quad= 0. \qquad \square\end{aligned} \tag{4.73}$$

Exercise 4.5 Chebyscheff orthogonality relation.

Prove eq. (4.12d).

Answer for Exercise 4.5

First consider the 0,0 inner product, making an $x = \cos\theta$, so that $dx = -\sin\theta d\theta$, and

$$\begin{aligned}\langle T_0, T_0\rangle &= \int_{-1}^{1}\frac{1}{\left(1-x^2\right)^{1/2}}dx \\ &= \int_{-\pi}^{0}\left(-\frac{1}{\sin\theta}\right) - \sin\theta d\theta \\ &= 0 - (-\pi) \\ &= \pi.\end{aligned} \tag{4.74}$$

Note that since the $[-\pi, 0]$ interval was chosen, the negative root of $\sin^2\theta = 1 - x^2$ was chosen, since $\sin\theta$ is negative in that interval.

The m,m inner product with $m \neq 0$ is

$$\begin{aligned}
\langle T_m, T_m \rangle &= \int_{-1}^{1} \frac{1}{\left(1 - x^2\right)^{1/2}} \left(T_m(x)\right)^2 dx \\
&= \int_{-\pi}^{0} \left(-\frac{1}{\sin\theta}\right) \cos^2(m\theta) - \sin\theta d\theta \\
&= \int_{-\pi}^{0} \cos^2(m\theta) d\theta \\
&= \frac{1}{2} \int_{-\pi}^{0} \left(\cos(2m\theta) + 1\right) d\theta \\
&= \frac{\pi}{2}.
\end{aligned} \tag{4.75}$$

So far so good. For $m \neq n$ the inner product is

$$\begin{aligned}
\langle T_m, T_m \rangle &= \int_{-\pi}^{0} \cos(m\theta)\cos(n\theta) d\theta \\
&= \frac{1}{4} \int_{-\pi}^{0} \left(e^{jm\theta} + e^{-jm\theta}\right)\left(e^{jn\theta} + e^{-jn\theta}\right) d\theta \\
&= \frac{1}{4} \int_{-\pi}^{0} \left(e^{j(m+n)\theta} + e^{-j(m+n)\theta} + e^{j(m-n)\theta} + e^{j(-m+n)\theta}\right) d\theta \\
&= \frac{1}{2} \int_{-\pi}^{0} \left(\cos((m+n)\theta) + \cos((m-n)\theta)\right) d\theta \\
&= \frac{1}{2} \left(\frac{\sin((m+n)\theta)}{m+n} + \frac{\sin((m-n)\theta)}{m-n} \right) \Bigg|_{-\pi}^{0} \\
&= 0. \qquad \square
\end{aligned} \tag{4.76}$$

Exercise 4.6 **Schelkunoff z-axis array, binary array.** (*2015 ps4, p1*)

A three-element array is placed along the z-axis. Assume that the spacing between the elements is $d = \lambda/2$ and the relative amplitude excitations are $I_1 = I_3 = 1$ and $I_2 = 2$

Use the Schelkunoff method to

a. Determine the angles of the nulls when the corresponding progressive phase shifts ad are $0, \pi/2, \pi, 3\pi/2$. Do this for each case.

b. For each case plot the corresponding array factor

Answer for Exercise 4.6

Part a. With the array elements placed at $\mathbf{r}_m = md\hat{\mathbf{z}}, m \in [0, 2]$, the array factor is

$$\text{AF} = 1 \times \left(e^{j(kd\cos\theta + ad)}\right)^0 + 2 \times \left(e^{j(kd\cos\theta + ad)}\right)^1 + 1 \times \left(e^{j(kd\cos\theta + ad)}\right)^2. \tag{4.77}$$

With $z = e^{j(kd\cos\theta + ad)}$, this is

$$\text{AF} = 1 + 2z + z^2 = (1 + z)^2. \tag{4.78}$$

This is a binary array with nulls located at $z = -1$. The angles where that is the case are

$$kd\cos\theta + ad = (2N + 1)\pi, \tag{4.79}$$

which is, for the separation of this problem,

$$\frac{2\pi}{\lambda}\frac{\lambda}{2}\cos\theta + ad = (2N + 1)\pi, \tag{4.80}$$

or

$$\theta = \cos^{-1}\left(2N + 1 - \frac{ad}{\pi}\right). \tag{4.81}$$

1. Case I: $ad = 0$. Here

$$\theta = \cos^{-1}(2N + 1), \tag{4.82}$$

which has solutions at $N = 0, -1$ of

$$\begin{aligned} \theta &= \cos^{-1} 1 = 0 \\ \theta &= \cos^{-1}(-1) = \pi = 180^\circ. \end{aligned} \tag{4.83}$$

2. Case II: $ad = \pi/2$. Here

$$\theta = \cos^{-1}\left(2N + 1 - \frac{1}{2}\right), \tag{4.84}$$

which has solutions at $N = 0$ of

$$\theta = \cos^{-1}(1/2) = \pi/3 = 60^\circ. \tag{4.85}$$

3. Case III: $ad = \pi$. Here

$$\theta = \cos^{-1}(2N), \tag{4.86}$$

which has solutions at $N = 0$ of

$$\theta = \cos^{-1} 0 = \pi/2 = 90^\circ. \tag{4.87}$$

4. Case IV: $ad = 3\pi/2$. Here

$$\theta = \cos^{-1}\left(2N - \frac{1}{2}\right), \tag{4.88}$$

which has solutions at $N = 0$ of

$$\theta = \cos^{-1}(-1/2) = 2\pi/3 = 120^\circ. \tag{4.89}$$

Part b. These are plotted in fig. 4.10.

Exercise 4.7 Schelkunoff z-axis, zero phase shifts. (*2015 ps4, p2*)

Use the Schelkunoff method to design a linear array of isotropic elements placed along the z-axis such that the zeros of the array factor are located at $\theta = 0^\circ, 60^\circ, 120^\circ$. The inter-element spacing is $d = \lambda/2$ and the progressive phase shift is zero degrees.

a. What is the required number of the elements?
b. Determine the corresponding current excitation coefficients
c. Find the array factor
d. Plot the corresponding array factor

Answer for Exercise 4.7

Part a. With $d = \lambda/2$, we write $z = e^{j\pi\cos\theta}$. The zeros of the array factor occur at

$$\begin{aligned}\pi \cos 0 &= \pi \\ \pi \cos(\pi/3) &= \pi/2 \\ \pi \cos(2\pi/3) &= -\pi/2,\end{aligned} \tag{4.90}$$

so the array factor is

$$\begin{aligned}\mathrm{AF} &= \left(z - e^{j\pi}\right)\left(z - e^{j\pi/2}\right)\left(z - e^{-j\pi/2}\right) \\ &= (z+1)(z-j)(z+j) \\ &= (z+1)\left(z^2 - j^2\right) \\ &= z^2 + 1 + z^3 + z.\end{aligned} \tag{4.91}$$

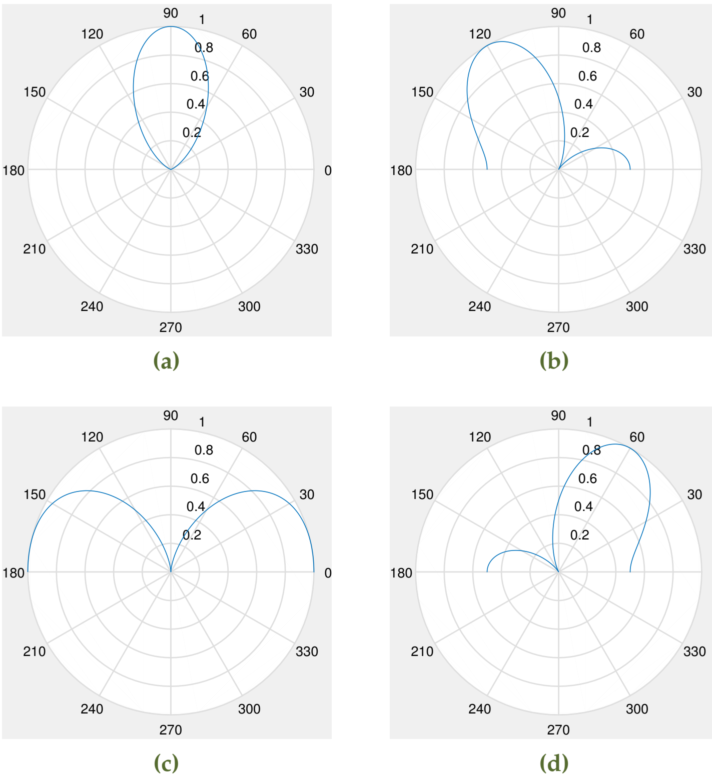

(a) (b)

(c) (d)

Figure 4.10: Plot |AF| for $ad = 0, \pi/2, \pi, 3\pi/2$.

Normalized this is

$$\mathrm{AF}(z) = \frac{1}{4}\left(1 + z + z^2 + z^3\right). \tag{4.92}$$

Four elements are required.

Part b. The currents at positions $\mathbf{r}_m = md\hat{\mathbf{z}}, m \in \{0, 1, 2, 3\}$ are

$$\begin{aligned} I_0 &= \frac{1}{4} \\ I_1 &= \frac{1}{4} \\ I_2 &= \frac{1}{4} \\ I_3 &= \frac{1}{4}. \end{aligned} \tag{4.93}$$

Part c. A phase term may be factored out of the array factor to put it in real form

$$\mathrm{AF} = \frac{z^{3/2}}{4}\left(z^{-3/2} + z^{-1/2} + z^{1/2} + z^{3/2}\right). \tag{4.94}$$

Substituting $z = e^{j\pi\cos\theta}$, and discarding the leading $z^{3/2}$ term, the array factor is

$$\begin{aligned} \mathrm{AF} &= \frac{1}{2}\left(\cos\left(\frac{\pi}{2}\cos\theta\right) + \cos\left(\frac{3\pi}{2}\cos\theta\right)\right) \\ &= \frac{1}{4}\frac{\sin\left(2\pi\cos\theta\right)}{\sin\left(\frac{\pi}{2}\cos\theta\right)}. \end{aligned} \tag{4.95}$$

Part d. This is plotted in fig. 4.11, which also clearly shows the zeros at $\theta = 0, 60^\circ, 120^\circ$ as desired.

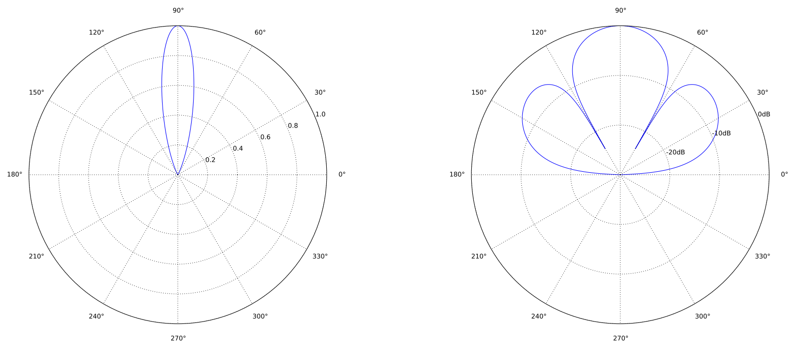

(a) (b)

Figure 4.11: Array factor for specified zeros.

Exercise 4.8 Binomial array. (*2015 ps4, p3*)

Five antenna elements are placed symmetrically along the z-axis. The distance between the elements is $kd = 5\pi/4$. For a binomial array, find

a. the excitation coefficients (currents)
b. an expression for the array factor
c. the normalized power pattern (for the array factor)
d. the angles in degrees where the nulls (if any) occur.
   Plot the power array factor with a tool like Matlab to verify your predictions.

Answer for Exercise 4.8

Part a. The array geometry assuming is illustrated in fig. 4.12. With $\mathbf{r}_m = md\hat{\mathbf{z}}, m \in [-2, 2]$, the array factor is

$$\begin{aligned}\text{AF} &= \sum_{m=-2}^{2} I_m e^{jk\mathbf{r}_m \cdot \hat{\mathbf{r}}} \\ &= \sum_{m=-2}^{2} I_m e^{jkdm\cos\theta}.\end{aligned} \tag{4.96}$$

Recall that the binomial expansion for $N = 4$ is

$$(z+1)^4 = 1 + 4z + 6z^2 + 4z^3 + z^4, \tag{4.97}$$

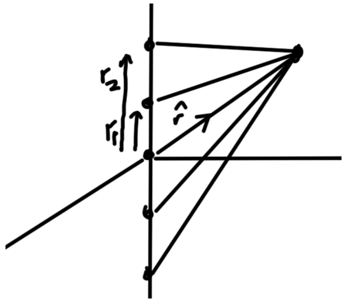

Figure 4.12: Five element array on z-axis.

so the currents are

$$\begin{aligned} I_{-2} &= 1 \\ I_{-1} &= 4 \\ I_0 &= 6 \\ I_1 &= 4 \\ I_2 &= 1. \end{aligned} \tag{4.98}$$

Part b. With $z = e^{jkd\cos\theta}$, we can assume a binomial representation of the form

$$\begin{aligned} \text{AF} &= \sum_{m=-2}^{2} \binom{4}{m+2} e^{jkdm\cos\theta} \\ &= \binom{4}{2} + 2\sum_{m=1}^{2} \binom{4}{m+2} \cos\left(kdm\cos\theta\right) \\ &= 6 + 2\left(4\cos\left(kd\cos\theta\right) + \cos\left(2kd\cos\theta\right)\right). \end{aligned} \tag{4.99}$$

Part c. Normalizing so that AF = 1 at $\Omega = kd\cos\theta \to 0$, gives

$$\begin{aligned} \text{AF} &= \frac{1}{8}\left(3 + 4\cos u + \cos 2u\right) \\ &= \cos^4(u/2), \end{aligned} \tag{4.100}$$

where $u = 5\pi\cos\theta/4$. The substitution $u = -j\ln z$, puts the array factor in explicit polynomial form

$$\text{AF}(z) = \frac{1}{16z^2}\left(1+z\right)^4. \tag{4.101}$$

The leading $1/z^2$ factor, which introduces negative power polynomial terms but does not change the roots, is because the expansion eq. (4.99) effectively factored out a pure phase term. This does not impact the power array factor $|\text{AF}|^2$. Had the array elements not been placed symmetrically about the origin, instead being located at $\mathbf{r}_m = md\hat{\mathbf{z}}, m \in \{0, 1, 2, 3, 5\}$, this factor would have been eliminated. A leading z^N factor in $\text{AF}(z)$ is seen to be associated with the location of the origin of the coordinate system.

Part d. Solutions for the nulls are found for integer N solutions of

$$\frac{5\pi}{4}\cos\theta = \pi(1 + 2N), \tag{4.102}$$

Two solutions in the visible range can be found

$$\theta = \cos^{-1}\left(\pm 4/5\right), \tag{4.103}$$

or

$$\theta \in \{143.1^\circ, 36.9^\circ\}. \tag{4.104}$$

The power array factor is plotted in fig. 4.13, and fig. 4.14.

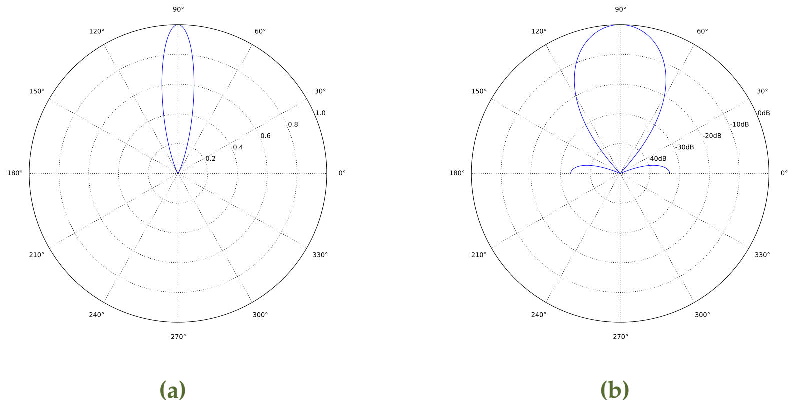

(a) **(b)**

Figure 4.13: Polar plot of 5 element binomial power array factor.

Exercise 4.9 Dolph-Chebyshev. (*2015 ps4, p4*)

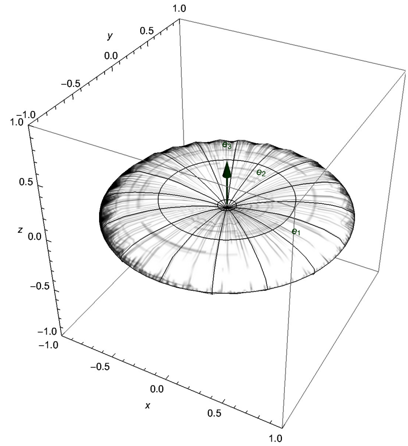

Figure 4.14: Spherical polar plot of 5 element binomial power array factor.

Design a five-element, −40dB sidelobe level Dolph-Chebyshev array of isotropic elements. The elements are placed along the x-axis with an inter-element spacing $d = \lambda/2$. Determine,

a. the normalized amplitude coefficients
b. the array factor
c. Use numerical integration to calculate the directivity
d. and the null-to-null beamwidth
e. Repeat part a-c for a uniform broadside array of the same spacing
f. Plot the power array-factor patterns for the two arrays on the same plot.

Answer for Exercise 4.9

Part a. The 40dB level is equivalent to

$$20 \log_{10} R = 40, \tag{4.105}$$

or

$$R = 10^2 = 100. \tag{4.106}$$

The Chebyshev scaling factor for a five element array is

$$x_0 = \cosh\left(\frac{1}{4}\cosh^{-1} R\right) = 2.01. \tag{4.107}$$

With $x = x_0 \cos(u/2)$, the unnormalized array factor is

$$\begin{aligned} \mathrm{AF}(u) &= T_4(x) \\ &= T_4(x_0 \cos(u/2)) \\ &= 8x_0^4 \cos^4(u/2) - 8x_0^2 \cos^2(u/2) + 1. \end{aligned} \tag{4.108}$$

Since

$$\begin{aligned} \cos^2(u/2) &= \frac{1}{2}\left(\cos(u) + 1\right) \\ \cos^4(u/2) &= \frac{1}{8}\left(\cos(2u) + 4\cos(u) + 3\right), \end{aligned} \tag{4.109}$$

the array factor can be expanded in $\cos(mu)$, as

$$\begin{aligned} \mathrm{AF}(u) &= x_0^4 \left(\cos(2u) + 4\cos(u) + 3\right) - 4x_0^2 \left(\cos(u) + 1\right) + 1 \\ &= x_0^4 \cos(2u) + \left(4x_0^4 - 4x_0^2\right) \cos(u) + 3x_0^4 - 4x_0^2 + 1. \end{aligned} \tag{4.110}$$

After normalization this is

$$\begin{aligned} \mathrm{AF}(u) &= \alpha \cos(2u) + \beta \cos(u) + \gamma \\ \alpha &= \frac{x_0^4}{8x_0^4 - 8x_0^2 + 1} \\ \beta &= \frac{4x_0^4 - 4x_0^2}{8x_0^4 - 8x_0^2 + 1} \\ \gamma &= \frac{3x_0^4 - 4x_0^2 + 1}{8x_0^4 - 8x_0^2 + 1}. \end{aligned} \tag{4.111}$$

The array coefficients are found to have the values

$$\begin{aligned} I_{-2} &= \frac{\alpha}{2} = 0.082 \\ I_{-1} &= \frac{\beta}{2} = 0.25 \\ I_0 &= \gamma = 0.34 \\ I_1 &= \frac{\beta}{2} = 0.25 \\ I_2 &= \frac{\alpha}{2} = 0.082. \end{aligned} \tag{4.112}$$

Part b. The array factor is defined by eq. (4.111), eq. (4.112), where $u = \pi \sin\theta \cos\phi$.

Part c. The directivity is found to be 3.97 (5.98 dB).

Part d. The zeros of the array factor occur where the argument of

$$T_m(x_0 \cos(u/2)) = \cos(m \cos^{-1}\left(x_0 \cos(u/2)\right)), \tag{4.113}$$

equals $-\pi/2 + n\pi$, or

$$u = 2\cos^{-1}\left(\frac{1}{x_0}\cos\left(\frac{\pi}{2m}(2n-1)\right)\right). \tag{4.114}$$

Compare this to the zeros of the uniform array factor, which was

$$\mathrm{AF}(z) = \sum_{n=0}^{N-1} z^n = \frac{1-z^N}{1-z} = z^{(N-1)/2}\frac{z^{N/2} - z^{-N/2}}{z^{1/2} - z^{-1/2}}, \tag{4.115}$$

so with $z = e^{ju}$, the absolute array factor is

$$\left|\mathrm{AF}(u)\right| = \frac{1}{N}\frac{\left|\sin\left(Nu/2\right)\right|}{\left|\sin\left(u/2\right)\right|}. \tag{4.116}$$

This has zeros where

$$u = \frac{2n\pi}{N}, \qquad n \neq 0 \in \mathbb{Z}. \tag{4.117}$$

These two sets of zeros are plotted on the unit circle in the z-domain in fig. 4.15. The Chebyshev and uniform array factors are plotted the z-x plane for $u = kd\sin\theta\cos(0)$ in dB in fig. 4.16. For the Chebyshev array the zeros are found to be at $\{44^\circ, 61^\circ, 119^\circ, 136^\circ\}$, so the null to null beamwidth is 88°. The 3 dB beamwidth for the main lobe is found to be 28°.

For the uniform array the zeros are found at $\{24^\circ, 53^\circ, 127^\circ, 156^\circ\}$ so that arrays' null to null beamwidth is 48°.

Part e. The normalized uniform array amplitude coefficients are $1/5$. The array factor is given by eq. (4.116). The directivity for the linear array is found numerically to be 5.0 (6.99 dB).

Part f. This array configuration has a donut shaped power pattern, as shown in fig. 4.17. The two array factor power patterns (normalized) are plotted in fig. 4.18.

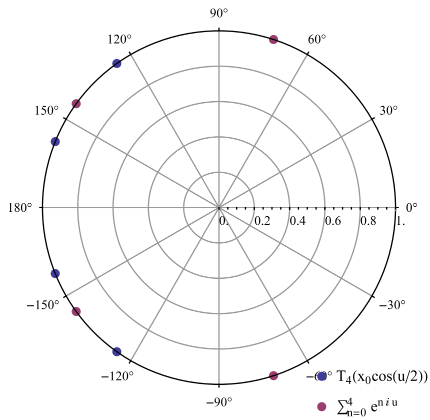

Figure 4.15: Zeros of five element Chebyshev and uniform array elements on z-domain unit circle.

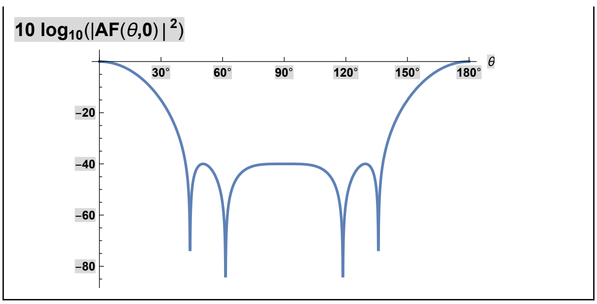

(a)

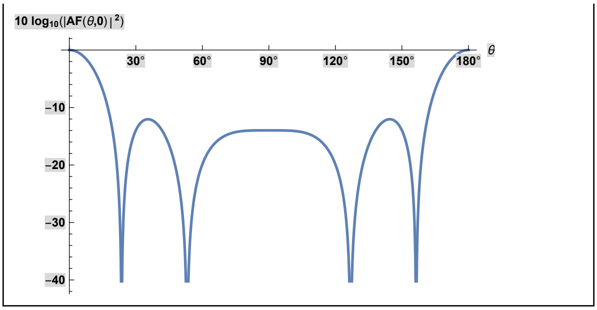

(b)

Figure 4.16: Chebyshev and uniform power array factor in z-x plane (dB).

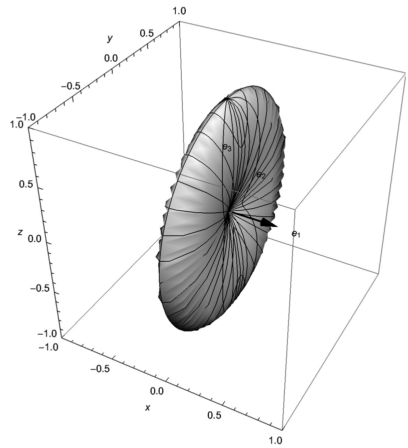

Figure 4.17: 5 element Chebyshev array power pattern in 3D.

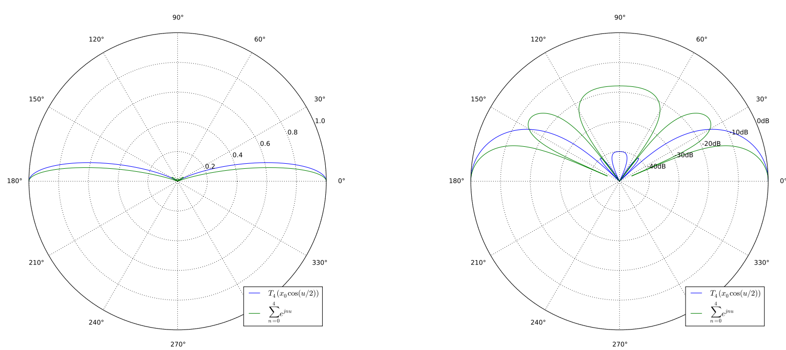

(a) **(b)**

Figure 4.18: Plots of 5 element Chebyshev and uniform array power patterns for $u = kd \sin\theta \cos 0$.

5 APERATURE ANTENNAS.

5.1 PROBLEMS.

Exercise 5.1 Aperture antenna. (*2015 ps5, p1*)

A rectangular aperture lies along the x-y plane and has dimensions $a \times b$. Let the electric field aperture distribution be given by,

$$\mathbf{E}_{\text{ap}} = \hat{\mathbf{y}} \cos\left(\frac{\pi}{a} x\right). \tag{5.1}$$

The aperture is cut out of an infinite perfectly electric conductor. The origin of the coordinate system is at the center of the aperture.

Using the theory of radiation from apertures based on the equivalence principle, calculate:

1. An expression for $E_\theta(\theta, \phi)$.
2. An expression for $E_\phi(\theta, \phi)$.
3. Consider an aperture of dimensions $a = b = 10\text{cm}$ at $f = 9.8\text{GHz}$.

a. Plot the E-plane and H-plane patterns (power).
b. Calculate the positions of the first nulls in the E and H planes.
c. From the plot determine the levels of the first sidelobe in the E and H planes.
d. From the plot determine the 3dB beamwidth of the main lobe in the E and H planes.

Answer for Exercise 5.1

Following the transformation procedure of [5] fig. 12.5, the equivalent source for this electric field is a magnetic current

$$\mathbf{M}_s = -2\hat{\mathbf{z}} \times \hat{\mathbf{y}} \cos\left(\frac{\pi}{a} x\right) = 2\hat{\mathbf{x}} \cos\left(\frac{\pi}{a} x\right). \tag{5.2}$$

producing an electric vector potential that is approximately

$$\begin{aligned}
\mathbf{F} &= \frac{\epsilon}{4\pi r}\int_{-a/2}^{a/2} dx' \int_{-b/2}^{b/2} dy' \mathbf{M}_s e^{-jk(r-\hat{\mathbf{r}}\cdot\mathbf{r}')} \\
&= \frac{\epsilon}{2\pi r} e^{-jkr}\hat{\mathbf{x}} \int_{-a/2}^{a/2} dx' \int_{-b/2}^{b/2} dy' \cos\left(\frac{\pi}{a}x'\right) e^{jk\hat{\mathbf{r}}\cdot\mathbf{r}'} \\
&= \frac{\epsilon}{2\pi r} e^{-jkr}\hat{\mathbf{x}} \int_{-a/2}^{a/2} dx' \int_{-b/2}^{b/2} dy' \cos\left(\frac{\pi}{a}x'\right) e^{jk\sin\theta(\cos\phi x' + \sin\phi y')} \\
&= \frac{\epsilon}{4\pi r} e^{-jkr}\hat{\mathbf{x}} \int_{-a/2}^{a/2} dx' \left(e^{jk\sin\theta\cos\phi x' + j\pi x'/a} + e^{jk\sin\theta\cos\phi x' - j\pi x'/a} \right) \times \\
&\quad \int_{-b/2}^{b/2} dy' e^{jk\sin\theta\sin\phi y'}.
\end{aligned} \tag{5.3}$$

A symmetric interval around the origin has been chosen to avoid the introduction of complex phases. Each of these integrals is of the form

$$\int_{-c/2}^{c/2} dz' e^{j\alpha z'} = \left.\frac{e^{j\alpha z'}}{j\alpha}\right|_{-c/2}^{c/2} = \frac{e^{j\alpha c/2} - e^{-j\alpha c/2}}{j\alpha} = \frac{\sin\left(\alpha c/2\right)}{\alpha/2}. \tag{5.4}$$

With

$$X = k\sin\theta\cos\phi \tag{5.5a}$$

$$Y = k\sin\theta\sin\phi, \tag{5.5b}$$

the electric vector potential is

$$\begin{aligned}
\mathbf{F} &= \frac{\epsilon}{4\pi r} e^{-jkr}\hat{\mathbf{x}} \frac{\sin\left(Yb/2\right)}{Y/2} \times \\
&\quad \left(\frac{\sin\left((X+\pi/a)a/2\right)}{(X+\pi/a)/2} + \frac{\sin\left((X-\pi/a)a/2\right)}{(X-\pi/a)/2} \right) \\
&= \frac{\epsilon}{2\pi r} e^{-jkr}\hat{\mathbf{x}} \frac{\sin\left(Yb/2\right)}{Y/2} \times \\
&\quad \frac{(X-\pi/a)\sin\left(Xa/2+\pi/2\right) + (X+\pi/a)\sin\left(Xa/2-\pi/2\right)}{X^2 - (\pi/a)^2}.
\end{aligned} \tag{5.6}$$

Since

$$\sin(z + \pi/2) + \sin(z - \pi/2) = 0 \tag{5.7a}$$

$$\sin(z + \pi/2) - \sin(z - \pi/2) = 2\cos z, \tag{5.7b}$$

this reduces to

$$\mathbf{F} = -\frac{\epsilon ab}{4r} e^{-jkr} \hat{\mathbf{x}} \frac{\cos\left(Xa/2\right)}{(Xa/2)^2 - (\pi/2)^2} \frac{\sin\left(Yb/2\right)}{Yb/2}. \tag{5.8}$$

The far field magnetic field is

$$\begin{aligned}
\mathbf{H} &= -j\omega \mathbf{F}_T \\
&= jkc \frac{\epsilon ab}{4r} e^{-jkr} \left(\hat{\mathbf{x}} - \left(\hat{\mathbf{x}} \cdot \hat{\mathbf{r}}\right) \hat{\mathbf{r}}\right) \frac{\cos\left(Xa/2\right)}{a^2 X^2/4 - (\pi/2)^2} \frac{\sin\left(Yb/2\right)}{Yb/2} \\
&= \frac{jkab}{4r\eta} e^{-jkr} \left(\hat{\mathbf{x}} - \left(\hat{\mathbf{x}} \cdot \hat{\mathbf{r}}\right) \hat{\mathbf{r}}\right) \frac{\cos\left(Xa/2\right)}{(Xa/2)^2 - (\pi/2)^2} \frac{\sin\left(Yb/2\right)}{Yb/2}.
\end{aligned} \tag{5.9}$$

Since

$$\hat{\mathbf{x}} = \sin\theta\cos\phi \hat{\mathbf{r}} + \cos\theta\cos\phi \hat{\boldsymbol{\theta}} - \sin\phi \hat{\boldsymbol{\phi}}, \tag{5.10}$$

the far field magnetic field is

$$\mathbf{H} = \frac{jkab}{4r\eta} e^{-jkr} \left(\cos\theta\cos\phi \hat{\boldsymbol{\theta}} - \sin\phi \hat{\boldsymbol{\phi}}\right) \frac{\cos\left(Xa/2\right)}{(Xa/2)^2 - (\pi/2)^2} \frac{\sin\left(Yb/2\right)}{Yb/2}. \tag{5.11}$$

This can be related to the electric field noting that that the dual of the far field relationship

$$\mathbf{H}_A = \frac{1}{\eta} \hat{\mathbf{r}} \times \mathbf{E}_A, \tag{5.12}$$

is

$$-\mathbf{E}_F = \eta \hat{\mathbf{r}} \times \mathbf{H}_F, \tag{5.13}$$

so the far field electric field is

$$\begin{aligned}
\mathbf{E} &= -\eta \hat{\mathbf{r}} \times \mathbf{H} \\
&= -\frac{jkab}{4r} e^{-jkr} \hat{\mathbf{r}} \times \hat{\mathbf{x}} \frac{\cos\left(Xa/2\right)}{(Xa/2)^2 - (\pi/2)^2} \frac{\sin\left(Yb/2\right)}{Yb/2}.
\end{aligned} \tag{5.14}$$

That electric field direction is

$$\begin{aligned}\hat{\mathbf{r}} \times \hat{\mathbf{x}} &= \cos\theta\cos\phi\hat{\mathbf{r}} \times \hat{\boldsymbol{\theta}} - \sin\phi\hat{\mathbf{r}} \times \hat{\boldsymbol{\phi}} \\ &= \cos\theta\cos\phi\hat{\boldsymbol{\phi}} + \sin\phi\hat{\boldsymbol{\theta}},\end{aligned} \tag{5.15}$$

so the electric field is

$$\mathbf{E} = -\frac{jkab}{4r}e^{-jkr}\left(\cos\theta\cos\phi\hat{\boldsymbol{\phi}} + \sin\phi\hat{\boldsymbol{\theta}}\right)\frac{\cos\left(Xa/2\right)}{(Xa/2)^2 - (\pi/2)^2}\frac{\sin\left(Yb/2\right)}{Yb/2}. \tag{5.16}$$

Note that the electric and magnetic fields are perpendicular, as expected.

1. The polar coordinate of the electric field is

$$E_\theta = -\frac{jkab}{4r}e^{-jkr}\sin\phi\frac{\cos\left(Xa/2\right)}{(Xa/2)^2 - (\pi/2)^2}\frac{\sin\left(Yb/2\right)}{Yb/2}. \tag{5.17}$$

2. The azimuthal coordinate of the electric field is

$$E_\phi = -\frac{jkab}{4r}e^{-jkr}\cos\theta\cos\phi\frac{\cos\left(Xa/2\right)}{(Xa/2)^2 - (\pi/2)^2}\frac{\sin\left(Yb/2\right)}{Yb/2}. \tag{5.18}$$

3. Now for the plots and numeric values requested for the given aperture size and source frequency.

   The electric field power pattern for an aperture of dimensions $a = b = 10\text{cm}$ at $f = 9.8\text{GHz}$ is plotted in dB scale from 0 dB down to 40 dB in fig. 5.1.

Part a. The maximum field is found at $\theta = 0$. The value of ϕ is inconsequential, so we have an infinite number of E-plane surfaces, and can pick the $\theta = \phi = 0$ wave vector direction for simplicity. For such a wave vector direction $\hat{\mathbf{E}} = \hat{\mathbf{y}}, \hat{\mathbf{H}} = \hat{\mathbf{x}}$, and the corresponding E-plane and H-plane power fields are plotted in fig. 5.2. These fields are also plotted on a log scale in fig. 5.3 , from 0 dB down to -50 dB.

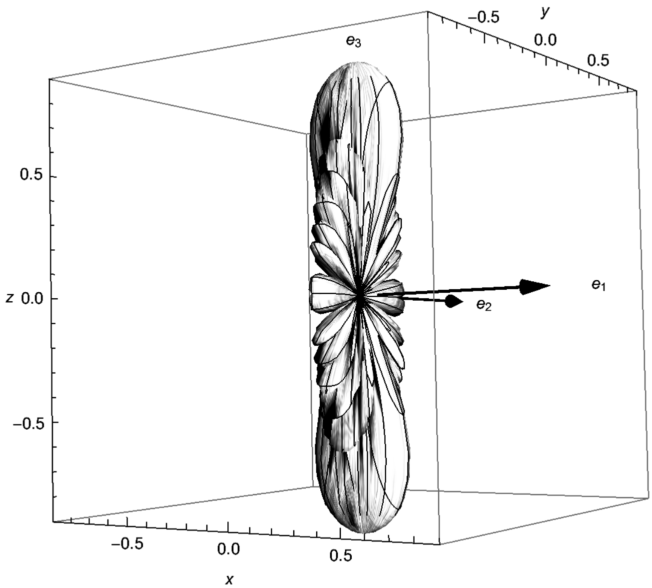

Figure 5.1: Electric field power pattern, 0 dB to -40 dB.

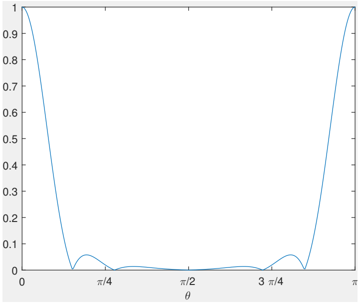

(a)

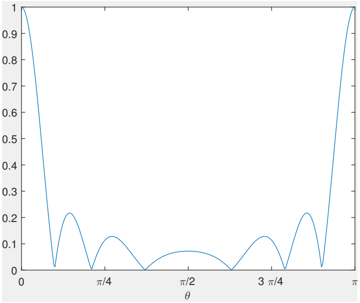

(b)

Figure 5.2: E-H-plane (power) for $\phi = 0$.

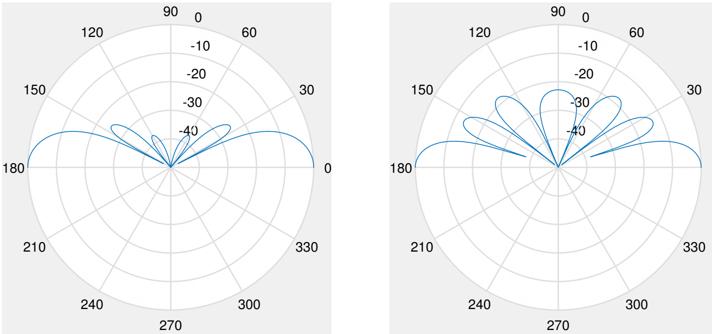

(a) (b)

Figure 5.3: E,H-plane (power) for $\phi = 0$, dB scale.

Part b. For the E-plane the zeros are found at 27°, 50°, 90°, 130°, and 153°.

For the H-plane the zeros are found at 18°, 38°, 67°, 113°, 142°, 162°.

These were determined numerically, but these can also be visually verified against the dB power plots above, which are marked in degrees.

Part c. For the E-plane the sidelobe peaks are found at 35°, 60°, 120°, 145°, with respective levels (dB) of -25, -37, -37, -25.

For the H-plane the sidelobe peaks are found at 26°, 49°, 90°, 131°, 154°, with respective levels (dB) of -13.2666, -17.8436, -22.8361, -17.8436, -13.2666.

These were also calculated numerically, but can also be visually verified against the dB power plots above.

Part d. The -3 dB point of the main lobe is found where $|\mathbf{E}| = 10^{-3/20}$. For the E-plane this is at 10°, and for the H-plane this is found at 8°.

6 MICROSTRIP ANTENNAS.

6.1 PROBLEMS.

Exercise 6.1 Patch antenna. (*2015 ps5, p2*)

A microstrip patch antenna is printed on a substrate with $h = 0.1588\text{cm}$, $\epsilon_r = 2.2$ at $f_0 = 10\text{GHz}$. Give your length answers in cm. Using the transmission-line model :

a. Calculate the width W.

b. Calculate the effective relative permittivity ϵ_{eff}.

c. Calculate the length of the patch L_0 if no fringing-field effects are accounted for.

d. Calculate the corrected length $L = L_0 - m\Delta L$ where $m = 2$ and ΔL is the correction due to the fringing fields.

e. Estimate the admittance of each radiating slot $Y_s = G + jB$.

f. Now transform Y_s of the second slot (right) to the plane of the first slot (left) using the impedance transformation,

$$Z_{\text{in2}} = Z_0 \frac{Z_s + jZ_0 \tan(\beta L)}{Z_0 + jZ_s \tan(\beta L)}, \tag{6.1}$$

where $\beta = k_0\sqrt{\epsilon_{\text{eff}}}$ is the effective propagation constant, and use $Z_0 = 26\Omega$ as the characteristic impedance of the microstrip line. What is the value of Z_{in2} and $Y_{\text{in2}} = 1/Z_{\text{in2}}$.

g. Based on the above, calculate the total input impedance of the patch antenna Z_{in} at the terminals of the first slot.

h. If the imaginary part of Z_{in} is not zero, adjust the length parameter m (in part d) between $0 < 3 < m$ to make the patch resonant (i.e. make the imaginary part of Z_{in} vanish). What is the new input impedance in this case?

Answer for Exercise 6.1

Part a.

$$\begin{aligned} W &= \frac{1}{2f_0\sqrt{\mu_0\epsilon_0}}\sqrt{\frac{2}{\epsilon_r+1}} \\ &= \frac{c}{2f_0}\sqrt{\frac{2}{2.2+1}} \\ &= \frac{3\times10^8 \mathrm{m/s}\times 100 \mathrm{cm/m}}{(2)10\times10^9 \mathrm{s}^{-1}}\sqrt{\frac{2}{2.2+1}} \\ &= 1.186 \mathrm{cm}. \end{aligned} \tag{6.2}$$

Part b.

$$\begin{aligned} \epsilon_{\mathrm{eff}} &= \frac{\epsilon_{\mathrm{r}}+1}{2}+\frac{\epsilon_{\mathrm{r}}-1}{2}\left(1+\frac{12h}{W}\right)^{-1/2} \\ &= 1.9716. \end{aligned} \tag{6.3}$$

Part c.

$$\begin{aligned} L_0 &= \frac{\lambda_0}{2} \\ &= \frac{c}{2f_0\sqrt{\epsilon_{\mathrm{eff}}}} \\ &= 1.068 \mathrm{cm}. \end{aligned} \tag{6.4}$$

Part d.

$$\begin{aligned} \frac{\Delta L}{h} &= 0.412\frac{\epsilon_{\mathrm{eff}}+0.3}{\epsilon_{\mathrm{eff}}-0.258}\,\frac{\frac{W}{h}+0.264}{\frac{W}{h}+0.8} \\ &= 0.5108, \end{aligned} \tag{6.5}$$

$$\begin{aligned} \Delta L &= 0.5108h \\ &= 0.081 \mathrm{cm}, \end{aligned} \tag{6.6}$$

$$\begin{aligned} L &= L_0 - 2\Delta L \\ &= 0.9061 \mathrm{cm}. \end{aligned} \tag{6.7}$$

Part e.

$$\begin{aligned}\lambda_0 &= c/f_0 \\ &= 3\text{cm},\end{aligned} \tag{6.8}$$

$$\begin{aligned}k_0 &= \frac{2\pi}{\lambda_0} \\ &= 2.0944\text{cm}^{-1}.\end{aligned} \tag{6.9}$$

The constraint for the calculation of G requires

$$\frac{h}{\lambda_0} = 0.053 < \frac{1}{10}, \tag{6.10}$$

which is satisfied, so

$$\begin{aligned}G &= \frac{W}{120\lambda_0}\left(1 - \frac{1}{24}(k_0 h)^2\right) \\ &= 0.0033\mho,\end{aligned} \tag{6.11}$$

$$\begin{aligned}B &= \frac{W}{120\lambda_0}(1 - 0.636\ln(k_0 h)) \\ &= 0.0056\mho,\end{aligned} \tag{6.12}$$

$$\begin{aligned}Y_s &= G + jB \\ &= (0.0033 + 0.0056j)\,\mho \\ &= 0.00649\underline{/60^\circ}\mho,\end{aligned} \tag{6.13}$$

$$\begin{aligned}Z_s &= (78 - 133j)\,\Omega \\ &= 154\underline{/-59^\circ}\Omega.\end{aligned} \tag{6.14}$$

Part f.

$$\begin{aligned}Z_{\text{in2}} &= (19 + 71j)\,\Omega \\ &= 73\underline{/75^\circ}\Omega,\end{aligned} \tag{6.15}$$

$$\begin{aligned}Y_{\text{in2}} &= (0.0036 - 0.0131j)\,\mho \\ &= 0.0136\underline{/-75^\circ}\mho.\end{aligned} \tag{6.16}$$

Part g.

$$\begin{aligned} Z_{\text{in}} &= \frac{1}{Y_s + Y_{\text{in2}}} \\ &= (66 + 73j)\ \Omega \\ &= 98\underline{/48^\circ}\Omega. \end{aligned} \tag{6.17}$$

Part h. The imaginary part of Z_{in} is plotted in fig. 6.1. The zero

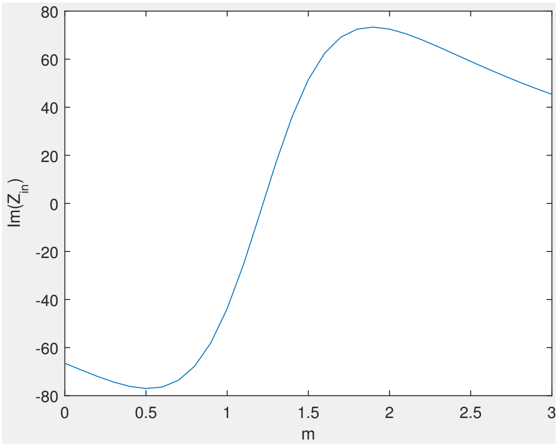

Figure 6.1: Im Z_{in} variation with m.

is found at

$$m = 1.22097, \tag{6.18}$$

at which point the new impedance is

$$Z_{\text{in}} = 152.3\Omega. \tag{6.19}$$

7 FIELDS AND WAVES.

7.1 COUPLED WAVE EQUATION IN CYLINDRICAL COORDINATES.

In [2], for a sourceless configuration, it is noted that the electric field equations $\boldsymbol{\nabla}^2 \mathbf{E} = -\beta^2 \mathbf{E}$ have the form

$$\boldsymbol{\nabla}^2 E_\rho - \frac{E_\rho}{\rho^2} - \frac{2}{\rho^2}\frac{\partial E_\phi}{\partial \phi} = -\beta^2 E_\rho \tag{7.1a}$$

$$\boldsymbol{\nabla}^2 E_\phi - \frac{E_\phi}{\rho^2} + \frac{2}{\rho^2}\frac{\partial E_\rho}{\partial \phi} = -\beta^2 E_\phi \tag{7.1b}$$

$$\boldsymbol{\nabla}^2 E_z = -\beta^2 E_z, \tag{7.1c}$$

where

$$\boldsymbol{\nabla}^2 \psi = \frac{1}{\rho}\frac{\partial}{\partial \rho}\left(\rho \frac{\partial \psi}{\partial \rho}\right) + \frac{1}{\rho^2}\frac{\partial^2 \psi}{\partial \phi^2} + \frac{\partial^2 \psi}{\partial z^2}. \tag{7.2}$$

He applies separation of variables to the last equation, ending up with the usual Bessel function solution, but the first two coupled equations are dismissed as coupled and difficult. It looks like separation of variables works for this too, but we have to prep the system slightly by writing $\psi = E_\rho + jE_\phi$, which gives

$$\boldsymbol{\nabla}^2 \psi - \frac{\psi}{\rho^2} + \frac{2j}{\rho^2}\frac{\partial \psi}{\partial \phi} = -\beta^2 \psi, \tag{7.3}$$

or

$$\frac{1}{\rho}\frac{\partial}{\partial \rho}\left(\rho \frac{\partial \psi}{\partial \rho}\right) + \frac{1}{\rho^2}\frac{\partial^2 \psi}{\partial \phi^2} + \frac{\partial^2 \psi}{\partial z^2} - \frac{\psi}{\rho^2} + \frac{2j}{\rho^2}\frac{\partial \psi}{\partial \phi} = -\beta^2 \psi. \tag{7.4}$$

With a separation of variables substitution $\psi = f(\rho)g(\phi)h(z)$ this gives

$$\frac{1}{\rho f}\frac{\partial}{\partial \rho}\left(\rho \frac{\partial f}{\partial \rho}\right) + \frac{1}{\rho^2 g}\frac{\partial^2 g}{\partial \phi^2} + \frac{1}{z}\frac{\partial^2 h}{\partial z^2} - \frac{1}{\rho^2} + \frac{2j}{\rho^2 g}\frac{\partial g}{\partial \phi} = -\beta^2. \tag{7.5}$$

Assuming a solution for the function h of

$$\frac{1}{z}\frac{\partial^2 h}{\partial z^2} = -\alpha^2, \tag{7.6}$$

the PDE is reduced to an equation in two functions

$$\frac{1}{\rho f}\frac{\partial}{\partial \rho}\left(\rho \frac{\partial f}{\partial \rho}\right) + \frac{1}{\rho^2 g}\frac{\partial}{\partial \phi}\left(g + 2jg\right) + \beta^2 - \alpha^2 - \frac{1}{\rho^2} = 0, \tag{7.7}$$

or

$$\frac{\rho}{f}\frac{\partial}{\partial \rho}\left(\rho \frac{\partial f}{\partial \rho}\right) + \frac{1}{g}\frac{\partial}{\partial \phi}\left(g + 2jg\right) + \left(\beta^2 - \alpha^2\right)\rho^2 = 1. \tag{7.8}$$

With the term in g having only ϕ dependence, we can assume

$$\frac{1}{g}\frac{\partial}{\partial \phi}\left(g + 2jg\right) = 1 - \gamma^2, \tag{7.9}$$

for

$$\frac{\rho}{f}\frac{\partial}{\partial \rho}\left(\rho \frac{\partial f}{\partial \rho}\right) - \gamma^2 + \left(\beta^2 - \alpha^2\right)\rho^2 = 0. \tag{7.10}$$

I'm not sure off hand if these can be solved in known special functions, especially since the constants in the mix are complex.

7.2 IMPEDANCE TRANSFORMATION.

In our final problem set we used the impedance transformation for calculations related to a microslot antenna. This transformation wasn't familiar to me, and is apparently covered in the third year ECE fields class. I found a derivation of this in [4], but the idea is really simple and follows from the reflection coefficient calculation for a normal reflection configuration. Consider a normal field reflection between two interfaces, as sketched in fig. 7.1. The fields are

$$\mathbf{E}^{\mathrm{i}} = \hat{\mathbf{x}} E_0 e^{-jk_1 z} \tag{7.11a}$$

$$\mathbf{H}^{\mathrm{i}} = \hat{\mathbf{y}} \frac{E_0}{\eta_1} e^{-jk_1 z} \tag{7.11b}$$

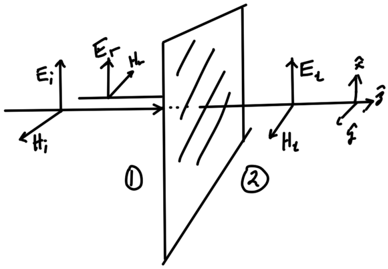

Figure 7.1: Normal reflection and transmission between two media.

$$\mathbf{E}^{\mathrm{r}} = \hat{\mathbf{x}}\Gamma E_0 e^{jk_1 z} \tag{7.11c}$$

$$\mathbf{H}^{\mathrm{r}} = -\hat{\mathbf{y}}\Gamma \frac{E_0}{\eta_1} e^{jk_1 z} \tag{7.11d}$$

$$\mathbf{E}^{\mathrm{t}} = \hat{\mathbf{x}} E_0 T e^{-jk_2 z} \tag{7.11e}$$

$$\mathbf{H}^{\mathrm{t}} = \hat{\mathbf{y}} \frac{E_0}{\eta_1} T e^{-jk_2 z}. \tag{7.11f}$$

The field orientations have been picked so that the tangential component of the electric field is $\hat{\mathbf{x}}$ oriented for all of the incident, reflected, and transmitted components. Requiring equality of the tangential field components at the interface gives

$$1 + \Gamma = T \tag{7.12a}$$

$$\frac{1}{\eta_1} - \frac{\Gamma}{\eta_1} = \frac{T}{\eta_2}. \tag{7.12b}$$

Solving for the transmission coefficient gives

$$\begin{aligned} T &= \frac{2}{1 + \frac{\eta_1}{\eta_2}} \\ &= \frac{2\eta_2}{\eta_2 + \eta_1}, \end{aligned} \tag{7.13}$$

and for the reflection coefficient

$$\begin{aligned}\Gamma &= T - 1 \\ &= \frac{2\eta_2 - \eta_1 - \eta_2}{\eta_2 + \eta_1} \\ &= \frac{\eta_2 - \eta_1}{\eta_2 + \eta_1}.\end{aligned} \tag{7.14}$$

The total fields in medium 1 at the point $z = -l$ are

$$\mathbf{E}^{\mathrm{i}} + \mathbf{E}^{\mathrm{r}} = \hat{\mathbf{x}} E_0 \left(e^{-jk_1(-l)} + \Gamma e^{jk_1(-l)} \right) \tag{7.15a}$$

$$\mathbf{H}^{\mathrm{i}} + \mathbf{H}^{\mathrm{r}} = \hat{\mathbf{y}} \frac{E_0}{\eta_1} \left(e^{-jk_1(-l)} - \Gamma e^{jk_1(-l)} \right). \tag{7.15b}$$

The ratio of the electric field strength to the magnetic field strength is defined as the input impedance

$$Z_{\mathrm{in}} \equiv \left. \frac{E^{\mathrm{i}} + E^{\mathrm{r}}}{H^{\mathrm{i}} + H^{\mathrm{r}}} \right|_{z=-l}. \tag{7.16}$$

That is

$$\begin{aligned}Z_{\mathrm{in}} &= \eta_1 \frac{e^{jk_1 l} + \Gamma e^{-jk_1 l}}{e^{jk_1 l} - \Gamma e^{-jk_1 l}} \\ &= \eta_1 \frac{(\eta_1 + \eta_2) e^{jk_1 l} + (\eta_2 - \eta_1) e^{-jk_1 l}}{(\eta_1 + \eta_2) e^{jk_1 l} - (\eta_2 - \eta_1) e^{-jk_1 l}} \\ &= \eta_1 \frac{\eta_2 \cos(k_1 l) + \eta_1 j \sin(k_1 l)}{\eta_2 j \sin(k_1 l) + \eta_1 \cos(k_1 l)},\end{aligned} \tag{7.17}$$

or

$$\boxed{Z_{\mathrm{in}} = \eta_1 \frac{\eta_2 + j\eta_1 \tan(k_1 l)}{\eta_1 + j\eta_2 \tan(k_1 l)}.} \tag{7.18}$$

7.3 PROBLEMS.

Exercise 7.1 $\hat{\mathbf{x}}$ oriented plane wave electric field. ([2] *ex. 4.1*)

A uniform plane wave having only an x component of the electric field is traveling in the $+z$ direction in an unbounded lossless, source-ofree region. Using Maxwell's equations write expressions for the electric and corresponding magnetic field intensities.

Answer for Exercise 7.1

The phasor form of Maxwell's equations for a source free region are

$$\boldsymbol{\nabla} \times \mathbf{E} = -j\omega\mathbf{B} \tag{7.19a}$$

$$\boldsymbol{\nabla} \times \mathbf{H} = j\omega\mathbf{D} \tag{7.19b}$$

$$\boldsymbol{\nabla} \cdot \mathbf{D} = 0 \tag{7.19c}$$

$$\boldsymbol{\nabla} \cdot \mathbf{B} = 0. \tag{7.19d}$$

Since $\mathbf{E} = \hat{\mathbf{x}}E(z)$, the magnetic field follows from eq. (7.19a)

$$\begin{aligned}
-j\omega\mathbf{B} &= \boldsymbol{\nabla} \times \mathbf{E} \\
&= \begin{vmatrix} \hat{\mathbf{x}} & \hat{\mathbf{y}} & \hat{\mathbf{z}} \\ \partial_x & \partial_y & \partial_z \\ E & 0 & 0 \end{vmatrix} \\
&= \hat{\mathbf{y}}\partial_z E(z) - \hat{\mathbf{z}}\cancel{\partial_y E(z)},
\end{aligned} \tag{7.20}$$

or

$$\mathbf{B} = -\frac{1}{j\omega}\partial_z E. \tag{7.21}$$

This is constrained by eq. (7.19b)

$$\begin{aligned}
j\omega\epsilon\hat{\mathbf{x}}E &= \frac{1}{\mu}\boldsymbol{\nabla} \times \mathbf{B} \\
&= -\frac{1}{\mu j\omega}\begin{vmatrix} \hat{\mathbf{x}} & \hat{\mathbf{y}} & \hat{\mathbf{z}} \\ \partial_x & \partial_y & \partial_z \\ 0 & \partial_z E & 0 \end{vmatrix} \\
&= -\frac{1}{\mu j\omega}\left(-\hat{\mathbf{x}}\partial_{zz}E + \hat{\mathbf{z}}\partial_x\partial_z E\right).
\end{aligned} \tag{7.22}$$

Since $\partial_x \partial_z E = \partial_z (\partial_x E) = \partial_z \frac{1}{\epsilon} \boldsymbol{\nabla} \cdot \mathbf{D} = \partial_z 0$, this means

$$\partial_{zz} E = -\omega^2 \epsilon \mu E = -k^2 E. \tag{7.23}$$

This is the usual starting place that we use to show that the plane wave has an exponential form

$$\mathbf{E}(z) = \hat{\mathbf{x}} \left(E_+ e^{-jkz} + E_- e^{jkz} \right). \tag{7.24}$$

The magnetic field from eq. (7.21) is

$$\begin{aligned} \mathbf{B} &= \frac{j}{\omega} \left(-jkE_+ e^{-jkz} + jkE_- e^{jkz} \right) \\ &= \frac{1}{c} \left(E_+ e^{-jkz} - E_- e^{jkz} \right), \end{aligned} \tag{7.25}$$

or

$$\begin{aligned} \mathbf{H} &= \frac{1}{\mu c} \left(E_+ e^{-jkz} - E_- e^{jkz} \right) \\ &= \frac{1}{\eta} \left(E_+ e^{-jkz} - E_- e^{jkz} \right). \end{aligned} \tag{7.26}$$

A solution requires zero divergence for the magnetic field, but that can be seen to be the case by inspection.

A

PROF. ELEFTHERIADES' HANDWRITING DECODER RING.

I found Prof. Eleftheriades' handwriting tricky to decode in a number of cases. Here's a handy dandy codex should anybody else have the same troubles

(a) Greek letter Ω is written as a circle floating above a face up square bracket.

(b) Greek letter σ is written like a number 6, slightly tipped.

(c) J looks like pi with a tail.

(d) Greek letter λ looks like a mirror image of his 'h'.

(e) Greek letter μ can look like an M.

(a) **(b)** **(c)** **(d)** **(e)**

Figure A.1: Prof. Eleftheriades' handwriting decoder ring.

B

ELECTRIC SOURCES (GA).

In [5] §3.2 is a demonstration of the required (curl) form for the magnetic field, and potential form for the electric field.

I was wondering how this derivation would proceed using the Geometric Algebra (GA) formalism.

B.1 MAXWELL'S EQUATION IN GA PHASOR FORM.

Maxwell's equations, omitting magnetic charges and currents, are

$$\boldsymbol{\nabla} \times \mathcal{E} = -\frac{\partial \mathcal{B}}{\partial t} \tag{B.1a}$$

$$\boldsymbol{\nabla} \times \mathcal{H} = \mathcal{J} + \frac{\partial \mathcal{D}}{\partial t} \tag{B.1b}$$

$$\boldsymbol{\nabla} \cdot \mathcal{D} = \rho \tag{B.1c}$$

$$\boldsymbol{\nabla} \cdot \mathcal{B} = 0. \tag{B.1d}$$

Assuming linear media $\mathcal{B} = \mu_0 \mathcal{H}$, $\mathcal{D} = \epsilon_0 \mathcal{E}$, and phasor relationships of the form $\mathcal{E} = \operatorname{Re}\left(\mathbf{E}(\mathbf{r}) e^{j\omega t}\right)$ for the fields and the currents, these reduce to

$$\boldsymbol{\nabla} \times \mathbf{E} = -j\omega \mathbf{B} \tag{B.2a}$$

$$\boldsymbol{\nabla} \times \mathbf{B} = \mu_0 \mathbf{J} + j\omega \epsilon_0 \mu_0 \mathbf{E} \tag{B.2b}$$

$$\boldsymbol{\nabla} \cdot \mathbf{E} = \rho/\epsilon_0 \tag{B.2c}$$

$$\boldsymbol{\nabla} \cdot \mathbf{B} = 0. \tag{B.2d}$$

These four equations can be assembled into a single equation form using the GA identities

$$\mathbf{f}\mathbf{g} = \mathbf{f} \cdot \mathbf{g} + \mathbf{f} \wedge \mathbf{g} = \mathbf{f} \cdot \mathbf{g} + I \mathbf{f} \times \mathbf{g}. \tag{B.3a}$$

$$I = \hat{\mathbf{x}}\hat{\mathbf{y}}\hat{\mathbf{z}}. \tag{B.3b}$$

The electric and magnetic field equations, respectively, are

$$\boldsymbol{\nabla}\mathbf{E} = \rho/\epsilon_0 - jkc\mathbf{B}I \tag{B.4a}$$

$$\boldsymbol{\nabla}c\mathbf{B} = \frac{I}{\epsilon_0 c}\mathbf{J} + jk\mathbf{E}I, \tag{B.4b}$$

where $\omega = kc$, and $1 = c^2\epsilon_0\mu_0$ have also been used to eliminate some of the mess of constants. Summing these (first scaling eq. (B.4b) by I), gives Maxwell's equation in its GA phasor form

$$\boxed{\left(\boldsymbol{\nabla} + jk\right)\left(\mathbf{E} + c\mathbf{B}I\right) = \frac{1}{\epsilon_0 c}\left(c\rho - \mathbf{J}\right).} \tag{B.5}$$

B.2 PRELIMINARIES. DUAL MAGNETIC FORM OF MAXWELL'S EQUATIONS.

The arguments of the text showing that a potential representation for the electric and magnetic fields is possible easily translates into GA. To perform this translation, some duality lemmas are required

First consider the cross product of two vectors $\mathbf{x}, \mathbf{y}$ and the right handed dual $-\mathbf{y}I$ of $\mathbf{y}$, a bivector, of one of these vectors. Noting that the Euclidean pseudoscalar I commutes with all grade multivectors in a Euclidean geometric algebra space, the cross product can be written

$$\begin{aligned}(\mathbf{x} \times \mathbf{y}) &= -I\left(\mathbf{x} \wedge \mathbf{y}\right) \\ &= -I\frac{1}{2}\left(\mathbf{x}\mathbf{y} - \mathbf{y}\mathbf{x}\right) \\ &= \frac{1}{2}\left(\mathbf{x}(-\mathbf{y}I) - (-\mathbf{y}I)\mathbf{x}\right) \\ &= \mathbf{x} \cdot \left(-\mathbf{y}I\right).\end{aligned} \tag{B.6}$$

The last step makes use of the fact that the wedge product of a vector and vector is antisymmetric, whereas the dot product (vector grade selection) of a vector and bivector is antisymmetric. Details on grade selection operators and how to characterize symmetric and antisymmetric products of vectors with blades as either dot or wedge products can be found in [14], [8].

Similarly, the dual of the dot product can be written as

$$\begin{aligned} -I(\mathbf{x} \cdot \mathbf{y}) &= -I\frac{1}{2}(\mathbf{x}\mathbf{y} + \mathbf{y}\mathbf{x}) \\ &= \frac{1}{2}(\mathbf{x}(-\mathbf{y}I) + (-\mathbf{y}I)\mathbf{x}) \\ &= \mathbf{x} \wedge (-\mathbf{y}I). \end{aligned} \tag{B.7}$$

These duality transformations are motivated by the observation that in the GA form of Maxwell's equation the magnetic field shows up in its dual form, a bivector. Spelled out in terms of the dual magnetic field, those equations are

$$\boldsymbol{\nabla} \wedge \mathbf{E} = -j\omega \mathbf{B}I \tag{B.8a}$$

$$\boldsymbol{\nabla} \cdot (-\mathbf{B}I) = \mu_0 \mathbf{J} + j\omega\epsilon_0\mu_0 \mathbf{E} \tag{B.8b}$$

$$\boldsymbol{\nabla} \cdot \mathbf{E} = \rho/\epsilon_0 \tag{B.8c}$$

$$\boldsymbol{\nabla} \wedge (-\mathbf{B}I) = 0. \tag{B.8d}$$

B.3 CONSTRUCTING A POTENTIAL REPRESENTATION.

The starting point of the argument in the text was the observation that the triple product $\boldsymbol{\nabla} \cdot (\boldsymbol{\nabla} \times \mathbf{x}) = 0$ for any (sufficiently continuous) vector $\mathbf{x}$. This triple product is a completely antisymmetric sum, and the equivalent statement in GA is $\boldsymbol{\nabla} \wedge \boldsymbol{\nabla} \wedge \mathbf{x} = 0$ for any vector $\mathbf{x}$. This follows from $\mathbf{a} \wedge \mathbf{a} = 0$, true for any vector $\mathbf{a}$, including the gradient operator $\boldsymbol{\nabla}$, provided those gradients are acting on a sufficiently continuous blade. In the absence of magnetic charges, eq. (B.8d) shows that the divergence of the dual magnetic field is zero. It it therefore possible to find a potential $\mathbf{A}$ such that

$$\mathbf{B}I = \boldsymbol{\nabla} \wedge \mathbf{A}. \tag{B.9}$$

Substituting this into Maxwell-Faraday eq. (B.8a) gives

$$\boldsymbol{\nabla} \wedge \left(\mathbf{E} + j\omega \mathbf{A}\right) = 0. \tag{B.10}$$

This relation is a bivector identity with zero, so will be satisfied if

$$\mathbf{E} + j\omega\mathbf{A} = -\boldsymbol{\nabla}\phi, \tag{B.11}$$

for some scalar ϕ. Unlike the $\mathbf{B}I = \boldsymbol{\nabla} \wedge \mathbf{A}$ solution to eq. (B.8d), the grade of ϕ is fixed by the requirement that $\mathbf{E} + j\omega\mathbf{A}$ is unity (a vector), so a $\mathbf{E} + j\omega\mathbf{A} = \boldsymbol{\nabla} \wedge \psi$, for a higher grade blade ψ would not work, despite satisfying the condition $\boldsymbol{\nabla} \wedge \boldsymbol{\nabla} \wedge \psi = 0$.

Substitution of eq. (B.11) and eq. (B.9) into Ampere's law eq. (B.8b) gives

$$\begin{aligned} -\boldsymbol{\nabla} \cdot (\boldsymbol{\nabla} \wedge \mathbf{A}) &= \mu_0 \mathbf{J} + j\omega\epsilon_0\mu_0 (-\boldsymbol{\nabla}\phi - j\omega\mathbf{A}) \\ -\boldsymbol{\nabla}^2\mathbf{A} - \boldsymbol{\nabla}(\boldsymbol{\nabla} \cdot \mathbf{A}) &= \end{aligned} \tag{B.12}$$

Rearranging gives

$$\boldsymbol{\nabla}^2\mathbf{A} + k^2\mathbf{A} = -\mu_0\mathbf{J} - \boldsymbol{\nabla}\left(\boldsymbol{\nabla} \cdot \mathbf{A} + j\frac{k}{c}\phi\right). \tag{B.13}$$

The fields $\mathbf{A}$ and ϕ are assumed to be phasors, say $\mathcal{A} = \operatorname{Re} \mathbf{A} e^{jkct}$ and $\varphi = \operatorname{Re} \phi e^{jkct}$. Grouping the scalar and vector potentials into the standard four vector form $A^\mu = (\phi/c, \mathbf{A})$, and expanding the Lorentz gauge condition

$$\begin{aligned} 0 &= \partial_\mu \left(A^\mu e^{jkct}\right) \\ &= \partial_a \left(A^a e^{jkct}\right) + \frac{1}{c}\frac{\partial}{\partial t}\left(\frac{\phi}{c} e^{jkct}\right) \\ &= \boldsymbol{\nabla} \cdot \mathbf{A} e^{jkct} + \frac{1}{c} jk\phi e^{jkct} \\ &= \left(\boldsymbol{\nabla} \cdot \mathbf{A} + jk\phi/c\right) e^{jkct}, \end{aligned} \tag{B.14}$$

shows that in eq. (B.13) the quantity in braces is in fact the Lorentz gauge condition, so in the Lorentz gauge, the vector potential satisfies a non-homogeneous Helmholtz equation.

$$\boxed{\boldsymbol{\nabla}^2\mathbf{A} + k^2\mathbf{A} = -\mu_0\mathbf{J}.} \tag{B.15}$$

B.4 MAXWELL'S EQUATION IN FOUR VECTOR FORM.

The four vector form of Maxwell's equation follows from eq. (B.5) after pre-multiplying by γ^0. With

$$A = A^\mu \gamma_\mu = (\phi/c, \mathbf{A}) \tag{B.16a}$$

$$F = \nabla \wedge A = \frac{1}{c}(\mathbf{E} + c\mathbf{B}I) \tag{B.16b}$$

$$\nabla = \gamma^\mu \partial_\mu = \gamma^0 (\boldsymbol{\nabla} + jk) \tag{B.16c}$$

$$J = J^\mu \gamma_\mu = (c\rho, \mathbf{J}), \tag{B.16d}$$

Maxwell's equation is

$$\boxed{\nabla F = \mu_0 J.} \tag{B.17}$$

Here $\{\gamma_\mu\}$ is used as the basis of the four vector Minkowski space, with $\gamma_0^2 = -\gamma_k^2 = 1$ (i.e. $\gamma^\mu \cdot \gamma_\nu = \delta^\mu{}_\nu$), and $\gamma_a \gamma_0 = \sigma_a$ where $\{\sigma_a\}$ is the Pauli basic (i.e. standard basis vectors for $\mathbb{R}^3$). Let's demonstrate this, one piece at a time. Observe that the action of the spacetime gradient on a phasor, assuming that all time dependence is in the exponential, is

$$\begin{aligned}
\gamma^\mu \partial_\mu \left(\psi e^{jkct}\right) &= (\gamma^a \partial_a + \gamma_0 \partial_{ct}) \left(\psi e^{jkct}\right) \\
&= \gamma_0 \left(\gamma_0 \gamma^a \partial_a + jk\right) \left(\psi e^{jkct}\right) \\
&= \gamma_0 \left(\sigma_a \partial_a + jk\right) \psi e^{jkct} \\
&= \gamma_0 \left(\boldsymbol{\nabla} + jk\right) \psi e^{jkct}.
\end{aligned} \tag{B.18}$$

This allows the operator identification of eq. (B.16c). The four current portion of the equation comes from

$$\begin{aligned}
c\rho - \mathbf{J} &= \gamma_0 \left(\gamma_0 c\rho - \gamma_0 \gamma_a \gamma_0 J^a\right) \\
&= \gamma_0 \left(\gamma_0 c\rho + \gamma_a J^a\right) \\
&= \gamma_0 \left(\gamma_\mu J^\mu\right) \\
&= \gamma_0 J.
\end{aligned} \tag{B.19}$$

Taking the curl of the four potential gives

$$\begin{aligned}\nabla \wedge A &= \left(\gamma^a \partial_a + \gamma_0 jk\right) \wedge \left(\gamma_0 \phi/c + \gamma_b A^b\right) \\ &= -\sigma_a \partial_a \phi/c + \gamma^a \wedge \gamma_b \partial_a A^b - jk\sigma_b A^b \\ &= -\sigma_a \partial_a \phi/c + \sigma_a \wedge \sigma_b \partial_a A^b - jk\sigma_b A^b \\ &= \frac{1}{c}\left(-\boldsymbol{\nabla}\phi - j\omega \mathbf{A} + c\boldsymbol{\nabla} \wedge \mathbf{A}\right) \\ &= \frac{1}{c}\left(\mathbf{E} + c\mathbf{B}I\right).\end{aligned} \tag{B.20}$$

Substituting all of these into Maxwell's eq. (B.5) gives

$$\gamma_0 \nabla c F = \frac{1}{\epsilon_0 c} \gamma_0 J, \tag{B.21}$$

which recovers eq. (B.17) as desired.

B.5 HELMHOLTZ EQUATION DIRECTLY FROM THE GA FORM.

It is easier to find eq. (B.15) from the GA form of Maxwell's eq. (B.17) than the traditional curl and divergence equations. Note that

$$\begin{aligned}\nabla F &= \nabla \left(\nabla \wedge A\right) \\ &= \nabla \cdot \left(\nabla \wedge A\right) + \cancel{\nabla \wedge \left(\nabla \wedge A\right)} \\ &= \nabla^2 A - \nabla \left(\nabla \cdot A\right),\end{aligned} \tag{B.22}$$

however, the Lorentz gauge condition $\partial_\mu A^\mu = \nabla \cdot A = 0$ kills the latter term above. This leaves

$$\begin{aligned}\nabla F &= \nabla^2 A \\ &= \gamma_0 \left(\boldsymbol{\nabla} + jk\right) \gamma_0 \left(\boldsymbol{\nabla} + jk\right) A \\ &= \gamma_0^2 \left(-\boldsymbol{\nabla} + jk\right) \left(\boldsymbol{\nabla} + jk\right) A \\ &= -\left(\boldsymbol{\nabla}^2 + k^2\right) A \\ &= \mu_0 J.\end{aligned} \tag{B.23}$$

The timelike component of this gives

$$\left(\boldsymbol{\nabla}^2 + k^2\right) \phi = -\rho/\epsilon_0, \tag{B.24}$$

and the spacelike components give

$$\left(\boldsymbol{\nabla}^2 + k^2\right) \mathbf{A} = -\mu_0 \mathbf{J}, \tag{B.25}$$

recovering eq. (B.15) as desired.

C

MAGNETIC SOURCES (GA).

In [5] §3.3, treating magnetic charges and currents, and no electric charges and currents, is a demonstration of the required (curl) form for the electric field, and potential form for the electric field. Not knowing what to name this, I'll call the associated equations the dual-Maxwell's equations. I was wondering how this derivation would proceed using the Geometric Algebra (GA) formalism.

C.1 DUAL-MAXWELL'S EQUATION IN GA PHASOR FORM.

The dual-Maxwell's equations, omitting electric charges and currents, are

$$\boldsymbol{\nabla} \times \mathcal{E} = -\frac{\partial \mathcal{B}}{\partial t} - \mathcal{m} \tag{C.1a}$$

$$\boldsymbol{\nabla} \times \mathcal{H} = \frac{\partial \mathcal{D}}{\partial t} \tag{C.1b}$$

$$\boldsymbol{\nabla} \cdot \mathcal{D} = 0 \tag{C.1c}$$

$$\boldsymbol{\nabla} \cdot \mathcal{B} = \rho_{\mathrm{m}}. \tag{C.1d}$$

Assuming linear media $\mathcal{B} = \mu_0 \mathcal{H}$, $\mathcal{D} = \epsilon_0 \mathcal{E}$, and phasor relationships of the form $\mathcal{E} = \mathrm{Re}\left(\mathbf{E}(\mathbf{r}) e^{j\omega t}\right)$ for the fields and the currents, these reduce to

$$\boldsymbol{\nabla} \times \mathbf{E} = -j\omega \mathbf{B} - \mathbf{M} \tag{C.2a}$$

$$\boldsymbol{\nabla} \times \mathbf{B} = j\omega \epsilon_0 \mu_0 \mathbf{E} \tag{C.2b}$$

$$\boldsymbol{\nabla} \cdot \mathbf{E} = 0 \tag{C.2c}$$

$$\boldsymbol{\nabla} \cdot \mathbf{B} = \rho_{\mathrm{m}}. \tag{C.2d}$$

These four equations can be assembled into a single equation form using the GA identities

$$\mathbf{f}\mathbf{g} = \mathbf{f} \cdot \mathbf{g} + \mathbf{f} \wedge \mathbf{g} = \mathbf{f} \cdot \mathbf{g} + I\mathbf{f} \times \mathbf{g}. \tag{C.3a}$$

$$I = \hat{\mathbf{x}}\hat{\mathbf{y}}\hat{\mathbf{z}}. \tag{C.3b}$$

The electric and magnetic field equations, respectively, are

$$\boldsymbol{\nabla}\mathbf{E} = -\left(\mathbf{M} + jkc\mathbf{B}\right) I \tag{C.4a}$$

$$\boldsymbol{\nabla} c\mathbf{B} = c\rho_{\mathrm{m}} + jk\mathbf{E}I, \tag{C.4b}$$

where $\omega = kc$, and $1 = c^2\epsilon_0\mu_0$ have also been used to eliminate some of the mess of constants. Summing these (first scaling eq. (C.4b) by I), gives Maxwell's equation in its GA phasor form

$$\boxed{\left(\boldsymbol{\nabla} + jk\right)\left(\mathbf{E} + c\mathbf{B}I\right) = \left(c\rho_{\mathrm{m}} - \mathbf{M}\right) I.} \tag{C.5}$$

C.2 PRELIMINARIES. DUAL MAGNETIC FORM OF MAXWELL'S EQUATIONS.

The arguments of the text showing that a potential representation for the electric and magnetic fields is possible easily translates into GA. To perform this translation, some duality lemmas are required

First consider the cross product of two vectors $\mathbf{x}, \mathbf{y}$ and the right handed dual $-\mathbf{y}I$ of $\mathbf{y}$, a bivector, of one of these vectors. Noting that the Euclidean pseudoscalar I commutes with all grade multivectors in a Euclidean geometric algebra space, the cross product can be written

$$\begin{aligned}
(\mathbf{x} \times \mathbf{y}) &= -I\left(\mathbf{x} \wedge \mathbf{y}\right) \\
&= -I\frac{1}{2}\left(\mathbf{x}\mathbf{y} - \mathbf{y}\mathbf{x}\right) \\
&= \frac{1}{2}\left(\mathbf{x}(-\mathbf{y}I) - (-\mathbf{y}I)\mathbf{x}\right) \\
&= \mathbf{x} \cdot \left(-\mathbf{y}I\right).
\end{aligned} \tag{C.6}$$

The last step makes use of the fact that the wedge product of a vector and vector is antisymmetric, whereas the dot product (vector grade selection) of a vector and bivector is antisymmetric. Details on grade selection operators and how to characterize symmetric and antisymmetric products of vectors with blades as either dot or wedge products can be found in [14], [8].

Similarly, the dual of the dot product can be written as

$$\begin{aligned} -I\left(\mathbf{x}\cdot\mathbf{y}\right) &= -I\frac{1}{2}\left(\mathbf{x}\mathbf{y}+\mathbf{y}\mathbf{x}\right) \\ &= \frac{1}{2}\left(\mathbf{x}(-\mathbf{y}I)+(-\mathbf{y}I)\mathbf{x}\right) \\ &= \mathbf{x}\wedge\left(-\mathbf{y}I\right). \end{aligned} \tag{C.7}$$

These duality transformations are motivated by the observation that in the GA form of Maxwell's equation the magnetic field shows up in its dual form, a bivector. Spelled out in terms of the dual magnetic field, those equations are

$$\boldsymbol{\nabla}\cdot\left(-\mathbf{E}I\right) = -j\omega\mathbf{B} - \mathbf{M} \tag{C.8a}$$

$$\boldsymbol{\nabla}\wedge\mathbf{H} = j\omega\epsilon_0\mathbf{E}I \tag{C.8b}$$

$$\boldsymbol{\nabla}\wedge\left(-\mathbf{E}I\right) = 0 \tag{C.8c}$$

$$\boldsymbol{\nabla}\cdot\mathbf{B} = \rho_{\mathrm{m}}. \tag{C.8d}$$

C.3 CONSTRUCTING A POTENTIAL REPRESENTATION.

The starting point of the argument in the text was the observation that the triple product $\boldsymbol{\nabla}\cdot\left(\boldsymbol{\nabla}\times\mathbf{x}\right) = 0$ for any (sufficiently continuous) vector $\mathbf{x}$. This triple product is a completely antisymmetric sum, and the equivalent statement in GA is $\boldsymbol{\nabla}\wedge\boldsymbol{\nabla}\wedge\mathbf{x} = 0$ for any vector $\mathbf{x}$. This follows from $\mathbf{a}\wedge\mathbf{a} = 0$, true for any vector $\mathbf{a}$, including the gradient operator $\boldsymbol{\nabla}$, provided those gradients are acting on a sufficiently continuous blade.

In the absence of electric charges, eq. (C.8c) shows that the divergence of the dual electric field is zero. It it therefore possible to find a potential $\mathbf{F}$ such that

$$-\epsilon_0\mathbf{E}I = \boldsymbol{\nabla}\wedge\mathbf{F}. \tag{C.9}$$

Substituting this eq. (C.8b) gives

$$\nabla \wedge \left(\mathbf{H} + j\omega \mathbf{F} \right) = 0. \tag{C.10}$$

This relation is a bivector identity with zero, so will be satisfied if

$$\mathbf{H} + j\omega \mathbf{F} = -\nabla \phi_m, \tag{C.11}$$

for some scalar ϕ_m. Unlike the $-\epsilon_0 \mathbf{E} I = \nabla \wedge \mathbf{F}$ solution to eq. (C.8c), the grade of ϕ_m is fixed by the requirement that $\mathbf{E} + j\omega \mathbf{F}$ is unity (a vector), so a $\mathbf{E} + j\omega \mathbf{F} = \nabla \wedge \psi$, for a higher grade blade ψ would not work, despite satisfying the condition $\nabla \wedge \nabla \wedge \psi = 0$.

Substitution of eq. (C.11) and eq. (C.9) into eq. (C.8b) gives

$$\begin{aligned} \nabla \cdot \left(\nabla \wedge \mathbf{F} \right) &= -\epsilon_0 \mathbf{M} - j\omega \epsilon_0 \mu_0 \left(-\nabla \phi_m - j\omega \mathbf{F} \right) \\ \nabla^2 \mathbf{F} - \nabla \left(\nabla \cdot \mathbf{F} \right) &= \end{aligned} \tag{C.12}$$

Rearranging gives

$$\nabla^2 \mathbf{F} + k^2 \mathbf{F} = -\epsilon_0 \mathbf{M} + \nabla \left(\nabla \cdot \mathbf{F} + j \frac{k}{c} \phi_m \right). \tag{C.13}$$

The fields $\mathbf{F}$ and ϕ_m are assumed to be phasors, say $\mathcal{A} = \operatorname{Re} \mathbf{F} e^{jkct}$ and $\varphi = \operatorname{Re} \phi_m e^{jkct}$. Grouping the scalar and vector potentials into the standard four vector form $F^\mu = (\phi_m / c, \mathbf{F})$, and expanding the Lorentz gauge condition

$$\begin{aligned} 0 &= \partial_\mu \left(F^\mu e^{jkct} \right) \\ &= \partial_a \left(F^a e^{jkct} \right) + \frac{1}{c} \frac{\partial}{\partial t} \left(\frac{\phi_m}{c} e^{jkct} \right) \\ &= \nabla \cdot \mathbf{F} e^{jkct} + \frac{1}{c} jk \phi_m e^{jkct} \\ &= \left(\nabla \cdot \mathbf{F} + jk \phi_m / c \right) e^{jkct}, \end{aligned} \tag{C.14}$$

shows that in eq. (C.13) the quantity in braces is in fact the Lorentz gauge condition, so in the Lorentz gauge, the vector potential satisfies a non-homogeneous Helmholtz equation.

$$\boxed{\nabla^2 \mathbf{F} + k^2 \mathbf{F} = -\epsilon_0 \mathbf{M}.} \tag{C.15}$$

C.4 MAXWELL'S EQUATION IN FOUR VECTOR FORM.

The four vector form of Maxwell's equation follows from eq. (C.5) after pre-multiplying by γ^0. With

$$F = F^\mu \gamma_\mu = (\phi_m/c, \mathbf{F}) \tag{C.16a}$$

$$G = \nabla \wedge F = -\epsilon_0 \left(\mathbf{E} + c\mathbf{B}I\right) I \tag{C.16b}$$

$$\nabla = \gamma^\mu \partial_\mu = \gamma^0 \left(\boldsymbol{\nabla} + jk\right) \tag{C.16c}$$

$$M = M^\mu \gamma_\mu = \left(c\rho_{\mathrm{m}}, \mathbf{M}\right), \tag{C.16d}$$

Maxwell's equation is

$$\boxed{\nabla G = -\epsilon_0 M.} \tag{C.17}$$

Here $\{\gamma_\mu\}$ is used as the basis of the four vector Minkowski space, with $\gamma_0^2 = -\gamma_k^2 = 1$ (i.e. $\gamma^\mu \cdot \gamma_\nu = \delta^\mu{}_\nu$), and $\gamma_a \gamma_0 = \sigma_a$ where $\{\sigma_a\}$ is the Pauli basic (i.e. standard basis vectors for $\mathbb{R}^3$).

Let's demonstrate this, one piece at a time. Observe that the action of the spacetime gradient on a phasor, assuming that all time dependence is in the exponential, is

$$\begin{aligned}
\gamma^\mu \partial_\mu \left(\psi e^{jkct}\right) &= \left(\gamma^a \partial_a + \gamma_0 \partial_{ct}\right) \left(\psi e^{jkct}\right) \\
&= \gamma_0 \left(\gamma_0 \gamma^a \partial_a + jk\right) \left(\psi e^{jkct}\right) \\
&= \gamma_0 \left(\sigma_a \partial_a + jk\right) \psi e^{jkct} \\
&= \gamma_0 \left(\boldsymbol{\nabla} + jk\right) \psi e^{jkct}.
\end{aligned} \tag{C.18}$$

This allows the operator identification of eq. (C.16c). The four current portion of the equation comes from

$$\begin{aligned}
c\rho_{\mathrm{m}} - \mathbf{M} &= \gamma_0 \left(\gamma_0 c\rho_{\mathrm{m}} - \gamma_0 \gamma_a \gamma_0 M^a\right) \\
&= \gamma_0 \left(\gamma_0 c\rho_{\mathrm{m}} + \gamma_a M^a\right) \\
&= \gamma_0 \left(\gamma_\mu M^\mu\right) \\
&= \gamma_0 M.
\end{aligned} \tag{C.19}$$

Taking the curl of the four potential gives

$$\begin{aligned}\nabla \wedge F &= \left(\gamma^a \partial_a + \gamma_0 jk\right) \wedge \left(\gamma_0 \phi_m / c + \gamma_b F^b\right) \\ &= -\sigma_a \partial_a \phi_m / c + \gamma^a \wedge \gamma_b \partial_a F^b - jk\sigma_b F^b \\ &= -\sigma_a \partial_a \phi_m / c + \sigma_a \wedge \sigma_b \partial_a F^b - jk\sigma_b F^b \\ &= \frac{1}{c}\left(-\boldsymbol{\nabla} \phi_m - j\omega \mathbf{F} + c\boldsymbol{\nabla} \wedge \mathbf{F}\right) \\ &= \epsilon_0 \left(c\mathbf{B} - \mathbf{E} I\right) \\ &= -\epsilon_0 \left(\mathbf{E} + c\mathbf{B} I\right) I.\end{aligned} \tag{C.20}$$

Substituting all of these into Maxwell's eq. (C.5) gives

$$-\frac{\gamma_0}{\epsilon_0} \nabla G = \gamma_0 M, \tag{C.21}$$

which recovers eq. (C.17) as desired.

C.5 HELMHOLTZ EQUATION DIRECTLY FROM THE GA FORM.

It is easier to find eq. (C.15) from the GA form of Maxwell's eq. (C.17) than the traditional curl and divergence equations. Note that

$$\begin{aligned}\nabla G &= \nabla \left(\nabla \wedge F\right) \\ &= \nabla \cdot \left(\nabla \wedge F\right) + \cancel{\nabla \wedge \left(\nabla \wedge F\right)} \\ &= \nabla^2 F - \nabla \left(\nabla \cdot F\right),\end{aligned} \tag{C.22}$$

however, the Lorentz gauge condition $\partial_\mu F^\mu = \nabla \cdot F = 0$ kills the latter term above. This leaves

$$\begin{aligned}\nabla G &= \nabla^2 F \\ &= \gamma_0 \left(\boldsymbol{\nabla} + jk\right) \gamma_0 \left(\boldsymbol{\nabla} + jk\right) F \\ &= \gamma_0^2 \left(-\boldsymbol{\nabla} + jk\right) \left(\boldsymbol{\nabla} + jk\right) F \\ &= -\left(\boldsymbol{\nabla}^2 + k^2\right) F \\ &= -\epsilon_0 M.\end{aligned} \tag{C.23}$$

The timelike component of this gives

$$\left(\boldsymbol{\nabla}^2 + k^2\right) \phi_m = -\epsilon_0 c \rho_{\mathrm{m}}, \tag{C.24}$$

and the spacelike components give

$$\left(\boldsymbol{\nabla}^2 + k^2\right) \mathbf{F} = -\epsilon_0 \mathbf{M}, \tag{C.25}$$

recovering eq. (C.15) as desired.

D

ELECTRIC AND MAGNETIC SOURCES (GA).

Separate examinations of the phasor form of Maxwell's equation (with electric charges and current densities), and the Dual Maxwell's equation (i.e. allowing magnetic charges and currents) were just performed. Here the structure of these equations with both electric and magnetic charges and currents will be examined.

D.1 SPACE TIME SPLIT.

The vector curl and divergence form of Maxwell's equations are

$$\boldsymbol{\nabla} \times \mathcal{E} = -\frac{\partial \mathcal{B}}{\partial t} - \mathcal{M} \tag{D.1a}$$

$$\boldsymbol{\nabla} \times \mathcal{H} = \mathcal{J} + \frac{\partial \mathcal{D}}{\partial t} \tag{D.1b}$$

$$\boldsymbol{\nabla} \cdot \mathcal{D} = \rho \tag{D.1c}$$

$$\boldsymbol{\nabla} \cdot \mathcal{B} = \rho_{\mathrm{m}}. \tag{D.1d}$$

In phasor form these are

$$\boldsymbol{\nabla} \times \mathbf{E} = -jkc\mathbf{B} - \mathbf{M} \tag{D.2a}$$

$$\boldsymbol{\nabla} \times \mathbf{H} = \mathbf{J} + jkc\mathbf{D} \tag{D.2b}$$

$$\boldsymbol{\nabla} \cdot \mathbf{D} = \rho \tag{D.2c}$$

$$\boldsymbol{\nabla} \cdot \mathbf{B} = \rho_{\mathrm{m}}. \tag{D.2d}$$

Switching to $\mathbf{E} = \mathbf{D}/\epsilon_0, \mathbf{B} = \mu_0 \mathbf{H}$ fields (even though these aren't the primary fields in engineering), gives

$$\boldsymbol{\nabla} \times \mathbf{E} = -jk(c\mathbf{B}) - \mathbf{M} \tag{D.3a}$$

$$\nabla \times (c\mathbf{B}) = \frac{\mathbf{J}}{\epsilon_0 c} + jk\mathbf{E} \tag{D.3b}$$

$$\nabla \cdot \mathbf{E} = \rho/\epsilon_0 \tag{D.3c}$$

$$\nabla \cdot (c\mathbf{B}) = c\rho_{\mathrm{m}}. \tag{D.3d}$$

Finally, using

$$\mathbf{fg} = \mathbf{f} \cdot \mathbf{g} + I\mathbf{f} \times \mathbf{g}, \tag{D.4}$$

the divergence and curl contributions of each of the fields can be grouped

$$\nabla \mathbf{E} = \rho/\epsilon_0 - \left(jk(c\mathbf{B}) + \mathbf{M}\right) I \tag{D.5a}$$

$$\nabla (c\mathbf{B}I) = c\rho_{\mathrm{m}} I - \left(\frac{\mathbf{J}}{\epsilon_0 c} + jk\mathbf{E}\right), \tag{D.5b}$$

or

$$\nabla \left(\mathbf{E} + c\mathbf{B}I\right) = \rho/\epsilon_0 - \left(jk(c\mathbf{B}) + \mathbf{M}\right) I + c\rho_{\mathrm{m}} I - \left(\frac{\mathbf{J}}{\epsilon_0 c} + jk\mathbf{E}\right). \tag{D.6}$$

Regrouping gives Maxwell's equation including both electric and magnetic sources

$$\boxed{\left(\nabla + jk\right)\left(\mathbf{E} + c\mathbf{B}I\right) = \frac{1}{\epsilon_0 c}\left(c\rho - \mathbf{J}\right) + \left(c\rho_{\mathrm{m}} - \mathbf{M}\right) I.} \tag{D.7}$$

D.2 COVARIANT FORM.

It was observed that these can be put into a tidy four vector form by premultiplying by γ_0, where

$$J = \gamma_\mu J^\mu = \left(c\rho, \mathbf{J}\right) \tag{D.8a}$$

$$M = \gamma_\mu M^\mu = \left(c\rho_{\mathrm{m}}, \mathbf{M}\right) \tag{D.8b}$$

$$\nabla = \gamma_0 \left(\boldsymbol{\nabla} + jk\right) = \gamma^k \partial_k + jk\gamma_0, \tag{D.8c}$$

That gives

$$\boxed{\nabla \left(\mathbf{E} + c\mathbf{B}I\right) = \frac{J}{\epsilon_0 c} + MI.} \tag{D.9}$$

D.3 TRIAL POTENTIAL SOLUTION.

When there were only electric sources, it was observed that potential solutions were of the form $\mathbf{E} + c\mathbf{B}I \propto \nabla \wedge A$, whereas when there was only magnetic sources it was observed that potential solutions were of the form $\mathbf{E} + c\mathbf{B}I \propto (\nabla \wedge F)I$. It seems reasonable to attempt a trial solution that contains both such contributions, say

$$\mathbf{E} + c\mathbf{B}I = \nabla \wedge A_{\mathrm{e}} + (\nabla \wedge A_{\mathrm{m}})\, I. \tag{D.10}$$

Without any loss of generality Lorentz gauge conditions can be imposed on the four-vector fields $A_{\mathrm{e}}, A_{\mathrm{m}}$. Those conditions are

$$\nabla \cdot A_{\mathrm{e}} = \nabla \cdot A_{\mathrm{m}} = 0. \tag{D.11}$$

Since $\nabla X = \nabla \cdot X + \nabla \wedge X$, for any four vector X, the trial solution eq. (D.10) is reduced to

$$\mathbf{E} + c\mathbf{B}I = \nabla A_{\mathrm{e}} + \nabla A_{\mathrm{m}} I. \tag{D.12}$$

Maxwell's equation is now

$$\begin{aligned}\frac{J}{\epsilon_0 c} + MI &= \nabla^2 (A_{\mathrm{e}} + A_{\mathrm{m}} I) \\ &= \gamma_0 \left(\boldsymbol{\nabla} + jk\right) \gamma_0 \left(\boldsymbol{\nabla} + jk\right) (A_{\mathrm{e}} + A_{\mathrm{m}} I) \\ &= \left(-\boldsymbol{\nabla} + jk\right) \left(\boldsymbol{\nabla} + jk\right) (A_{\mathrm{e}} + A_{\mathrm{m}} I) \\ &= -\left(\boldsymbol{\nabla}^2 + k^2\right) (A_{\mathrm{e}} + A_{\mathrm{m}} I)\,. \end{aligned} \tag{D.13}$$

Notice how tidily this separates into vector and trivector components. Those are

$$-\left(\boldsymbol{\nabla}^2 + k^2\right) A_{\mathrm{e}} = \frac{J}{\epsilon_0 c} \tag{D.14a}$$

$$-\left(\boldsymbol{\nabla}^2 + k^2\right) A_{\mathrm{m}} = M. \tag{D.14b}$$

The result is a single Helmholtz equation for each of the electric and magnetic four-potentials, and both can be solved completely independently. This was claimed in class, but now the underlying reason is clear.

D.4 LORENTZ GAUGE APPLICATION TO HELMHOLTZ.

Because a single frequency phasor relationship was implied the scalar components of each of these four potentials is determined by the Lorentz gauge condition. For example

$$
\begin{aligned}
0 &= \boldsymbol{\nabla} \cdot \left(A_{\mathrm{e}} e^{jkct} \right) \\
&= \left(\gamma^0 \frac{1}{c} \frac{\partial}{\partial t} + \gamma^k \frac{\partial}{\partial x^k} \right) \cdot \left(\gamma_0 A_{\mathrm{e}}^0 e^{jkct} + \gamma_m A_{\mathrm{e}}^m e^{jkct} \right) \\
&= \left(\gamma^0 jk + \gamma^r \frac{\partial}{\partial x^r} \right) \cdot \left(\gamma_0 A_{\mathrm{e}}^0 + \gamma_s A_{\mathrm{e}}^s \right) e^{jkct} \\
&= \left(jk A_{\mathrm{e}}^0 + \boldsymbol{\nabla} \cdot \mathbf{A}_{\mathrm{e}} \right) e^{jkct},
\end{aligned}
\tag{D.15}
$$

so

$$
A_{\mathrm{e}}^0 = \frac{j}{k} \boldsymbol{\nabla} \cdot \mathbf{A}_{\mathrm{e}}. \tag{D.16}
$$

The same sort of relationship will apply to the magnetic potential too. This means that the Helmholtz equations can be solved in the three vector space as

$$
\left(\boldsymbol{\nabla}^2 + k^2 \right) \mathbf{A}_{\mathrm{e}} = -\frac{\mathbf{J}}{\epsilon_0 c} \tag{D.17a}
$$

$$
\left(\boldsymbol{\nabla}^2 + k^2 \right) \mathbf{A}_{\mathrm{m}} = -\mathbf{M}. \tag{D.17b}
$$

D.5 RECOVERING THE FIELDS.

Relative to the observer frame implicitly specified by γ_0, here's an expansion of the curl of the electric four potential

$$
\begin{aligned}
\nabla \wedge A_{\mathrm{e}} &= \frac{1}{2} \left(\nabla A_{\mathrm{e}} - A_{\mathrm{e}} \nabla \right) \\
&= \frac{1}{2} \left(\gamma_0 \left(\boldsymbol{\nabla} + jk \right) \gamma_0 \left(A_{\mathrm{e}}^0 - \mathbf{A}_{\mathrm{e}} \right) - \gamma_0 \left(A_{\mathrm{e}}^0 - \mathbf{A}_{\mathrm{e}} \right) \gamma_0 \left(\boldsymbol{\nabla} + jk \right) \right) \\
&= \frac{1}{2} \left(\left(-\boldsymbol{\nabla} + jk \right) \left(A_{\mathrm{e}}^0 - \mathbf{A}_{\mathrm{e}} \right) - \left(A_{\mathrm{e}}^0 + \mathbf{A}_{\mathrm{e}} \right) \left(\boldsymbol{\nabla} + jk \right) \right) \\
&= \frac{1}{2} \left(-2 \boldsymbol{\nabla} A_{\mathrm{e}}^0 + \cancel{jk A_{\mathrm{e}}^0} - \cancel{jk A_{\mathrm{e}}^0} + \boldsymbol{\nabla} \mathbf{A}_{\mathrm{e}} - \mathbf{A}_{\mathrm{e}} \boldsymbol{\nabla} - 2 jk \mathbf{A}_{\mathrm{e}} \right) \\
&= - \left(\boldsymbol{\nabla} A_{\mathrm{e}}^0 + jk \mathbf{A}_{\mathrm{e}} \right) + \boldsymbol{\nabla} \wedge \mathbf{A}_{\mathrm{e}}.
\end{aligned}
\tag{D.18}
$$

In the above expansion when the gradients appeared on the right of the field components, they are acting from the right (i.e. implicitly using the Hestenes dot convention.)

The electric and magnetic fields can be picked off directly from above, and in the units implied by this choice of four-potential are

$$\mathbf{E}_\mathrm{e} = -\left(\boldsymbol{\nabla} A_\mathrm{e}^0 + jk\mathbf{A}_\mathrm{e}\right) = -j\left(\frac{1}{k}\boldsymbol{\nabla}\boldsymbol{\nabla}\cdot\mathbf{A}_\mathrm{e} + k\mathbf{A}_\mathrm{e}\right) \tag{D.19a}$$

$$c\mathbf{B}_\mathrm{e} = \boldsymbol{\nabla}\times\mathbf{A}_\mathrm{e}. \tag{D.19b}$$

For the fields due to the magnetic potentials

$$(\nabla\wedge A_\mathrm{e})\,I = -\left(\boldsymbol{\nabla} A_\mathrm{e}^0 + jk\mathbf{A}_\mathrm{e}\right) I - \boldsymbol{\nabla}\times\mathbf{A}_\mathrm{e}, \tag{D.20}$$

so the fields are

$$c\mathbf{B}_\mathrm{m} = -\left(\boldsymbol{\nabla} A_\mathrm{m}^0 + jk\mathbf{A}_\mathrm{m}\right) = -j\left(\frac{1}{k}\boldsymbol{\nabla}\boldsymbol{\nabla}\cdot\mathbf{A}_\mathrm{m} + k\mathbf{A}_\mathrm{m}\right) \tag{D.21a}$$

$$\mathbf{E}_\mathrm{m} = -\boldsymbol{\nabla}\times\mathbf{A}_\mathrm{m}. \tag{D.21b}$$

Including both electric and magnetic sources the fields are

$$\mathbf{E} = -\boldsymbol{\nabla}\times\mathbf{A}_\mathrm{m} - j\left(\frac{1}{k}\boldsymbol{\nabla}\boldsymbol{\nabla}\cdot\mathbf{A}_\mathrm{e} + k\mathbf{A}_\mathrm{e}\right) \tag{D.22a}$$

$$c\mathbf{B} = \boldsymbol{\nabla}\times\mathbf{A}_\mathrm{e} - j\left(\frac{1}{k}\boldsymbol{\nabla}\boldsymbol{\nabla}\cdot\mathbf{A}_\mathrm{m} + k\mathbf{A}_\mathrm{m}\right). \tag{D.22b}$$

Observe that the alternation of signs is exactly that of a superposition of electric dipole and magnetic dipole fields. This is consistent with the fact that the dual form of Maxwell's equations has been designed explicitly to model infinitesimal current loops as sources.

E

RECIPROCITY THEOREM (GA).

The reciprocity theorem involves a Poynting like antisymmetric difference of the following form

$$\mathbf{E}^{(a)} \times \mathbf{H}^{(b)} - \mathbf{E}^{(b)} \times \mathbf{H}^{(a)}. \tag{E.1}$$

This smells like something that can probably be related to a combined electromagnetic field multivectors in some sort of structured fashion. Guessing that this is related to the antisymmetric sum of two electromagnetic field multivectors turns out to be correct. Let

$$F^{(a)} = \mathbf{E}^{(a)} + c\mathbf{B}^{(a)} I \tag{E.2a}$$

$$F^{(b)} = \mathbf{E}^{(b)} + c\mathbf{B}^{(b)} I. \tag{E.2b}$$

Now form the antisymmetric sum

$$\begin{aligned}
\frac{1}{2}\left(F^{(a)}F^{(b)} - F^{(b)}F^{(a)}\right) &= \frac{1}{2}\left(\mathbf{E}^{(a)} + c\mathbf{B}^{(a)} I\right)\left(\mathbf{E}^{(b)} + c\mathbf{B}^{(b)} I\right) \\
&\quad - \frac{1}{2}\left(\mathbf{E}^{(b)} + c\mathbf{B}^{(b)} I\right)\left(\mathbf{E}^{(a)} + c\mathbf{B}^{(a)} I\right) \\
&= \frac{1}{2}\left(\mathbf{E}^{(a)}\mathbf{E}^{(b)} - \mathbf{E}^{(b)}\mathbf{E}^{(a)}\right) \\
&\quad + \frac{Ic}{2}\left(\mathbf{E}^{(a)}\mathbf{B}^{(b)} - \mathbf{B}^{(b)}\mathbf{E}^{(a)}\right) \\
&\quad + \frac{Ic}{2}\left(\mathbf{B}^{(a)}\mathbf{E}^{(b)} - \mathbf{E}^{(b)}\mathbf{B}^{(a)}\right) \\
&\quad + \frac{c^2}{2}\left(\mathbf{B}^{(b)}\mathbf{B}^{(a)} - \mathbf{B}^{(a)}\mathbf{B}^{(b)}\right) \\
&= \mathbf{E}^{(a)} \wedge \mathbf{E}^{(b)} + c^2\left(\mathbf{B}^{(b)} \wedge \mathbf{B}^{(a)}\right) \\
&\quad + Ic\left(\mathbf{E}^{(a)} \wedge \mathbf{B}^{(b)} + \mathbf{B}^{(a)} \wedge \mathbf{E}^{(b)}\right) \\
&= I\mathbf{E}^{(a)} \times \mathbf{E}^{(b)} + c^2 I\left(\mathbf{B}^{(b)} \times \mathbf{B}^{(a)}\right) \\
&\quad - c\left(\mathbf{E}^{(a)} \times \mathbf{B}^{(b)} + \mathbf{B}^{(a)} \times \mathbf{E}^{(b)}\right).
\end{aligned} \tag{E.3}$$

This has two components, the first is a bivector (pseudoscalar times vector) that includes all the non-mixed products, and the second is a vector that includes all the mixed terms. We can therefore write the antisymmetric difference of the reciprocity theorem by extracting just the grade one terms of the antisymmetric sum of the combined electromagnetic field

$$\mathbf{E}^{(a)} \times \mathbf{H}^{(b)} - \mathbf{E}^{(b)} \times \mathbf{H}^{(a)} = -\frac{1}{2c\mu_0} \left\langle \left(F^{(a)} F^{(b)} - F^{(b)} F^{(a)} \right) \right\rangle_1 . \quad \text{(E.4)}$$

Observing that the antisymmetrization used in the reciprocity theorem is only one portion of the larger electromagnetic field antisymmetrization, introduces two new questions

1. How would the reciprocity theorem be derived directly in terms of $F^{(a)} F^{(b)} - F^{(b)} F^{(a)}$?

2. What is the significance of the other portion of this antisymmetrization $\mathbf{E}^{(a)} \times \mathbf{E}^{(b)} - c^2 \mu_0^2 \left(\mathbf{H}^{(a)} \times \mathbf{H}^{(b)} \right)$?

F

RELATION TO TENSOR FORM (GA).

Following the principle that one should always relate new formalisms to things previously learned, I'd like to know what Maxwell's equations look like in tensor form when magnetic sources are included. As a verification that the previous Geometric Algebra form of Maxwell's equation that includes magnetic sources is correct, I'll start with the GA form of Maxwell's equation, find the tensor form, and then verify that the vector form of Maxwell's equations can be recovered from the tensor form.

Tensor form. With four-vector potential A, and bivector electromagnetic field $F = \nabla \wedge A$, the GA form of Maxwell's equation is

$$\nabla F = \frac{J}{\epsilon_0 c} + MI. \tag{F.1}$$

The left hand side can be unpacked into vector and trivector terms $\nabla F = \nabla \cdot F + \nabla \wedge F$, which happens to also separate the sources nicely as a side effect

$$\nabla \cdot F = \frac{J}{\epsilon_0 c} \tag{F.2a}$$

$$\nabla \wedge F = MI. \tag{F.2b}$$

The electric source equation can be unpacked into tensor form by dotting with the four vector basis vectors. With the usual definition $F^{\alpha\beta} = \partial^\alpha A^\beta - \partial^\beta A^\alpha$, that is

$$\begin{aligned}
\gamma^\mu \cdot (\nabla \cdot F) &= \gamma^\mu \cdot (\nabla \cdot (\nabla \wedge A)) \\
&= \gamma^\mu \cdot \left(\gamma^\nu \partial_\nu \cdot \left(\gamma_\alpha \partial^\alpha \wedge \gamma_\beta A^\beta\right)\right) \\
&= \gamma^\mu \cdot \left(\gamma^\nu \cdot \left(\gamma_\alpha \wedge \gamma_\beta\right)\right) \partial_\nu \partial^\alpha A^\beta \\
&= \frac{1}{2} \gamma^\mu \cdot \left(\gamma^\nu \cdot \left(\gamma_\alpha \wedge \gamma_\beta\right)\right) \partial_\nu F^{\alpha\beta} \\
&= \frac{1}{2} \delta^{\nu\mu}_{[\alpha\beta]} \partial_\nu F^{\alpha\beta} \\
&= \frac{1}{2} \partial_\nu F^{\nu\mu} - \frac{1}{2} \partial_\nu F^{\mu\nu} \\
&= \partial_\nu F^{\nu\mu}.
\end{aligned} \tag{F.3}$$

So the first tensor equation is

$$\boxed{\partial_\nu F^{\nu\mu} = \frac{1}{c\epsilon_0} J^\mu.} \tag{F.4}$$

To unpack the magnetic source portion of Maxwell's equation, put it first into dual form, so that it has four vectors on each side

$$\begin{aligned}
M &= -\left(\nabla \wedge F\right) I \\
&= -\frac{1}{2}\left(\nabla F + F \nabla\right) I \\
&= -\frac{1}{2}\left(\nabla F I - F I \nabla\right) \\
&= -\nabla \cdot \left(F I\right).
\end{aligned} \tag{F.5}$$

Dotting with γ^μ gives

$$\begin{aligned}
M^\mu &= \gamma^\mu \cdot (\nabla \cdot (-F I)) \\
&= \gamma^\mu \cdot \left(\gamma^\nu \partial_\nu \cdot \left(-\frac{1}{2} \gamma^\alpha \wedge \gamma^\beta I F_{\alpha\beta}\right)\right) \\
&= -\frac{1}{2} \left\langle \gamma^\mu \cdot \left(\gamma^\nu \cdot \left(\gamma^\alpha \wedge \gamma^\beta I\right)\right) \right\rangle \partial_\nu F_{\alpha\beta}.
\end{aligned} \tag{F.6}$$

This scalar grade selection is a complete antisymmetrization of the indexes

$$\begin{aligned}
&\left\langle \gamma^\mu \cdot \left(\gamma^\nu \cdot \left(\gamma^\alpha \wedge \gamma^\beta I \right) \right) \right\rangle \\
&= \left\langle \gamma^\mu \cdot \left(\gamma^\nu \cdot \left(\gamma^\alpha \gamma^\beta \gamma_0 \gamma_1 \gamma_2 \gamma_3 \right) \right) \right\rangle \\
&= \left\langle \gamma_0 \gamma_1 \gamma_2 \gamma_3 \gamma^\mu \gamma^\nu \gamma^\alpha \gamma^\beta \right\rangle \\
&= \delta^{\mu\nu\alpha\beta}_{3210} \\
&= \epsilon^{\mu\nu\alpha\beta},
\end{aligned} \tag{F.7}$$

so the magnetic source portion of Maxwell's equation, in tensor form, is

$$\boxed{\frac{1}{2}\epsilon^{\nu\alpha\beta\mu}\partial_\nu F_{\alpha\beta} = M^\mu.} \tag{F.8}$$

Relating the tensor to the fields. The electromagnetic field has been identified with the electric and magnetic fields by

$$F = \mathcal{E} + c\mu_0 \mathcal{H} I, \tag{F.9}$$

or in coordinates

$$\frac{1}{2}\gamma_\mu \wedge \gamma_\nu F^{\mu\nu} = E^a \gamma_a \gamma_0 + c\mu_0 H^a \gamma_a \gamma_0 I. \tag{F.10}$$

By forming the dot product sequence $F^{\alpha\beta} = \gamma^\beta \cdot (\gamma^\alpha \cdot F)$, the electric and magnetic field components can be related to the tensor components. The electric field components follow by inspection and are

$$\begin{aligned}
E^b &= \gamma^0 \cdot \left(\gamma^b \cdot F \right) \\
&= F^{b0}.
\end{aligned} \tag{F.11}$$

The magnetic field relation to the tensor components follow from

$$\begin{aligned}
F^{rs} &= F_{rs} \\
&= \gamma_s \cdot \left(\gamma_r \cdot \left(c\mu_0 H^a \gamma_a \gamma_0 I \right) \right) \\
&= c\mu_0 H^a \left\langle \gamma_s \gamma_r \gamma_a \gamma_0 I \right\rangle \\
&= c\mu_0 H^a \left\langle -\cancel{\gamma^0} \gamma^1 \gamma^2 \gamma^3 \gamma_s \gamma_r \gamma_a \cancel{\gamma_0} \right\rangle \\
&= -c\mu_0 H^a \delta^{[321]}_{sra} \\
&= c\mu_0 H^a \epsilon_{sra}.
\end{aligned} \tag{F.12}$$

Expanding this for each pair of spacelike coordinates gives

$$F^{12} = c\mu_0 H^3 \epsilon_{213} = -c\mu_0 H^3 \tag{F.13a}$$

$$F^{23} = c\mu_0 H^1 \epsilon_{321} = -c\mu_0 H^1 \tag{F.13b}$$

$$F^{31} = c\mu_0 H^2 \epsilon_{132} = -c\mu_0 H^2, \tag{F.13c}$$

or

$$\boxed{\begin{aligned} E^1 &= F^{10} \\ E^2 &= F^{20} \\ E^3 &= F^{30} \\ H^1 &= -\frac{1}{c\mu_0} F^{23} \\ H^2 &= -\frac{1}{c\mu_0} F^{31} \\ H^3 &= -\frac{1}{c\mu_0} F^{12}. \end{aligned}} \tag{F.14}$$

Recover the vector equations from the tensor equations. Starting with the non-dual Maxwell tensor equation, expanding the timelike index gives

$$\begin{aligned} \frac{1}{c\epsilon_0} J^0 &= \frac{1}{\epsilon_0}\rho \\ &= \partial_\nu F^{\nu 0} \\ &= \partial_1 F^{10} + \partial_2 F^{20} + \partial_3 F^{30}. \end{aligned} \tag{F.15}$$

This is Gauss's law

$$\boxed{\boldsymbol{\nabla} \cdot \boldsymbol{\mathcal{E}} = \rho/\epsilon_0.} \tag{F.16}$$

For a spacelike index, any one is representative. Expanding index 1 gives

$$\begin{aligned}\frac{1}{c\epsilon_0}J^1 &= \partial_\nu F^{\nu 1} \\ &= \frac{1}{c}\partial_t F^{01} + \partial_2 F^{21} + \partial_3 F^{31} \\ &= -\frac{1}{c}E^1 + \partial_2(c\mu_0 H^3) + \partial_3(-c\mu_0 H^2) \\ &= \left(-\frac{1}{c}\frac{\partial \mathcal{E}}{\partial t} + c\mu_0 \boldsymbol{\nabla} \times \mathcal{H}\right) \cdot \mathbf{e}_1.\end{aligned} \tag{F.17}$$

Extending this to the other indexes and multiplying through by $\epsilon_0 c$ recovers the Ampere-Maxwell equation (assuming linear media)

$$\boxed{\boldsymbol{\nabla} \times \mathcal{H} = \mathcal{J} + \frac{\partial \mathcal{D}}{\partial t}.} \tag{F.18}$$

The expansion of the 0th free (timelike) index of the dual Maxwell tensor equation is

$$\begin{aligned}M^0 &= \frac{1}{2}\epsilon^{\nu\alpha\beta 0}\partial_\nu F_{\alpha\beta} \\ &= -\frac{1}{2}\epsilon^{0\nu\alpha\beta}\partial_\nu F_{\alpha\beta} \\ &= -\frac{1}{2}\left(\partial_1(F_{23} - F_{32}) + \partial_2(F_{31} - F_{13}) + \partial_3(F_{12} - F_{21})\right) \\ &= -\left(\partial_1 F_{23} + \partial_2 F_{31} + \partial_3 F_{12}\right) \\ &= -\left(\partial_1(-c\mu_0 H^1) + \partial_2(-c\mu_0 H^2) + \partial_3(-c\mu_0 H^3)\right),\end{aligned} \tag{F.19}$$

but $M^0 = c\rho_\mathrm{m}$, giving us Gauss's law for magnetism (with magnetic charge density included)

$$\boxed{\boldsymbol{\nabla} \cdot \mathcal{H} = \rho_\mathrm{m}/\mu_0.} \tag{F.20}$$

For the spacelike indexes of the dual Maxwell equation, only one need be computed (say 1), and cyclic permutation will provide the rest. That is

$$\begin{aligned}
M^1 &= \frac{1}{2}\epsilon^{\nu\alpha\beta 1}\partial_\nu F_{\alpha\beta} \\
&= \frac{1}{2}\left(\partial_2\left(F_{30} - F_{03}\right)\right) + \frac{1}{2}\left(\partial_3\left(F_{02} - F_{02}\right)\right) + \frac{1}{2}\left(\partial_0\left(F_{23} - F_{32}\right)\right) \\
&= -\partial_2 F^{30} + \partial_3 F^{20} + \partial_0 F_{23} \\
&= -\partial_2 E^3 + \partial_3 E^2 + \frac{1}{c}\frac{\partial}{\partial t}\left(-c\mu_0 H^1\right) \\
&= -\left(\boldsymbol{\nabla} \times \mathcal{E} + \mu_0 \frac{\partial \mathcal{H}}{\partial t}\right) \cdot \mathbf{e}_1.
\end{aligned} \tag{F.21}$$

Extending this to the rest of the coordinates gives the Maxwell-Faraday equation (as extended to include magnetic current density sources)

$$\boxed{\boldsymbol{\nabla} \times \mathcal{E} = -\mathcal{M} - \mu_0 \frac{\partial \mathcal{H}}{\partial t}.} \tag{F.22}$$

This takes things full circle, going from the vector differential Maxwell's equations, to the Geometric Algebra form of Maxwell's equation, to Maxwell's equations in tensor form, and back to the vector form. Not only is the tensor form of Maxwell's equations with magnetic sources now known, the translation from the tensor and vector formalism has also been verified, and miraculously no signs or factors of 2 were lost or gained in the process.

G

PARALLEL PROJECTION OF ELECTROMAGNETIC FIELDS (GA).

When computing the components of a polarized reflecting ray that were parallel or not-parallel to the reflecting surface, it was found that the electric and magnetic fields could be written as

$$\mathbf{E} = \left(\mathbf{E} \cdot \hat{\mathbf{p}}\right) \hat{\mathbf{p}} + \left(\mathbf{E} \cdot \hat{\mathbf{q}}\right) \hat{\mathbf{q}} = E_\parallel \hat{\mathbf{p}} + E_\perp \hat{\mathbf{q}} \tag{G.1a}$$

$$\mathbf{H} = \left(\mathbf{H} \cdot \hat{\mathbf{p}}\right) \hat{\mathbf{p}} + \left(\mathbf{H} \cdot \hat{\mathbf{q}}\right) \hat{\mathbf{q}} = H_\parallel \hat{\mathbf{p}} + H_\perp \hat{\mathbf{q}}. \tag{G.1b}$$

where a unit vector $\hat{\mathbf{p}}$ that lies both in the reflecting plane and in the electromagnetic plane (tangential to the wave vector direction) was

$$\hat{\mathbf{p}} = \frac{\hat{\mathbf{k}} \times \hat{\mathbf{n}}}{\left|\hat{\mathbf{k}} \times \hat{\mathbf{n}}\right|} \tag{G.2a}$$

$$\hat{\mathbf{q}} = \hat{\mathbf{k}} \times \hat{\mathbf{p}}. \tag{G.2b}$$

Here $\hat{\mathbf{q}}$ is perpendicular to $\hat{\mathbf{p}}$ but lies in the electromagnetic plane. This logically subdivides the fields into two pairs, one with the electric field parallel to the reflection plane

$$\begin{aligned} \mathbf{E}_1 &= \left(\mathbf{E} \cdot \hat{\mathbf{p}}\right) \hat{\mathbf{p}} = E_\parallel \hat{\mathbf{p}} \\ \mathbf{H}_1 &= \left(\mathbf{H} \cdot \hat{\mathbf{q}}\right) \hat{\mathbf{q}} = H_\perp \hat{\mathbf{q}}, \end{aligned} \tag{G.3}$$

and one with the magnetic field parallel to the reflection plane

$$\begin{aligned} \mathbf{H}_2 &= \left(\mathbf{H} \cdot \hat{\mathbf{p}}\right) \hat{\mathbf{p}} = H_\parallel \hat{\mathbf{p}} \\ \mathbf{E}_2 &= \left(\mathbf{E} \cdot \hat{\mathbf{q}}\right) \hat{\mathbf{q}} = E_\perp \hat{\mathbf{q}}. \end{aligned} \tag{G.4}$$

Expressed in Geometric Algebra form, each of these pairs of fields should be thought of as components of a single multivector field. That is

$$F_1 = \mathbf{E}_1 + c\mu_0 \mathbf{H}_1 I \tag{G.5a}$$

$$F_2 = \mathbf{E}_2 + c\mu_0 \mathbf{H}_2 I, \tag{G.5b}$$

where the original total field is

$$F = \mathbf{E} + c\mu_0 \mathbf{H} I. \tag{G.6}$$

In eq. (G.5a) we have a composite projection operation, finding the portion of the electric field that lies in the reflection plane, and simultaneously finding the component of the magnetic field that lies perpendicular to that (while still lying in the tangential plane of the electromagnetic field). In eq. (G.5b) the magnetic field is projected onto the reflection plane and a component of the electric field that lies in the tangential (to the wave vector direction) plane is computed.

If we operate only on the complete multivector field, can we find these composite projection field components in a single operation, instead of working with the individual electric and magnetic fields?

Working towards this goal, it is worthwhile to point out consequences of the assumption that the fields are plane wave (or equivalently far field spherical waves). For such a wave we have

$$\begin{aligned}
\mathbf{H} &= \frac{1}{\mu_0} \hat{\mathbf{k}} \times \mathbf{E} \\
&= \frac{1}{\mu_0} (-I) \left(\hat{\mathbf{k}} \wedge \mathbf{E} \right) \\
&= \frac{1}{\mu_0} (-I) \left(\hat{\mathbf{k}} \mathbf{E} - \hat{\mathbf{k}} \cdot \mathbf{E} \right) \\
&= -\frac{I}{\mu_0} \hat{\mathbf{k}} \mathbf{E},
\end{aligned} \tag{G.7}$$

or

$$\mu_0 \mathbf{H} I = \hat{\mathbf{k}} \mathbf{E}. \tag{G.8}$$

This made use of the identity $\mathbf{a} \wedge \mathbf{b} = I \left(\mathbf{a} \times \mathbf{b} \right)$, and the fact that the electric field is perpendicular to the wave vector direction. The total multivector field is

$$\begin{aligned}
F &= \mathbf{E} + c\mu_0 \mathbf{H} I \\
&= \left(1 + c\hat{\mathbf{k}} \right) \mathbf{E}.
\end{aligned} \tag{G.9}$$

Expansion of magnetic field component that is perpendicular to the reflection plane gives

$$
\begin{aligned}
\mu_0 H_\perp &= \mu_0 \mathbf{H} \cdot \hat{\mathbf{q}} \\
&= \left\langle \left(-\hat{\mathbf{k}} \mathbf{E} I \right) \hat{\mathbf{q}} \right\rangle \\
&= -\left\langle \hat{\mathbf{k}} \mathbf{E} I \left(\hat{\mathbf{k}} \times \hat{\mathbf{p}} \right) \right\rangle \\
&= \left\langle \hat{\mathbf{k}} \mathbf{E} I I \left(\hat{\mathbf{k}} \wedge \hat{\mathbf{p}} \right) \right\rangle \\
&= -\left\langle \hat{\mathbf{k}} \mathbf{E} \hat{\mathbf{k}} \hat{\mathbf{p}} \right\rangle \\
&= \left\langle \hat{\mathbf{k}} \hat{\mathbf{k}} \mathbf{E} \hat{\mathbf{p}} \right\rangle \\
&= \mathbf{E} \cdot \hat{\mathbf{p}},
\end{aligned}
\tag{G.10}
$$

so

$$
F_1 = (\hat{\mathbf{p}} + c I \hat{\mathbf{q}}) \mathbf{E} \cdot \hat{\mathbf{p}}. \tag{G.11}
$$

Since $\hat{\mathbf{q}} \hat{\mathbf{k}} \hat{\mathbf{p}} = I$, the component of the complete multivector field in the $\hat{\mathbf{p}}$ direction is

$$
\begin{aligned}
F_1 &= (\hat{\mathbf{p}} - c \hat{\mathbf{p}} \hat{\mathbf{k}}) \mathbf{E} \cdot \hat{\mathbf{p}} \\
&= \hat{\mathbf{p}} (1 - c \hat{\mathbf{k}}) \mathbf{E} \cdot \hat{\mathbf{p}} \\
&= (1 + c \hat{\mathbf{k}}) \hat{\mathbf{p}} \mathbf{E} \cdot \hat{\mathbf{p}}.
\end{aligned}
\tag{G.12}
$$

It is reasonable to expect that F_2 has a similar form, but with $\hat{\mathbf{p}} \rightarrow \hat{\mathbf{q}}$. This is verified by expansion

$$
\begin{aligned}
F_2 &= E_\perp \hat{\mathbf{q}} + c \left(\mu_0 H_\parallel \right) \hat{\mathbf{p}} I \\
&= (\mathbf{E} \cdot \hat{\mathbf{q}}) \, \hat{\mathbf{q}} + c \left\langle -\hat{\mathbf{k}} \mathbf{E} I \hat{\mathbf{k}} \hat{\mathbf{q}} I \right\rangle \left(\hat{\mathbf{k}} \hat{\mathbf{q}} I \right) I \\
&= (\mathbf{E} \cdot \hat{\mathbf{q}}) \, \hat{\mathbf{q}} + c \left\langle \hat{\mathbf{k}} \mathbf{E} \hat{\mathbf{k}} \hat{\mathbf{q}} \right\rangle \hat{\mathbf{k}} \hat{\mathbf{q}} (-1) \\
&= (\mathbf{E} \cdot \hat{\mathbf{q}}) \, \hat{\mathbf{q}} + c \left\langle \hat{\mathbf{k}} \mathbf{E} (-\hat{\mathbf{q}} \hat{\mathbf{k}}) \right\rangle \hat{\mathbf{k}} \hat{\mathbf{q}} (-1) \\
&= (\mathbf{E} \cdot \hat{\mathbf{q}}) \, \hat{\mathbf{q}} + c \left\langle \hat{\mathbf{k}} \hat{\mathbf{k}} \mathbf{E} \hat{\mathbf{q}} \right\rangle \hat{\mathbf{k}} \hat{\mathbf{q}} \\
&= \left(1 + c \hat{\mathbf{k}} \right) \hat{\mathbf{q}} \, (\mathbf{E} \cdot \hat{\mathbf{q}})
\end{aligned}
\tag{G.13}
$$

This and eq. (G.12) before that makes a lot of sense. The original field can be written

$$
F = \left(\hat{\mathbf{E}} + c \left(\hat{\mathbf{k}} \times \hat{\mathbf{E}} \right) I \right) \mathbf{E} \cdot \hat{\mathbf{E}}, \tag{G.14}
$$

where the leading multivector term contains all the directional dependence of the electric and magnetic field components, and the trailing scalar has the magnitude of the field with respect to the reference direction $\hat{\mathbf{E}}$.

We have the same structure after projecting $\mathbf{E}$ onto either the $\hat{\mathbf{p}}$, or $\hat{\mathbf{q}}$ directions respectively

$$F_1 = \left(\hat{\mathbf{p}} + c\left(\hat{\mathbf{k}} \times \hat{\mathbf{p}}\right) I\right) \mathbf{E} \cdot \hat{\mathbf{p}} \tag{G.15a}$$

$$F_2 = \left(\hat{\mathbf{q}} + c\left(\hat{\mathbf{k}} \times \hat{\mathbf{q}}\right) I\right) \mathbf{E} \cdot \hat{\mathbf{q}}. \tag{G.15b}$$

The next question is how to achieve this projection operation directly in terms of F and $\hat{\mathbf{p}}, \hat{\mathbf{q}}$, without resorting to expression of F in terms of $\mathbf{E}$, and $\mathbf{B}$. I've not yet been able to determine the structure of that operation.

H

MATHEMATICA NOTEBOOKS.

These Mathematica notebooks, some just trivial ones used to generate figures, others more elaborate, and perhaps some even polished, can be found in

https://github.com/peeterjoot/mathematica/tree/master/ece1229/.

The free Wolfram CDF player, is capable of read-only viewing these notebooks to some extent.

Files saved explicitly as CDF have interactive content that can be explored with the CDF player.

- Jan 18, 2015 tableOfTrigIntegrals.nb

  Integrals of some powers of sine and cosine products

- Jan 19, 2015 sphericalPlot3d.nb

  Antenna intensity plots for sine and cosine powers 1,2.

- Jan 28, 2015 sphericalManipulate.cdf

  An interactive graphical visualization of a couple of radiation intensity functions.

- Feb 8, 2015 visualizeDipoleFields.cdf

  In chapter 4 of Balanis' "Antenna Theory: Analysis and Design", are some discussions of the $kr < 1$, $kr = 1$, and $kr > 1$ radial dependence of the fields and power of a solution to an infinitesimal dipole system. This discussion severely lacks some plots. Here's a Mathematica Manipulate that allows for inspection of the real and imaginary parts of these functions, plotted against both k and r, with a kr == constant contour overlaid on it. The value of that constant can be altered using one of the sliders, as can the maximum range of k and r, and upper and lower bounds of the value of the functions being plotted.

- Feb 8, 2015 selectedInfinitesimalDipolePlots.nb

  think this was plots to generate figures for ps2

- Feb 28, 2015 ps3/eAndMdipoleSuperposition.nb

  ps3 p1 3d plot Manipulator and figures generation for a superposition of electric and magnetic dipoles.

- Feb 28, 2015 eAndMdipoleSuperposition.cdf

  This is a Manipulator to show the far fields of a superposition of electric and magnetic infinestismal dipoles on the x and y axes respectively. The fields at one point on the surface can be controlled using the theta and phi sliders.

- Feb 28, 2015 ps3/longDipolesSelectedLengths.nb

  Polar plots of the radiation intensity for long z-axis electric current dipoles. This also does the radiation resistance numerical integrals.

- Feb 28, 2015 ps3/longDipolesSavedLabeledPlot.nb

  Saved labeled plot for ps3 p2a.

- Feb 28, 2015 ps3/longDipoleInteractiveLength.nb

  A manipulate for visualizing the polar pattern for a long electric dipole, and showing the directivity. A version without the 3D checkbox option and without the directivity display is deployed as cdf in longDipolesWithLengthControl.cdf

- Feb 28, 2015 longDipolesWithLengthControl.cdf

  A manipulate for visualizing the polar pattern for a long electric dipole.

- Mar 1, 2015 ps3/directivityLongDipole.nb

  Numerical directivity calculations for ps3 p2 b, long dipole.

- Mar 10, 2015 ps3/ps3Q3plotsAndMiscIntegrals.nb

  Trig integrals and plots for ps3, p3. Numerical calculations of the directivity for part e.

- Mar 13, 2015 chebychevPlots.nb

  A couple Cheybshev T plots.

- Mar 15, 2015 cornerCubeArrayFactorSq.cdf

  A manipulate to show the radiation intensity of the array factor in 3D for the corner cube configuration. This doesn't include any contribution from the field itself (i.e. no sine squared term.)

- Mar 15, 2015 ps3/ps3Q3plotsCorrected.nb

  Redo the plots and the numerical calculations for the corner cube configuration problem, ps3, q3.

- Mar 16, 2015 cornerCubeArrayFactorSqIn.cdf

  Standalone generator for cornerCubeArrayFactorSq.cdf

- Mar 17, 2015 simpleTrigIntegrals.nb

  Some simple trig integrals

- Mar 21, 2015 chebychevPlotsII.nb

  A Manipulate for Cheybshev plot exploration. A plot of the first few, and a plot with a scale factor.

- Mar 21, 2015 chebychevPlotsManipulate.cdf

  Deployed CDF manipulator for Cheybshev polynomial exploration.

- Mar 22, 2015 chebychevN4ArrayFitManipulate.cdf

  Manipulate to visualize the variation with d for an $N = 4$ Cheybshev fitting.

- Mar 22, 2015 polarPlot.nb

  This uses the Cheybshev design technique from the text to fit a 4 element array to a T_3 function, and visualize it with polar plots. This includes a Manipulate to visualize the variation with d, saved separately as chebychevN4ArrayFitManipulate.cdf.

- Mar 23, 2015 ChebychevSecondMethod.nb

  Exploring Dolph-Cheybshev method from the class notes. Plots and a Manipulator

- Mar 23, 2015 ChebychevSecondMethodManipulate.cdf

  Just the manipulator from ChebychevSecondMethod.nb

- Mar 23, 2015 ChebychevSecondMethodManipulate.nb

  Deployed version of the manipulator from ChebychevSecondMethod.nb

- Mar 24, 2015 ps4/problem3BinomialArray.nb

  Verify the paper calculations for this problem, and generate the plots and the numerical values of the angles for the nulls.

- Mar 25, 2015 BinomialArray5WithPhaseAndKDControls.cdf

  Add interactive controls to 2D PolarPlot of problem 3 notebook, deployed version.

- Mar 25, 2015 ps4/BinomialArray5WithPhaseAndKDControls.nb

  Add interactive controls to 2D PolarPlot of problem 3 notebook.

- Mar 28, 2015 ps4/ps4p4Chebychev.nb

  Plots and numerical integration results for p4.

- Mar 29, 2015 sphericalReflectedUnitVector.nb

  Calculate spherical coordinates for a reflected unit vector. Doesn't simplify nicely.

- Mar 31, 2015 ps4/checkAlgebra.nb

  Check some of the trig algebra done by hand.

- Apr 9, 2015 ps5/problem1plot.nb

  Plot the calculated electric field for the aperature problem. Here I did the 2D polar plots using a dB scale plot, which I hadn't done before, but makes a lot of sense to see the details of the lobes. Also did a similar log scale plot for the 3D view.

- Apr 11, 2015 testPlaneIntersectionMethods.nb

  Some experimentation on how to plot a 3D surface with an arbitrary plane cut through it.

- Apr 21, 2015 balanisProblem8_8.nb

  balanisProblem8_8

I

JULIA NOTEBOOKS.

These Julia notebooks, can be found in
https://github.com/peeterjoot/julia.

These notebooks are text files. The julia program, available freely at www.julialang.org, is required to execute them. Some Julia code can also be evaluated with Matlab.

- Feb 17, 2015 ece1229/ps2/ps2p5.jl

  Numerical calculations for ps2 p5 (simple).

- Feb 22, 2015 ece1229/misc/eta.jl

  Numerically compute the free space impedance to compare to 120 pi.

- Mar 25, 2015 ece1229/misc/mycrappypolar.jl

  A brute force polar plot before figuring out how to do it in PyPlot directly.

- Mar 25, 2015 ece1229/ps4/p2.jl

  A reimplementation of matlab/ece1229/ps4/p2.m in Julia. Figure out how to do a polar plot and save it to a file.

- Mar 25, 2015 ece1229/misc/pyplotPolarExample.jl

  A variation of [10] pyplot_windrose.jl to try a Julia implementation of ps4/p2.

- Mar 26, 2015 ece1229/ps4/p4.jl

  Calculation of the numeric values of the Chebyshev array coeffients, directivites, and plots.

- Apr 28, 2015 ece1229/ps3/p2.jl

  Log polar plot of finite length dipole power, to zoom in on the side lobes for the 1.25 case.

- Apr 29, 2015 ece1229/ps3/p3.jl

  Replot corner cube array factor in log scale. Original polar and 3D plots were done in the ps3Q3plotsCorrected.nb Mathematica notebook.

- Apr 30, 2015 ece1229/ps4/p2x.jl

  Replot ps4 p2 function in linear and log scales, based on code from ps3/p3.jl

- May 1, 2015 ece1229/ps4/p3.jl

  Call polarPlot() to generate plot in both linear and log scales

- May 1, 2015 ece1229/ps4/polarPlot.jl

  Turn p2x.jl into a generic polar plotting function.

- May 1, 2015 ece1229/cheb/c.jl

  Replot chebychevDesign.tex figures with linear and log scale plots, avoiding infinities that I had in the Mathematica polarPlot.nb plots of the same.

J

MATLAB NOTEBOOKS.

These Matlab notebooks, some just trivial ones used to generate figures, others more elaborate, and perhaps some even polished, can be found in

https://github.com/peeterjoot/matlab.

These notebooks are text files, but a matlab product is required to execute them.

- Mar 25, 2015 ece1229/ps4/p1plot.m

  Plot the ps4 p1 AF for one value of ad.

- Mar 25, 2015 ece1229/ps4/p1plots.m

  Generate all the plots for p1 and save the plots to files for the report.

- Mar 25, 2015 ece1229/ps4/p2.m

  Problem 2. Code to confirm the zeros numerically, and to plot the absolute array factor.

- Apr 13, 2015 ece1229/ps5/phicap.m

  spherical polar phicap function

- Apr 13, 2015 ece1229/ps5/rcap.m

  spherical polar rcap function

- Apr 13, 2015 ece1229/ps5/thetacap.m

  spherical polar thetacap function

- Apr 13, 2015 ece1229/ps5/vecE.m

  ps5 p1 compuation and plots

- Apr 13, 2015 ece1229/ps5/logscale.m

  db values for an input array rescaled to fit in the 0,1 interval.

- Apr 14, 2015 ece1229/ps5/pII.m

  Display the numeric substitutions, and compute the value of m for part h that has zero imaginary input impedance.

- Apr 14, 2015 ece1229/ps5/calculateZinAndStuff.m

  Calculate Zin given a single value of m. Returns all the intermediate calculations in a structure for display purposes.

INDEX

Ampere's law, 138
  differential form, 32
  integral form, 32
Ampere-Maxwell equation, 163
angle of incidence, 62
antenna array, 83
antenna gain, 25
antenna under test, 25
antisymmetric, 157
antisymmetrization, 161
aperture antenna, 117
aperture efficiency, 14
array antenna
  Cheybshev, 89
array factor, 93
AUT, 25
average power density, 13

binary array, 103
binomial array, 108
bivector, 137, 159
boundary conditions, 30

captured power, 24
Chebyscheff
  first order LDE, 101
  orthogonality, 102
  recurrence relation, 100
  second order LDE, 101
Chebyscheff polynomial, 83
Cheybshev array, 86
Cheybshev polynomials
  products, 85
circular polarization, 16
constitutive relations, 29
continuity equation, 28
corner cube, 93
corner cube antenna, 93
coupled PDE, 127
covariant form, 152
cross product, 144
  duality, 136
curl, 42, 49
  four vector, 140
current density, 45

dB, 3
dBi, 4
dipole
  long, 76
  near field, 70
  superposition, 74
dipole moment, 69
directivity, 13–15, 20
  approximation, 15
  E-plane, 22
  H-plane, 22
divergence, 35, 43, 137
  cross product, 45
  spherical coordinates, 51
divergence theorem, 29, 32, 44
Dolph-Chebyshev, 110
Dolph-Cheybshev, 89
dot product, 161
  dual, 137
dual-Maxwell's equation
  covariant, 147
  Geometric Algebra, 143

dual-Maxwell's equations, 143
duality, 37
duality transformation, 40, 55

effective area, 14
Effective Isotropic Receiving Power, 11
EIRP, 11
electic field
 in terms of potentials, 155
electric charge density, 27, 135
electric current density, 27, 135
electric dipole, 20
electric far field, 46
electric field, 161
 tangential, 32
 transverse projection, 55
 vector wave equation, 127
electric four potential, 153
electric potential, 49
electric source, 38
electric surface current density, 32, 33
electric vector potential, 49
electrical dipole
 horizontal, 20
electromagnetic field, 159
energy conservation, 35
energy momentum conservation, 35
energy momentum tensor, 36

far field, 1, 44, 51, 55
 electric field, 46
 magnetic, 53
four current, 139
four potential
 electric, 153
 magnetic, 153
four vector, 139, 147, 152
free space impedance, 12
free space loss, 14
free-space loss, 14
frequency domain, 38, 39
Fresnel equations, 58, 60
Friis equation, 17, 25, 74
Friis transmission equation, 15

gain, 15, 17
Gauss's law, 162
 differential form, 32
 differential form, magnetic, 32
 integral form, 32
 integral form, magnetic, 32
 magnetism, 163
Geometric Algebra, 135, 143, 151, 157, 164
geometric product, 136, 144
grade selection, 158
gradient
 spherical coordinates, 51
Green's function, 30
ground reflection, 59, 72, 73

half power beamwidth, 20
half-power beamwidth, 15
Helmholtz equation, 140, 148, 153
 electric current density, 154
 Green's function, 31
 magnetic current density, 154
 non-homogeneous, 138
homogeneous media, 29
horizontal dipole, 58

IERP, 74

image theorem, 64
impedance, 9
impedance transformation, 128
impulse response, 30
incident plane, 61
index of refraction, 58
infinite conducting plane, 65
infinitesimal dipole, 49
infinitesimal electric dipole, 68, 69
intrinsic impedance, 1
isotropic radiator, 4

Julia, 74

Laplacian, 127
line of sight, 17, 73
linear antenna, 49
linear media, 1, 29, 35, 135, 143, 163
linear polarization, 16
linear time invariant, 30
Lorentz force
  dual, 36
Lorentz force equation, 36
Lorentz gauge, 138, 140, 146, 148, 153, 154

magnetic charge, 143
magnetic charge density, 27, 163
magnetic current, 143
magnetic current density, 27, 164
magnetic current source, 46
magnetic field, 49, 161
  in terms of potentials, 155
  tangential, 33
magnetic four potential, 153
magnetic source, 35, 38, 43, 159
magnetic vector potential, 49
magnetization, 1
matched load, 15
Mathematica, 3, 169
Matlab, 74
max power density, 13
maximum directivity, 14
Maxwell equation, 135
  phasor, 135
Maxwell's equation, 135, 151, 164
  covariant, 152
  Geometric Algebra, 152
  integral forms, 29
  magnetic and electric potential separation, 153
  non-covariant GA form, 136
Maxwell's equations, 27, 151
  differential, 31
  tensor, 159
Maxwell-Faraday equation, 164
  differential form, 32
  integral form, 32
microstrip patch, 123
Mie scattering, 11
Minkowski space, 139
mobile reception, 71
momentum conservation, 36
momentum flux, 38
multivector, 157

normal reflection, 128
notation
  bold vectors, 12
  caligraphic vectors, 12
  phasor sign, 46

time average, 12

optical limit, 10

parallel projection, 165
ParametricPlot, 3
ParametricPlot3D, 3
patch antenna, 123
permittivity, 30, 70
phasor, 5, 35, 43, 138, 143, 151
dipole current, 70
plane of incidence, 58
plane of reflection, 58, 61
plane wave, 54, 60
PLF, 17
polarization, 5, 26
power loss, 15
polarization loss factor, 17
polarization mismatch, 17
polarization power loss, 15
polarization vector, 4
potential
curl of curl, 46
potential representation, 145
power
average, 9
complex, 9
phasor, 8
power density, 13, 23
Poynting theorem, 39
Poynting vector, 1, 21, 35
time average, 2
pseudoscalar, 136

radar cross section, 9, 10, 18, 23
radiated power density, 13
radiation intensity, 1, 4
RCS, 18, 23
corner reflector, 10
cylinder, 10
flat plate, 9
sphere, 10
reciprocity theorem, 39, 42, 157
rectangular aperture, 117
reflection coefficient, 56, 58, 72, 130
reflection plane, 61

scalar potential, 55
scattered power, 18
scattered power density, 24
scattering, 10
Schelkunoff
z-axis, 105
Schelkunoff array, 103
separation of variables, 127
signal to noise, 17
space time split, 151
spacetime gradient, 139, 153
spherical potential, 51
spherical scattering, 10
standard gain, 25
Stokes' theorem, 29, 32
superposition, 2, 3

tangential field components, 129
tensor, 157
tensor form, 159, 164
transmission coefficient, 129
transmission power, 17
transmitted power, 17
transverse field, 44
transverse nature, 54
triple product, 137
trivector, 159

vector potential, 49
vertical dipole, 56

polarization, 74

wave equation, 127
wave vector, 56
wavelength, 16
wedge product, 136, 144, 159
relation to cross product, 136

X-band, 18

zero phase, 105

BIBLIOGRAPHY

[1] M. Abramowitz and I.A. Stegun. *Handbook of mathematical functions with formulas, graphs, and mathematical tables*, volume 55. Dover publications, 1964. (Cited on page 85.)

[2] Constantine A Balanis. *Advanced engineering electromagnetics*. Wiley New York, 1989. (Cited on pages 127 and 131.)

[3] Constantine A Balanis. *Advanced engineering electromagnetics*, chapter Time-varying and time-harmonic electromagnetic fields. Wiley New York, 1989. (Cited on page 31.)

[4] Constantine A Balanis. *Advanced engineering electromagnetics*, chapter Reflection and transmission. Wiley New York, 1989. (Cited on page 128.)

[5] Constantine A Balanis. *Antenna theory: analysis and design*. John Wiley & Sons, 3rd edition, 2005. (Cited on pages xii, 12, 23, 30, 37, 49, 56, 58, 71, 80, 86, 89, 117, 135, and 143.)

[6] Jiuping Chen, Douglas W Oldenburg, and Edad Haber. Reciprocity in electromagnetics: application to modelling marine magnetometric resistivity data. *Physics of the earth and Planetary Interiors*, 150(1):45–61, 2005. URL http://www.mathcs.emory.edu/~haber/pubs/recip.pdf. (Cited on page 44.)

[7] digi.com. *Antenna Gain: dBi vs. dBd Decibel Detail*, 2015. URL http://www.digi.com/support/kbase/kbaseresultdetl?id=2146. [Online; accessed 15-Jan-2015]. (Cited on page 4.)

[8] C. Doran and A.N. Lasenby. *Geometric algebra for physicists*. Cambridge University Press New York, Cambridge, UK, 1st edition, 2003. (Cited on pages 137 and 145.)

[9] George V Eleftheriades and Keith G Balmain. *Negative-refraction metamaterials: fundamental principles and applications*. John Wiley & Sons, 2005. (Cited on page xii.)

[10] gizmaa. *Various Julia plotting examples using PyPlot*, 2020. URL https://gist.github.com/gizmaa/7214002. [Online; accessed 01-Jun-2020]. (Cited on page 173.)

[11] David Jeffrey Griffiths and Reed College. *Introduction to electrodynamics*. Prentice hall Upper Saddle River, NJ, 3rd edition, 1999. (Cited on pages 1, 2, 3, and 12.)

[12] David Jeffrey Griffiths and Reed College. *Introduction to electrodynamics*, chapter Electromagnetic Waves. Prentice hall Upper Saddle River, NJ, 3rd edition, 1999. (Cited on page 45.)

[13] E. Hecht. *Optics*. 1998. (Cited on pages 57, 58, and 72.)

[14] D. Hestenes. *New Foundations for Classical Mechanics*. Kluwer Academic Publishers, 1999. (Cited on pages 137 and 145.)

[15] J.D. Irwin. *Basic Engineering Circuit Analysis*. MacMillian, 1993. (Cited on pages 9 and 44.)

[16] JD Jackson. *Classical Electrodynamics*. John Wiley and Sons, 2nd edition, 1975. (Cited on pages 1, 2, 40, and 54.)

[17] JD Jackson. *Classical Electrodynamics*, chapter Simple Radiating Systems, Scattering, and Diffraction. John Wiley and Sons, 2nd edition, 1975. (Cited on page 45.)

[18] Peeter Joot. *Relativistic Electrodynamics.*, chapter Energy Momentum Tensor. peeterjoot.com, 2011. URL http://peeterjoot.com/archives/math2011/phy450.pdf. [Online; accessed 02-June-2020]. (Cited on page 36.)

[19] Peeter Joot. *Quantum Mechanics II.*, chapter Verifying the Helmholtz Green's function. peeterjoot.com, 2011. URL http://peeterjoot.com/archives/math2011/phy456.pdf. [Online; accessed 02-June-2020]. (Cited on page 30.)

[20] Peeter Joot. *Exploring physics with Geometric Algebra, Part I.*, chapter Stokes theorem. peeterjoot.com, 2014. URL http://peeterjoot.com/archives/math2015/gabookI.pdf. [Online; accessed 02-June-2020]. (Cited on page 29.)

[21] L.D. Landau and E.M. Lifshitz. *The classical theory of fields*. Butterworth-Heinemann, 1980. ISBN 0750627689. (Cited on page 1.)

[22] Adel S Sedra and Kenneth Carless Smith. *Microelectronic circuits*. Saunders College Publishing, 3rd edition, 1991. (Cited on page 44.)

[23] Warren L Stutzman and William A Davis. *Antenna theory*. Wiley Online Library, 1998. (Cited on page xii.)

[24] C-T Tai and CS Pereira. An approximate formula for calculating the directivity of an antenna. *IEEE Transactions on Antennas and Propagation*, 24:235, 1976. (Cited on pages 20 and 22.)

[25] Wikipedia. Impedance of free space — wikipedia, the free encyclopedia, 2014. URL `http://en.wikipedia.org/w/index.php?title=Impedance_of_free_space&oldid=605562113`. [Online; accessed 23-February-2015]. (Cited on page 12.)

[26] Wikipedia. *Magnetic potential — Wikipedia, The Free Encyclopedia*, 2015. URL `http://en.wikipedia.org/w/index.php?title=Magnetic_potential&oldid=642387563`. [Online; accessed 5-February-2015]. (Cited on page 49.)